# 國立交通大學

## 電控工程研究所

## 博 士 論 文

模 糊 邏 輯 控 制 系 統 之 穩 定 度 分 析 與 應 用

**The Stability Analysis and its Application in Fuzzy Control Systems**

研 究 生：馬立山

指導教授：吳炳飛　教授

中 華 民 國 九 十 八 年 十 二 月

# 模 糊 邏 輯 控 制 系 統 之 穩 定 度 分 析 與 應 用
## The Stability Analysis and its Application in Fuzzy Control Systems

研 究 生：馬立山　　　　　　　　　　Student：Li-Shan Ma

指導教授：吳炳飛　　　　　　　　　　Advisor：Prof. Bing-Fei Wu

國 立 交 通 大 學

電控工程研究所

博 士 論 文

A Dissertation

Submitted to Institute of Electrical and Control Engineering

College of Electrical Engineering

National Chiao Tung University

in partial Fulfillment of the Requirements

for the Degree of

Doctor of Philosophy

in

Electrical and Control Engineering

Dec. 2009

Hsinchu, Taiwan, Republic of China

中華民國九十八年十二月

# 模 糊 邏 輯 控 制 系 統 之 穩 定 度 分 析 與 應 用

研究生：馬立山　　　　　　　　　　　　　　指導教授：吳炳飛教授

## 國立交通大學電控工程研究所博士班

## 中文摘要

在本篇論文中，我們分析了 P 與 PD 型之模糊邏輯控制系統之絕對穩定度，另外也提出了一種基於模糊邏輯控制系統之應用，即只利用傳輸一狀態之數值信號，並利用適應性模糊類神經觀測器 (AFNO)去同步一類的未知混沌系統。關於穩定度分析，包括兩種狀況：確定與非確定性受控體。而穩定度分析包括以下參數：參考輸入、致動增益、區間(Interval )受控體參數。對確定性受控體而言，我們利用 Popov 或線性化的方法，針對 P 與 PD 型之模糊邏輯控制系統，在不同參考輸入信號與致動增益下，作絕對穩定度分析，另外，關於模糊邏輯控制系統在參數空間之穩態誤差也可被分析。針對非確定性受控體，我們利用基於 Lur'e 系統之參數化強健 Popov 準則，來作 P 型模糊邏輯控制系統之絕對穩定度分析，而關於非確定性受控體之 PD 型分析，在我們方法中，PD 型之模糊邏輯控制器，為一種單一輸入之 PD 型模糊邏輯控制器，而且此控制器可被轉成一種特殊 P 型模糊邏輯控制器，而再作進一步分析。與之前研究不同的是，我們利用參數化強健 Popov 準則，可針對非零之參考輸入，且非確定性之受控體，作絕對穩定度分析。我們亦利用 PSPICE 元件，設計了一個模糊電流控制 RC 電路，透過數值與 PSPICE 模擬驗證我們所作分析之結果。另外，在模擬例子中，我們也利用不同平衡點的觀念，解釋模糊邏輯控制系統之震盪機制。最後，我們也比較幾種非確定性系統之絕對穩定度準則，驗證我們的分析的有效性。另一方面，模糊邏輯控制系統也可以被設計用來智慧化同步混沌信號，其應用主要觀

念為只藉傳輸一狀態之數值信號，並利用 AFNO 去同步一類的未知混沌系統，如果此一非線性混沌系統可以藉由微分幾何的方法，被轉換成標準的 Lur'e 系統，則此方法便可以被應用來作同步。值得一提的是，在這一個方法中，AFNO 之適應性模糊類神經(FNN)可以被線上即時調整權重，去對傳送端之非線性項作建模。另外，藉由傳送端傳送一個狀態並利用接收端之觀測器可以對傳送端未知之所有狀態作重建，當所有狀態被觀測到，傳送端與接收端便達到同步。AFNO可以線上適應性估測傳送端之狀態，即使傳送端已經切換到另一個混沌系統，接收端之 AFNO還可以與新的混沌系統達到同步。另外一方面，即使存在建模誤差或外加有界干擾，AFNO 亦可強健的達到同步。模擬結果驗證 ANFO 對混沌系統之同步應用是有效的。
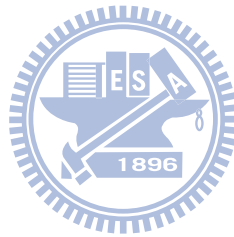
# The Stability Analysis and its Application in Fuzzy Control Systems

Student：Li-Shan Ma                    Advisor：Prof. Bing-Fei Wu

Institute of Electrical and Control Engineering
National Chiao Tung University

## ABSTRACT

This thesis analyzes the absolute stability in P and PD type fuzzy logic control systems with both certain and uncertain linear plants. In addition, the adaptive fuzzy-neural observer (AFNO) is applies to synchronize a class of unknown chaotic systems via scalar transmitting signal only. Stability analysis includes the reference input, actuator gain and interval plant parameters. For certain linear plants, the stability (i.e. the stable equilibriums of error) in P and PD types is analyzed with the Popov or linearization methods under various reference inputs and actuator gains. The steady state errors of fuzzy control systems are also addressed in the parameter plane. The parametric robust Popov criterion for parametric absolute stability based on Lur'e systems is also applied to the stability analysis of P type fuzzy control systems with uncertain plants. The PD type fuzzy logic controller in our approach is a single-input fuzzy logic controller and is transformed into the P type for analysis. In our work, the absolute stability analysis of fuzzy control systems is given with respect to a non-zero reference input and an uncertain linear plant with the parametric robust Popov criterion unlike previous works. Moreover, a fuzzy current controlled RC circuit is designed with PSPICE models. Both numerical and PSPICE simulations are provided to verify the analytical results. Furthermore, the oscillation mechanism in fuzzy control systems is specified with various equilibrium points of view in the simulation example. Eventually, the comparisons are also given to show the effectiveness of the analysis method. On the other hand, the fuzzy control system can be applied to synchronize the chaotic signals in the master end intelligently. With a scalar transmitting signal only, the AFNO is utilized to synchronize a class of unknown chaotic systems. The proposed method can be used for synchronization if nonlinear chaotic systems can be transformed into the canonical form of Lur'e system type by the differential geometric method. In this approach, the adaptive fuzzy-neural network (FNN) in AFNO is adopted on line to model the nonlinear term in the master end. Additionally, the

master's unknown states can be reconstructed from one transmitted state using observer design in the slave end. Synchronization is achieved when all states are observed. The utilized scheme can adaptively estimate the transmitter states on line, even if the transmitter is changed into another chaotic system. On the other hand, the robustness of AFNO can be guaranteed with respect to the modeling error, and external bounded disturbance. Simulation results confirm that the AFNO design is valid for the application of chaos synchronization.

# 致　　　　謝

顧壓力。

　另外，家中兩位寶貝兒子慕恩及瀚恩，雖然經常在我趕研究進度時候，意猶未盡地霸佔電腦，令人幾近抓狂，但您們卻也是鼓勵我奮鬥的泉源。您們的調皮，其實透露了無限的創造力，想到此時，真的會會心一笑。

　多年來，太太 憶如在我就讀研究所博士班期間，協助照料子女，尤其在留職停薪那一年，協助分擔家中許多事務，免除我後顧之憂，使我能一心向學，更是讓我無以回報。

　因篇幅有限，還有很多曾經教導我的師長、幫助我的同仁、鼓勵我朋友，無法一一致意，謹在此表達由衷的感謝，謝謝您們。

　博士求學過程中真的是一個漫長且艱辛的路程，有時看不到希望，甚至必須在絕望中持續奮鬥，不知何時光明會出現，尤其投稿論文被拒絕，畢業遙遙無期的時候。雖然未來前途也充滿了挑戰，希望透過如此一個真實的經驗，讓我體察到，即使未來處在困境中，仍要持續奮鬥，因為奮鬥才有希望。


最後將論文獻給所有關心、支持及協助我的人

<div align="right">立山 於交大CSSP 實驗室</div>

<div align="right">11/6/2009</div>

# Contents

# List of Figures

# List of Tables

# Chapter 1

## Introduction

### 1.1 Motivation

Fuzzy logic controller (FLC) has become a conventionally adopted control algorithm, and has been employed in various industrial applications [1], since Mamdani [2] proposed the first linguistic FLC based on expert experience to control a laboratory steam engine. The FLC design does not require an accurate mathematical model. Unlike traditional nonlinear controllers, FLC can work with imprecise inputs, and can deal with nonlinearity and uncertainty. Therefore, many studies are devoted to this field. Conversely, since the accurate mathematical model is not required to design FLC, the design procedure is still based on trial and error. Hence, the stability and performance of FLC cannot be guaranteed. Systematic analysis and synthesis schemes [3]-[26] have recently been developed to improve this issue.

Some methods [3]-[10] adopt the Takagi-Sugeno (T-S) fuzzy models to determine the stability of fuzzy control systems by the Lyapunov function or linear matrix inequality (LMI). The overall plant is first represented as a T-S fuzzy model by a fuzzy blending of each linear system model. The controller is then designed based on this T-S fuzzy model by Lyapunov function or LMI. However, an appropriate fuzzy model may be difficult to formulate for an arbitrary nonlinear dynamic system. Additionally, a common Lyapunov function for general cases, and an existing positive-definite matrix, are both difficult to obtain. Besides the T-S fuzzy model, Lyapunov functions are also adopted to design and analyze the robust PD fuzzy controller for bounded uncertainties or nonlinearities of the system, using the

Popov-Lyapunov approach [11]. In addition, the stability on the T-S fuzzy model is analyzed by the Kharitonov theorem incorporated with the Schur and Hurwitz criterions [12]. Recently, the developments of fuzzy logic control designs almost focus on the T-S fuzzy models control. The stability analyses all apply the time-domain LMI approach. The main research directions include model uncertainties [13]-[20] and time-delay [21]-[23] or both [24], [25]. The stability issues due to the reference input influence are not to be discussed in the T-S fuzzy models control.

Kickert and Mamdani [26] first applied the describing function approach (DF) to analyze the stability of fuzzy control systems by granting fuzzy control systems as a multi-level relay model. The describing function of FLC can, under reasonable assumptions, be obtained to predict the existence of a limit cycle in fuzzy logic control systems [27], [28]. DF provides an approximate approach to obtain the stability of unforced fuzzy control systems. DF may yield inaccurate or incorrect analysis results, because it is an aggressive and approximate approach. In other words, under some assumptions, DF can only be applied to analyze fuzzy system stability successfully. Additionally, the steady state error and transient response of fuzzy control systems with the sinusoidal and exponential input describing functions techniques are analyzed in [29] and [30], respectively.

The choice of parameters in fuzzy control systems with phase plane approach was proposed in [31]-[33]. Then, the phase plane analysis can be utilized to design fuzzy rules, or measure the performance and stability of a specific set of fuzzy rules. Phase plane analysis is a simple graphical approach, in which the system trajectories are inspected to provide information on system stability and performance. However, it is restricted to second order dynamic systems.

The extension of classical circle criteria is also applied to analyze the stability of linear systems with fuzzy logic controllers [34], [35]. The extended circle criteria can be employed to test the SISO and MIMO systems [34]. The extended circle criteria for MISO and MIMO

are presented in [35] for testing the robust stability in PI, such as fuzzy control systems with uncertain plant gains. This algorithm limits the nonlinearity of fuzzy controller to the sector bound.

The Popov is a frequency domain stability criterion for closed loop nonlinear systems of Lur'e type. Fuzzy control systems can be regarded as Lur'e type systems. Kandel et al. [36] adopted the Popov criterion to analyze the stability of fuzzy control systems with controller as multi-level relay. Furutani et al. [37] utilized the shifted Popov criterion to manage the fuzzy controller with both time-variant and time-invariant parts. However, the Popov criteria applied to the stability analyzes on the fuzzy logic control do not consider the effect of reference input.

On the other hand, the latest research developments on the Lur'e systems stability analyzes concentrate on the systems with model uncertainties [38]-[41] and time-delay [42]-[43] or both [44]-[46]. The main approaches include the time-domain LMI [38]-[44] and the classical frequency-domain [45], [46] methods. The stability issues due to the reference input influence are not even discussed except in [51]. By [51], we can predict that the stability of fuzzy control systems will crash due to reference input shift, so it is important to take the reference inputs as one of the parameters for stability analyzes of fuzzy control systems.

In short, the recent stability analysis developments on the Lur'e type systems almost always use the time-domain LMI approach. The concerned issues are on uncertainties and time-delay or both. However, the development directions don't concern the reference input influence on stability.

Other investigations on fuzzy logic control systems can be described as follows. Butkiewicz [47] investigated the steady error of a fuzzy control system with respect to different fuzzy reasoning processes [47]. Tao and Taur [48] designed a robust complexity-reduced PID-like fuzzy controller for a plant with fuzzy linear model in [48].

Malki et al. [49] derived a fuzzy PD controller from the conventional continuous-time linear PD controller [49], in which the proportional and derivative gains are a nonlinear function of the input signal. The stability of this new type fuzzy PD controller is ensured by the small gain theorem. Taur and Tao [50] analyzed and designed region-wise linear fuzzy controllers (RLFC) [50], and found that the RLFCs generally performed better than the PD controllers.

Our work analyzes the absolute stability in P and PD type fuzzy control systems with both certain and uncertain linear plants. The control functions in P and PD type fuzzy controllers are known to be piecewise linear, and can be described with mathematical equations. The equilibrium points of each piecewise linear surface in a P type fuzzy control system with a certain linear plant can be calculated by this description. The unique error equilibrium point of the overall system can be obtained by determining whether the error equilibrium point located in its own error region. Therefore, the error equilibrium points in the reference and actuator gain parameter space can be analyzed. Additionally, the absolute stability can be analyzed using the frequency and time domain approaches. Since a P type fuzzy control system is a Lur'e system, its stability can be tested by the Popov criteria in the frequency domain. In the time domain, the stability can be tested by linearizing the system with regard to the equilibrium point. Conversely, the stability of a P type fuzzy control system can be tested by the parametric robust Popov criterion [51] incorporated with the Kharitonov theorem for uncertain linear plant and interval parameters, including actuator gain, reference input and plant parameters. Notably, the actuator gain can be included in one of the plant parameters. For a PD type fuzzy control system, single-input fuzzy logic controller (SFLC) [52] is introduced into our analysis. In a certain linear plant situation, the equilibrium point of fuzzy control systems can be analyzed using the same P type fuzzy analysis concepts. A PD type fuzzy control system with an SFLC controller can be transformed into a P type system, so that its stability can be analyzed with the Popov and linearization methods. The parametric

4

absolute stability of Lur'e systems can also be applied to a transformed PD type fuzzy control system when the plant is uncertain. For comparison with theoretical analysis, a fuzzy current controlled RC circuit is designed with a PSPICE model. Simulation results including both numerical and PSPICE confirm the theoretical analysis. Additionally, the mechanism of oscillations in fuzzy control systems is interpreted with a viewpoint of equilibrium points in a simulation example. Finally, the comparisons also are made to exhibit the effectiveness of the analysis method. The applied method parametric robust Popov criterion will be compared with the robust Lur'e test [54], the robust circle criterion [54], and the robust Popov criterion [54]. In compared methods, the stability of uncertain fuzzy control systems which are considered as stable by compared methods will crash under the effect of the reference inputs. On the other hand, by the applied analysis method, the stability can be guaranteed for the certain interval reference inputs. In summary, this study can provide a valuable reference in designing fuzzy control systems.

In conclusion, the stability analysis is extended to a non-zero reference input and an uncertain linear plant. This is in contrast to the approach employed by Kim et al. [27], in which DF is derived and applied to analyze the stability of fuzzy control systems for zero reference inputs and certain linear plants. The DF method may yield inaccurate or incorrect analysis results without restricted assumptions. By contrast, the Popov criterion based on the Kharitonov theory can guarantee an exact stability investigation. Moreover, SFLC [52] is applied in the analysis of a PD type fuzzy control system. SFLC is an efficient FLC, owing to its 1-D fuzzy rules only. By this feature, the SLFC can be implemented as an analog circuit and applied for high frequency control. This work first investigates the steady state error and robust stability analysis for linear plants using the proposed structure transformation. Additionally, an analog fuzzy control system is designed with a PSPICE model to verify the analysis results. Finally, the explanations for unstable oscillations in fuzzy control systems are

presented with the equilibrium concept.

On the other hands, a kind of the applications based on fuzzy control systems is addressed in this thesis. In this application, the adaptive fuzzy-neural observer (AFNO) is applies to synchronize a class of unknown chaotic systems with a scalar transmitted signal only. The synchronization of chaotic systems has been extensively studied and given its potential application to security communications. Synchronization means that the master and slave have identical states as time goes to infinity. Pecora and Carroll first considered the synchronization of chaotic systems [55], in which the drive-response concept is introduced to achieve synchronization by a scalar transmitted signal. Perfectly identical parameters cannot be achieved in real applications. Therefore, the nonlinear robust control [56,57] concept is employed to chaos synchronization with previous known states within the margin of synchronization error. An adaptive recurrent neural controller can be utilized to synchronize with respect to unknown systems [58,59]. However, all states should be measurable with this algorithm. In contrast, the nonlinear observer is designed to synchronize chaotic systems [60,61,62]. Morgül and Solak [62] presented global synchronization is possible for a system with Brunowsky canonical form. Grassi and Mascolo [61] provided a systematic method for synchronizing using a scale transmitted signal. Message-free synchronization has been developed to permit communication with masking message in chaotic signals [63]. Messages can be extracted with message-free synchronization. Moreover, Boutayeb [60] proposed a scheme which is provided to synchronize and extract message simultaneously. Nevertheless, these systems do not consider the robustness of the state observer with respect to parameters mismatch [60,61,62]. Adaptive sliding observer design [64,65] can handle parameters mismatch. Furthermore, a robust observer [66] is designed for synchronization using the Takagi-Sugeno fuzzy model and the LMI approach. Millerioux and Daafouz recently introduced the input-independent global chaos synchronization [67]. In this method, the added

6

message does not affect the synchronization if the observer gain is appropriately designed. Other studies consider nonlinear observer designs for chaos synchronization [68,69]. However, by the methods of previous descriptions, the chaotic systems should be known previously before synchronization design. Recently, the system identification approaches [70,71,72] have been introduced for a scale signal identification and chaos synchronization respectively. In [71], the system identification concepts are applied to approximate the chaotic signal. The proposed identification scheme assumes a Lur'e type system as a reference model. This allows us to separate the identification process into two parts, adjusting alternatively the parameters of the linear and the nonlinear part. For modeling the linear system, the autoregressive moving average (ARMA) approach is utilized. On the other hand, the genetic algorithm is applied to optimize the break points parameters of nonlinear static functions to approximate nonlinear mapping. However, this approach is based on off-line identification, and it is not an on-line tuning scheme. Furthermore, the order in linear part identification should be by trial and error. The identification results just imitate the transmission signal and the other states in the master end cannot be achieved to synchronize simultaneously. In addition, the simulation results of this approach seem not very well. According to [70], the recursive identification is applied for chaos synchronization when the slave has exactly identical structure to the master system, but its parameters are unknown. It is shown that the unknown slave system parameters can be found by the concepts of adaptive synchronization. In other words, when the unknown slave system parameters are found, the synchronization is achieved. However, the structures in the master and slave ends should be known previously and exactly the same, although the parameters in the slave end can be estimated by recursive identification. The discussion of robustness is not included too. More recently, an alternative indirect Takagi–Sugeno fuzzy model based adaptive fuzzy observer design has been applied to chaos synchronization under assumptions that states are unmeasurable and parameters are

7

unknown [72]. The adaptive law is designed to estimate the unknown parameters in the T-S fuzzy model of the slave end. When the unknown parameters are estimated correctly, the synchronization is achieved. However, the form of the T-S fuzzy model should be known first, and then the adaptive fuzzy observer is designed by the T-S fuzzy model. In addition, the discussion of robustness is not included.

This investigation achieves synchronization with respect to a class of unknown master chaotic systems by introducing the concepts of AFNO [73], Brunowsky canonical form [62] and Lur'e systems [74]. The proposed system includes a chaos master with canonical form and the slave with AFNO. The AFNO combines a FNN and a linear observer. In this design, the slave should synchronize with the master by a scale transmitted signal .This approach employs adaptive FNN to model the nonlinear term of the master end. The output of the adaptive FNN, robust input and a transmitted state are sent to the linear observer to estimate the states of the slave. The master and slave achieve synchronization when all states are estimated at the slave. Additionally, the adaptive laws are needed to update the weights of the FNN, when the reconstructed and transmitted states differ from each other.

The benefits of provided AFNO for synchronization can be stated as follows. AFNO is first applied to chaos synchronization with only one transmitted signal. Since AFNO is on line learning at the slave, the synchronization can be achieved respect to a switched unknown chaotic system with the Lur'e type. Additionally, the adaptability for parameters change or even system switched in the mater and the robustness for modeling error and external bounded disturbance are also given. AFNO also has FNN's inherent properties of fault-tolerance, parallelism learning, linguistic information and logic control. By comparing with [70,71,72], our presentation provides the on-line, robust and adaptive synchronization for a class of chaotic systems. The form of nonlinear functions in the master end cannot be known in previous due to soft computing with FNN for fitting it in the slave end.

## 1.2 Organizations of the Dissertation

This thesis is organized as follows. Chapter 1 is an introduction. Chapter 2 describes the P and PD type fuzzy control systems. Chapter 3 analyzes the equilibrium points and stability in P type fuzzy control system. Chapter 4 then performs the same analyses in a PD type fuzzy control system. Chapter 5 provides simulation results with Matlab and PSPICE simulators. In Chapter 6, the comparisons are made to show the superiority of the applied analysis method. Furthermore, in Chapter 7, the observer-based synchronization for a class of unknown chaotic systems with adaptive fuzzy-neural network is presented. Finally, some conclusions are given in Chapter 8.
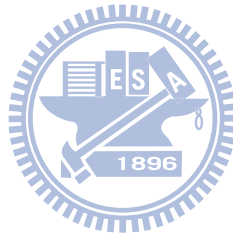
# Chapter 2

# The Fuzzy Logic Control Systems

## 2.1 Fuzzy Logic Controller

Both P and PD type fuzzy logic control systems include a linear plant with time-invariant uncertainty, adjustable actuator gain and reference input. Moreover, the fuzzy logic controllers are the cores of systems. An FLC can be taken as multiple bends of piecewise linear functions, since it has singleton and specific membership functions. Hence, a fuzzy logic control system can be treated as a Lur'e type system.

Consider the fuzzy logic control system in Fig. 2.1. The IF-THEN rules in single input fuzzy logic controller can be described as;

$$Rule_i :\text{If} \ e \ \text{is} \ M_i, \text{then} \ u_f \text{ is } \ u_i , \tag{1}$$

where $e$ is the control error and $M_i$ and $u_i$ denote fuzzy sets. If a singleton is applied in a fuzzifier, then the product inference and center average are formulated in the inference engine and defuzzifier, respectively. The output of the fuzzy logic controller can be represented as

$$u_f = \sum_i \mathbf{\Omega}_i(e)u_i , \tag{2}$$

where $\mathbf{\Omega}_i(e) = \dfrac{M_i(e)}{\sum_j M_j(e)}$ .

For simplification, this study uses the fuzzy rules and membership functions listed in Table 2.1 [27] and Fig. 2.2 are adopted in this thesis, respectively. Table 2.2 presents the fuzzy controller parameters. Figure 2.3 shows the control function of the fuzzy controller, which can

be described as:

$$u_f = \sigma(e) = \begin{cases} segment \ 1 : k_2 e + c_2, & e \in [a_2, a_3], \\ segment \ 2 : k_1 e + c_1, & e \in [a_1, a_2], \\ segment \ 3 : k_0 e, & e \in [-a_1, a_1], \\ segment \ 4 : k_1 e - c_1, & e \in [-a_2, -a_1], \\ segment \ 5 : k_2 e - c_2, & e \in [-a_3, -a_2], \end{cases} \tag{3}$$

where

$$0 < a_1 < a_2 < a_3, \ 0 < b_1 < b_2 < b_3, \ c_1 = b_2 - k_1 a_2, \ c_2 = b_3 - k_2 a_3, \ k_0 = \frac{b_1}{a_1}, \ k_1 = \frac{b_2 - b_1}{a_2 - a_1}, \text{ and}$$

$$k_2 = \frac{b_3 - b_2}{a_3 - a_2}.$$

**Remark 2.1**: The assumptions $0 < a_1 < a_2 < \cdots < a_n$ and $0 < b_1 < b_2 < \cdots < b_n$ are satisfied for $n$ multiple bends of a control function. The control output of the static fuzzy system is given by:
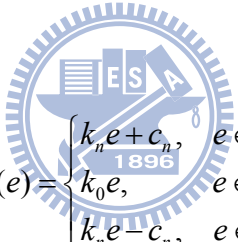
$$u_f = \sigma(e) = \begin{cases} k_n e + c_n, & e \in [a_n, a_{n+1}], \\ k_0 e, & e \in [-a_1, a_1], \\ k_n e - c_n, & e \in [-a_{n+1}, -a_n], \end{cases} \tag{4}$$

where $c_n = b_{n+1} - k_n a_{n+1}$, $k_n = \dfrac{b_{n+1} - b_n}{a_{n+1} - a_n}$, and $n = 1, 2, 3, \cdots, n$.

The control function $\sigma$ satisfies

$$0 \leq \hat{e}\left[\sigma(e + \hat{e}) - \sigma(e)\right] \leq k(e)\hat{e}^2, \quad \forall e \in \mathbf{O}, \quad \forall \hat{e} \in \Re, \tag{5}$$

where $\sigma(0) = 0$, $k > 0$ and $\mathbf{O}$ indicates some neighborhood of $e = 0$.


## 2.2 P Type Fuzzy Logic Control System

Figure 2.1 illustrates a P type fuzzy control system with a fuzzy logic controller, a parametric linear time-invariant system and adjustable parameters, which include actuator gain $K$ and reference input $r$. The control function of the fuzzy controller is a piecewise

linear function, and is depicted in Fig. 2.3.

The linear plant $H(s, p)$ shown in Fig. 2.1 can be presented as

$$H(s, p) = C(p)\left[sI - A(p)\right]^{-1} B'(p),$$ (6)

where $A(p) \in \mathfrak{R}^{n \times n}$ and $A(p)$ is a stable matrix; $B'(p) \in \mathfrak{R}^{n \times 1}$; $C(p) \in \mathfrak{R}^{1 \times n}$, the parameter vector $p$ exists in a compact and simple connected region $\mathbf{P} \subset \mathfrak{R}^l$.

The transfer function $G(s, p, K)$ with amplifier gain $K \in \mathfrak{R}$ can be stated as

$$G(s, p, K) = C(p)\left[sI - A(p)\right]^{-1} B(p, K)$$ (7)

where $B(p, K) = KB'(p) \in \mathfrak{R}^{n \times 1}$, and $K \in \mathfrak{R}$. The overall static fuzzy logic control system in Fig. 2.1 can be described as:

$$\dot{x} = A(p)x + B(p, K)u_f,$$

$$y = C(p)x,$$ (8)

where the control input $u_f = \sigma(e)$; the control error $e = r - y$, $x \in \mathfrak{R}^n$, $e \in \mathfrak{R}$ and $y \in \mathfrak{R}$; the reference input $r$ is a constant value, and $r$ is a constant value, and $r \in \mathfrak{R}$.

The closed loop system is given by

$$\dot{x} = A(p)x + B(p, K)\sigma\left[r - C(p)x\right].$$ (9)

The error equilibrium points and relative stability under the influence of parameters including actuator gain $K$, reference input $r$ and time invariant uncertainty in linear plants are addressed. The parameter vector is defined as $(r, p, K)$.


## 2.3 PD Type Fuzzy Logic Control System

This subchapter discusses the PD type SFLC depicted in Fig. 2.4. The SFLC's output $u_f$ is proportional to a negative signed distance $D_s$. Additionally, the number of the fuzzy rules,

as shown in Table 2.3 [52], is significantly reduced into 1-D space, as in Table 2.4, owing to the single input and skew-symmetric property. Due to the skew-symmetric property of the rule table, $(e,\dot{e})$ can be split into five regions. Figure 2.5 illustrates an example of this division of $(e,\dot{e})$. The reduced 1-D rules improve the efficiency of the controller by saving time cost for a look up rule table, although it also adds the calculation time of signed distance. Therefore, the SFLC is suitable for implementation in circuit control. The SFLC is introduced in this subchapter for further equilibrium points and stability analysis in the following subchapters.

## 2.3.1 Calculation of signed distance

The control error in SFLC is defined as

$$e_d(t) = y - r . \tag{10}$$

The switching line $s_l$ as shown in Fig. 2.5 is given by

$$s_l : \dot{e}_d + \lambda e_d = 0 . \tag{11}$$

The signed perpendicular distance $D_s$ of general point $Q(e_d,\dot{e}_d)$ to a switching line is calculated as follows:

$$D_s = \text{sgn}(s_l)D = \frac{\dot{e}_d + \lambda e_d}{\sqrt{1+\lambda^2}}, \tag{12}$$

where $D = \dfrac{\left|\dot{e}_d + \lambda e_d\right|}{\sqrt{1+\lambda^2}}$ is shown in Fig. 2.5 and $\text{sgn}(s_l) = \begin{cases} 1 & \text{for } s_l > 0 \\ -1 & \text{for } s_l < 0 \end{cases}$.

The control output $u_f = \phi(D_S)$ is defined according to the control rule in SFLC as given in Table 2.4 and Fig. 2.4.

## 2.3.2 The presentation of the SFLC system

The SFLC system can be described as:

$$\dot{x} = A(p)x + B(p,K)u_f ,$$

$$y = C(p)x, \tag{13}$$

where the control input $u_f = \phi(D_s)$.

## 2.3.3 The analytic representation of the SFLC system

If Tables 2.2, 2.4 and Fig. 2.2 are applied into the controller in SFLC, then the control function $\phi(\bullet)$ of the fuzzy controller is as displayed in Fig. 2.6. The surface of the fuzzy controller in SFLC is typically oddly symmetrical; therefore, the control force is given by

$$u_f = \phi(D_s) = \sigma(-D_S) = \sigma(\rho), \tag{14}$$

where $\rho = -D_s = \dfrac{\dot{e} + \lambda e}{\sqrt{1 + \lambda^2}}$.

In the following analysis, this representation as illustrated in Fig. 2.7 is applied to PD type analysis. In Chapter 3, the SFLC system is reformatted as a special P type fuzzy control system, and is employed to analyze the equilibrium
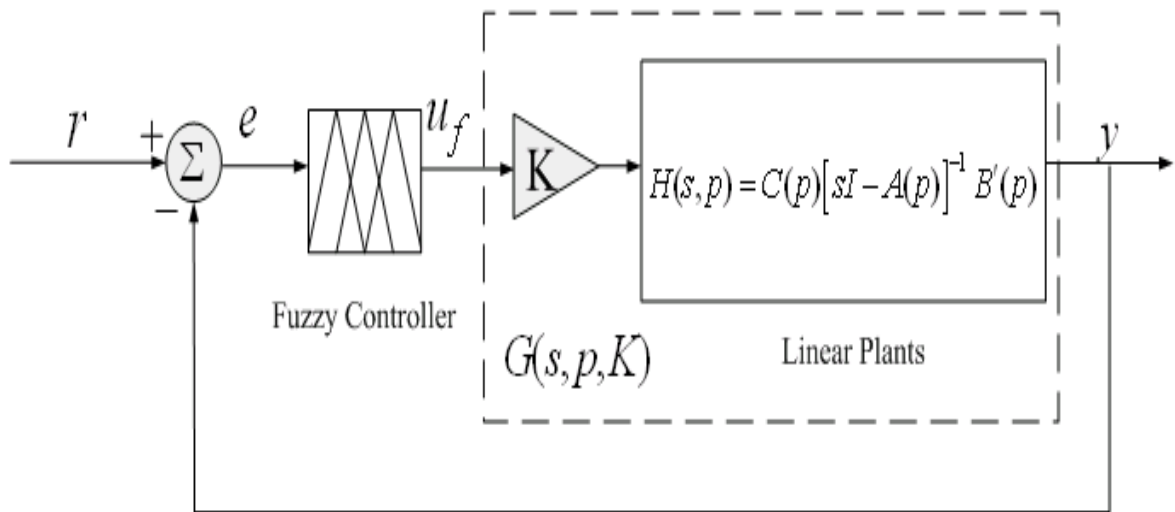
Fig. 2.1 The P type fuzzy control system.



(a)



(b)
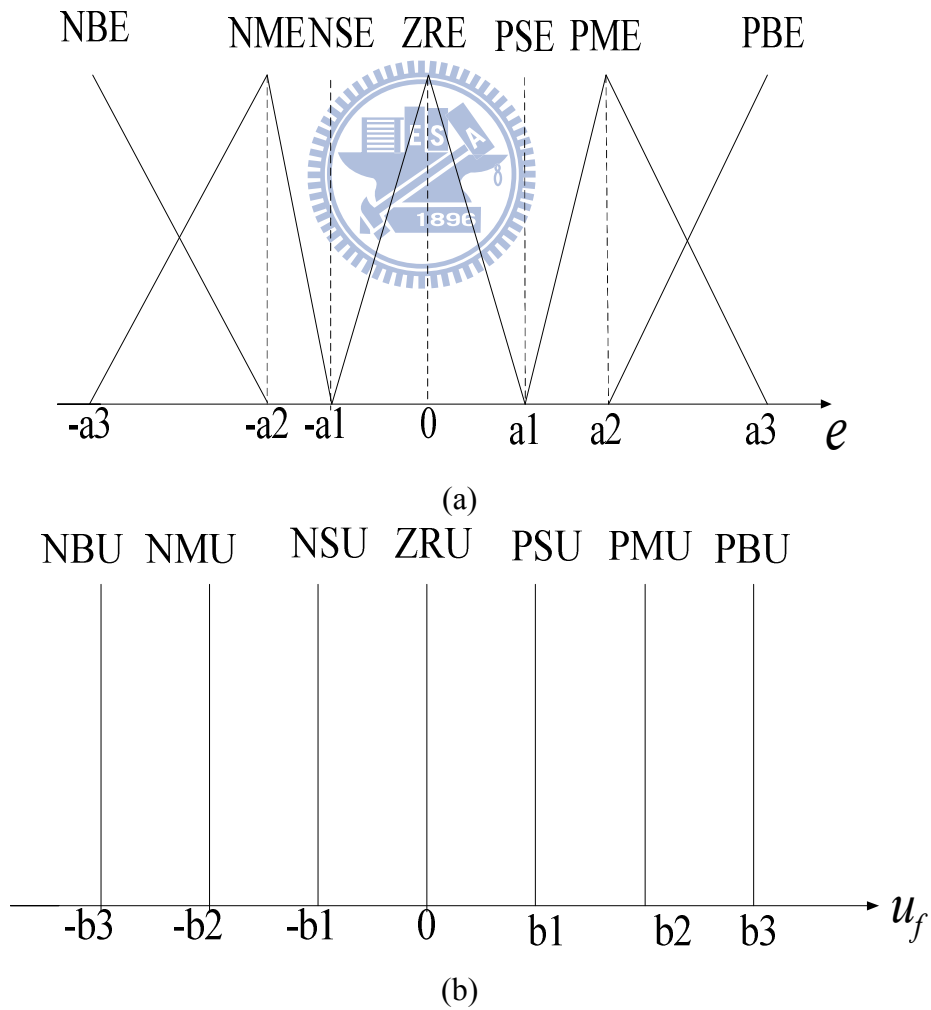
Fig.2.2 The membership functions of the fuzzy logic controller.

Table 2.1

Rules of the fuzzy logic controller

| $e$ | NBE | NME | NSE | ZRE | PSE | PME | PBE |
|---|---|---|---|---|---|---|---|
| $u_f$ | NBU | NMU | NSU | ZRU | PSU | PMU | PBU |

Table 2.2

Parameters of the fuzzy logic controller

| | NBE | NME | NSE | ZRE | PSE | PME | PBE |
|---|---|---|---|---|---|---|---|
| $e$ | $-a_3$ | $-a_2$ | $-a_1$ | 0 | $a_1$ | $a_2$ | $a_3$ |
| | NBU | NMU | NSU | ZRU | PSU | PMU | PBU |
| $u_f$ | $-b_3$ | $-b_2$ | $-b_1$ | 0 | $b_1$ | $b_2$ | $b_3$ |
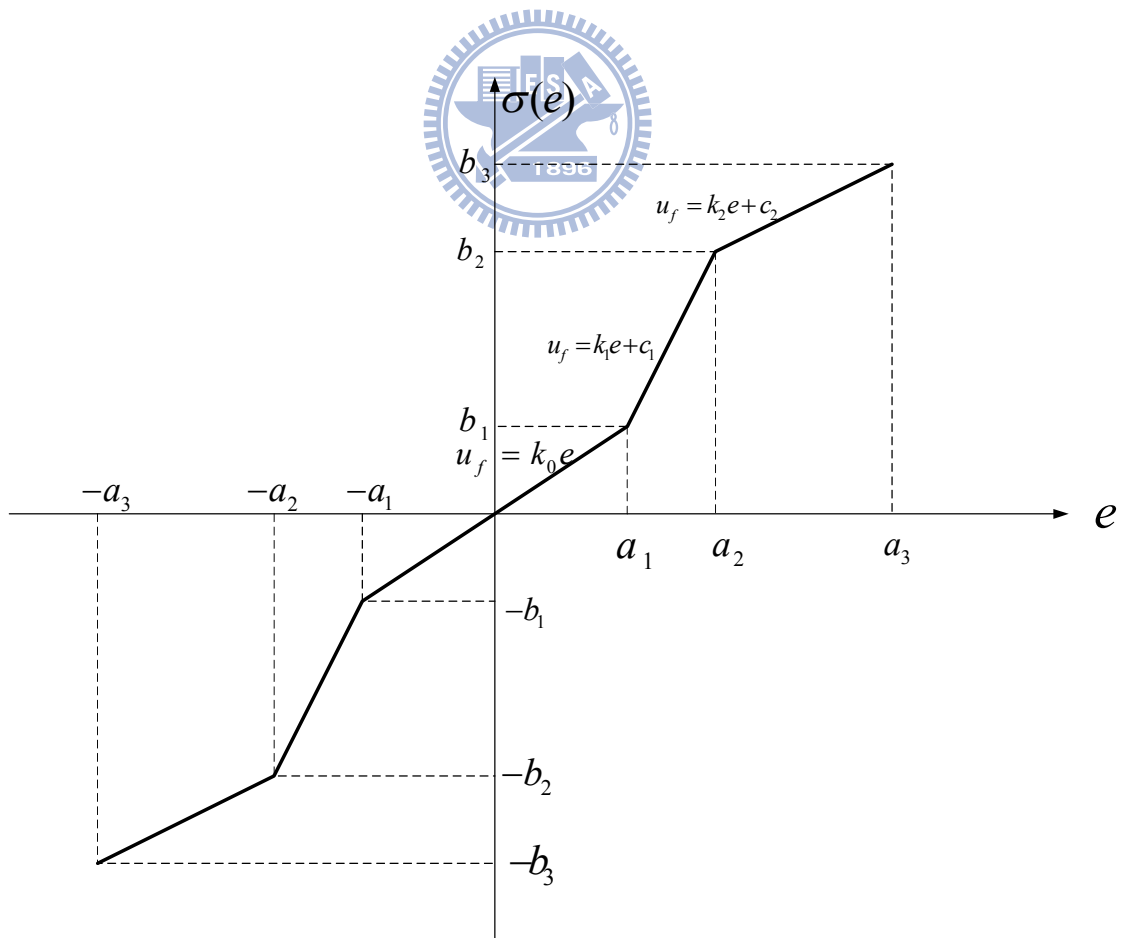


Fig. 2.3 The control function of the fuzzy logic controller.
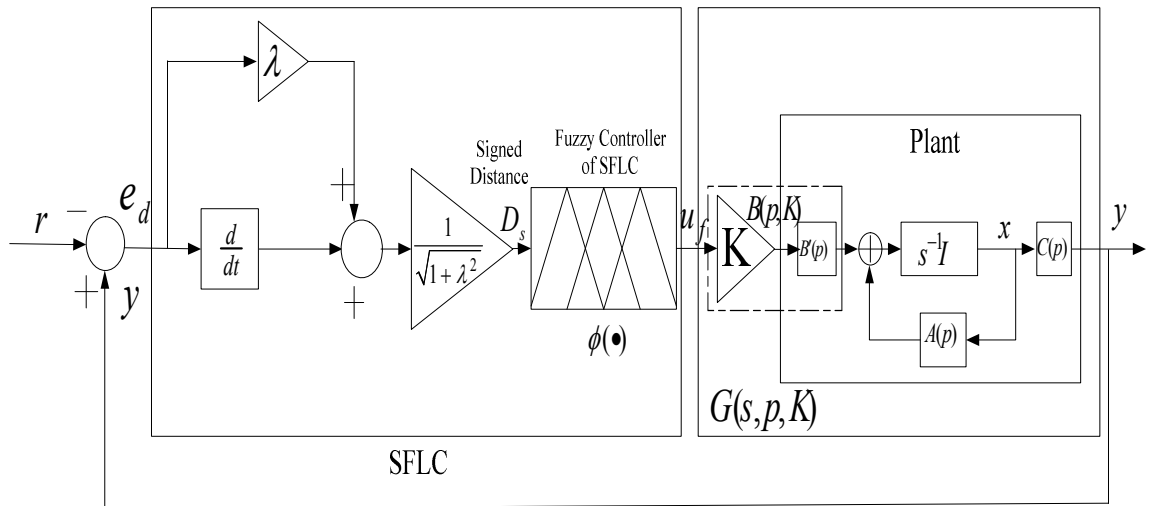
Fig. 2.4 The single-input fuzzy logic control system.

Table 2.3
Rules of conventional FLC with control error defined as $e_d$

| $\dot{e}_d$ \ $e_d$ | NB | NS | ZR | PS | PB |
|---|---|---|---|---|---|
| PB | ZR | NS | NS | NB | NB |
| PS | PS | ZR | NS | NS | NB |
| ZR | PS | PS | ZR | NS | NS |
| NS | PB | PS | PS | ZR | NS |
| NB | PB | PB | PS | PS | ZR |

Table 2.4
Rules of SFLC

| $D_S$ | NBE | NME | NSE | ZRE | PSE | PME | PBE |
|---|---|---|---|---|---|---|---|
| $u_f$ | PBU | PMU | PSU | ZRU | NSU | NMU | NBU |
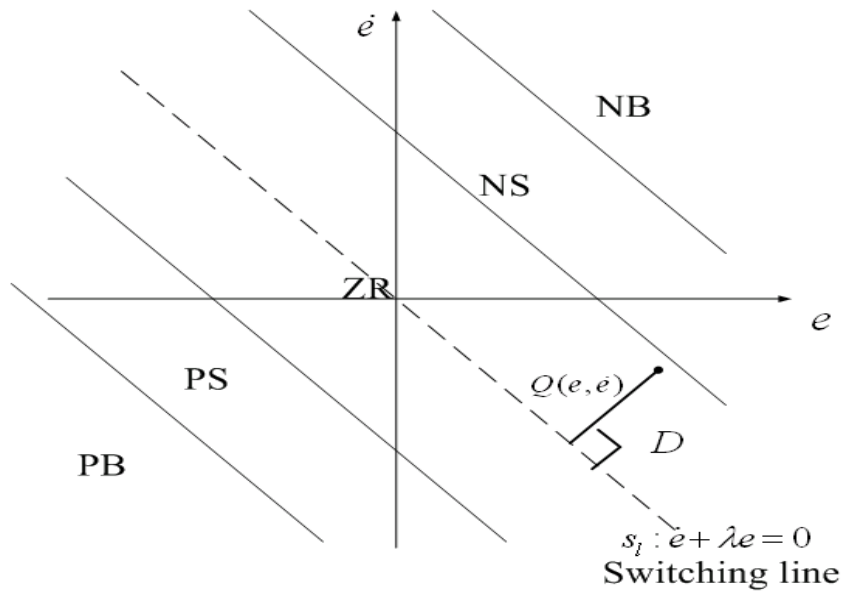
Fig. 2.5 The skew-symmetric property in ($e$, $\dot{e}$) and the calculation of signed distance.
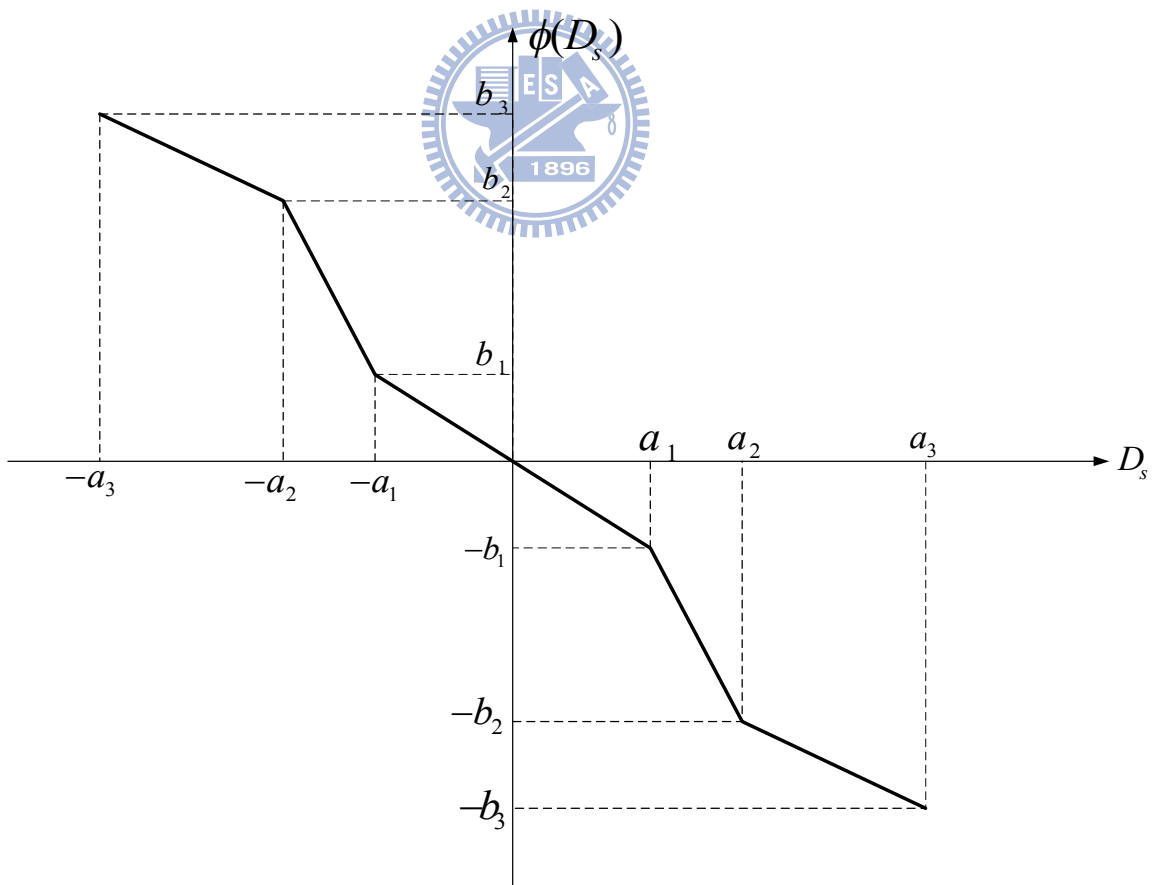


Fig. 2.6 The control function of the fuzzy logic controller in SFLC.
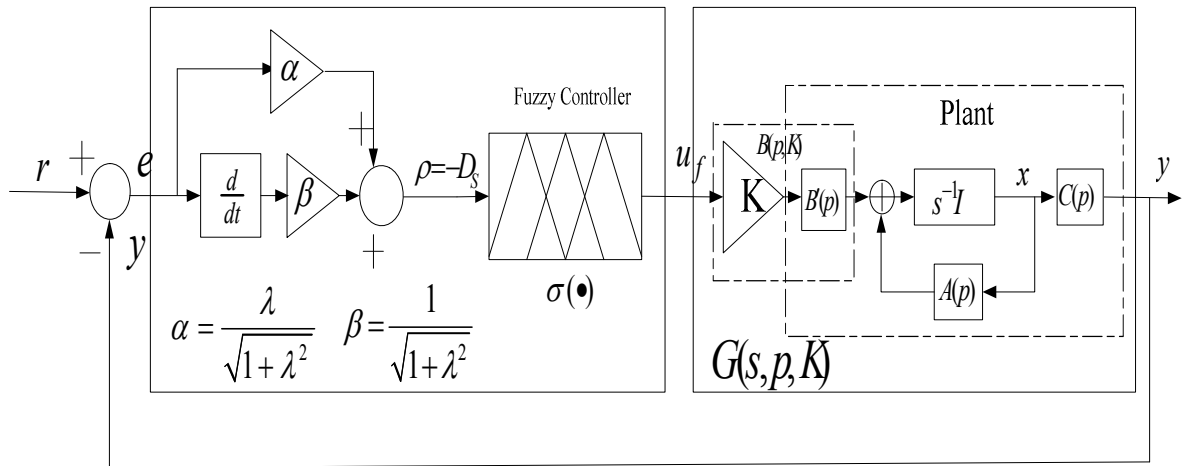
Fig. 2.7 The transition formation in the transformation.
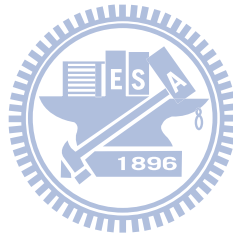
# Chapter 3

# Equilibrium Points and Stability Analysis in P and PD Type Fuzzy Control Systems

## 3.1 Equilibrium Point Analysis for P Type Fuzzy Control Systems with Linear Plants

This subchapter presents the analysis of error equilibrium points and stability in P type fuzzy control systems. The equilibrium point in fuzzy control systems can be derived when equilibrium points can be solved. Moreover, the stability of the equilibrium point can be judged with the linearizing system around the equilibrium or the Popov criterion in the following subchapter. If the error equilibrium points of the overall system are stable, then the steady state error can be derived from this result.

By (9), let $\dot{x} = 0$, then

$$Ax + B(K)\sigma[r - Cx] = 0. \tag{15}$$

If $A^{-1}$ exists, then (16) is obtained.

$$x + A^{-1}B(K)\sigma(e) = 0, \tag{16}$$

where $e = r - Cx$.

Multiply the result by $C$ in (16), and let $Cx = r - e$, then

$$e - r - CA^{-1}B(K)\sigma(e) = 0. \tag{17}$$

The state equilibrium points represented as $x^e$, and the error equilibrium points denoted as

$e^e$ , can be determined from (16) and (17), respectively.

**Assumption 3.1**: The unique solution exists in (17). In other words, an error equilibrium
point uniquely exists.

Under Assumption 3.1, the error equilibrium points can be solved from (18) by replacing (4)
in each segment.

$$
\begin{aligned}
e^e - r - CA^{-1}B(K)(k_n e^e + c_n) = 0 \quad & \textit{if } e \in [a_n, a_{n+1}], \\
e^e - r - CA^{-1}B(K)(k_0 e^e) = 0 \qquad & \textit{if } e \in [-a_1, a_1], \qquad n = 1, 2, 3, \cdots. \\
e^e - r - CA^{-1}B(K)(k_n e^e - c_n) = 0 \quad & \textit{if } e \in [-a_{n+1}, -a_n].
\end{aligned} \tag{18}
$$

One of these error equilibrium points is the unique point of the overall system. The unique
point is identified by checking whether $e^e$ is located in its own error region.

## 3.2. Stability Analysis for P Type Fuzzy Control Systems with a Certain Linear Plant

In the certain linear plant case, the stability can be determined by the time or frequency
domain approaches proposed in [51]. In the time domain approach, the eigenvalues of the
linearizied system (8) can be applied to determine the stability. In the frequency domain, the
Popov criterion is utilized to test stability.

### 3.2.1 Frequency domain approach

Consider the error dynamic system for a given parameter vector $(r, p, K)$.

$$
\dot{\hat{x}} = A(p)\hat{x} + B(p)\hat{\sigma}(-C(p)\hat{x}), \tag{19}
$$

where $\hat{x} = x - x^e(r, p, K)$,

and

$$
\hat{\sigma}(-C(p)\hat{x}) = \sigma\left[-C(p)\hat{x} + e^e(r, p, K)\right] - \sigma\left[e^e(r, p, K)\right].
$$

The error equilibrium point of the P type fuzzy control system is given by

$$e^e(r,p,K)=r-C(p)x^e(r,p,K). \tag{20}$$

The error dynamic system is also of Lur'e type. The function $\hat{\sigma}$ satisfies the following sector condition if $e^e(r,p,K)\in \mathbf{O}$.

$$0 \le \hat{e}\hat{\sigma}(\hat{e}) \le k[e^e(r,p,K)]\hat{e}^2, \quad \forall \hat{e} \in \Re, \tag{21}$$

where $\hat{e}=e-e^e(r,p,K)$ and $k>0$.

By the Popov criterion, (19) is absolutely stable for a given $(r,p,K)$, if there exists a real number $v=v(r,p,K)$ satisfying

$$\mathrm{Re}[(1+j\omega v)G(j\omega,p,K)]+\frac{1}{k[e^e(r,p,K)]}>0, \quad \forall \omega \in \Re, \tag{22}$$

where $G(s,p,K)=C(p)[sI-A(p)]^{-1}B(p,K)$.

## 3.2.2 Time domain approach

Under an arbitrary parameter vector $(r,p,K)$, if an equilibrium state $x^e(r,p,K)$ of the system exists, then the stability can be determined from the linearization of (9) near the state equilibrium point.

**Remark 3.1**: If the unique state equilibrium is stable, then the steady state error in fuzzy control systems can be obtained from the state equilibrium by $e^e=r-Cx^e$.

## 3.3 Stability Analysis for P Type Fuzzy Control Systems with an Uncertain Linear Plant

In this subchapter, the parametric absolute stability can be tested using the parametric robust Popov criterion incorporated with Kharitonov theorem, when the parameter vector $(r,p,K)\in R_{ref}\times \mathbf{P}\times \mathbf{K}$, where $R_{ref}=[\underline{r},\overline{r}]\subset \Re$.

The value of $e^e(r,p,K)$ is difficult to calculate from the results in the previous

subchapter, because fuzzy control function $\sigma(\bullet)$ is sometimes impossible to obtain mathematically, and parameters $(r, p, K)$ vary in a range in real application. Therefore, the stability analysis by the parametric robust Popov criterion in [51] is adopted to handle this situation.

Applying Theorem 1 in [51], let's consider the uncertain P type fuzzy control system (9) satisfying the following conditions. Then, the P type fuzzy control system is parametric absolute stable.

(1) If the fuzzy controller $\sigma$ is continuous, and for some neighborhood $\mathbf{O}$ of $e = 0$ satisfies

$$0 \le \hat{e}[\sigma(e+\hat{e}) - \sigma(e)] \le k(e)\hat{e}^2, \quad \forall e \in \mathbf{O}, \quad \forall \hat{e} \in \mathfrak{R}, \text{ and } \sigma(0) = 0, \qquad (23)$$

where $k(e)$ is a positive number depending on $e \in \mathbf{O}$.

(2) If $-C(p)A^{-1}(p)B(p,K) + \dfrac{1}{k(0)} > 0$, $\forall p \in \mathbf{P}$ \qquad (24)

holds, for any $(r, p, K) \in R_{ref} \times \mathbf{P} \times \mathbf{K}$ and any $\sigma$ satisfying the sector condition (23), there exists a solution $e = e^e(r, p, K)$ of (17) in $\mathbf{O}^e(r, p, K)$,

where

$$\mathbf{O}^e(r,p,K) = \begin{cases} \left[\dfrac{r}{\varsigma_0(p)}, r\right] & (\text{when } r\{C(p)A^{-1}(p)B(p,K)\} \le 0) \\[4mm] \left[r, \dfrac{r}{\varsigma_0(p)}\right] & (\text{when } r\{C(p)A^{-1}(p)B(p,K)\} > 0) \end{cases} \qquad (25)$$

and $\varsigma_0(p) = 1 - C(p)A^{-1}(p)B(p,K)k(0)$. A more detail proof on (15) and (16) can be referred in the Lemma 1 of [51].

(3) If for a given region $R_{ref}$ of $r$ and for any $p \in \mathbf{P}$, the condition $\mathbf{O}_R^e(p) \subset \mathbf{O}$ is satisfied, and a real number $v_o = v_o(r, p, K)$ exists such that the following inequality holds

23

$$\text{Re}[(1+j\omega v_o)G(j\omega, p, K)] + \frac{1}{k_R(r, p, K)} > 0, \quad \forall \omega \in \Re, \tag{26}$$

where

$$k_R(p) = \max\left\{k(e) : e \in \mathbf{O}_R^e(r, p, K)\right\}, \tag{27}$$

and $\mathbf{O}_R^e(r, p, K)$ represents the region containing $e^e(r, p, K)$ for all $r \in R_{ref}$.

**Remark 3.2**: $k_R(r, p, K)$ is hard to find, so we suppose that $R_{ref} \subset \mathbf{O}$. Moreover, assume

that for any $p \in \mathbf{P}$, $G(0, p, K) > 0$, $k_R^*(p) = \max\left\{k(e) : e \in R_{ref}\right\}$, and there exists a real

number $v_o = v_o(r, p, K)$ letting the inequality hold.

$$\text{Re}[(1+j\omega v_o)G(j\omega, p, K)] + \frac{1}{k_R^*} > 0, \quad \forall \omega \in \Re. \tag{28}$$

The P type fuzzy control system is then parametric absolute stable. [51]

**Remark 3.3**:

(1) This test can be extended to the general P type fuzzy control functions design.

(2) The assumption in Remark 3.2 does not lose generality, since most systems have

$G(0, p, K) > 0$.

(3) The effect of $K$ can be combined into plant parameters $p$.

The existence of $v_o = v_o(p)$ for every $p \in \mathbf{P}$ should be guaranteed in (28). This is

generally a difficult problem. Therefore, the parametric robust Popov criterion incorporated

with Kharitonov [51], [53], [54] for interval Lur'e systems is introduced into a parametric

absolute stable analysis.

Consider the following as a family of interval plants

$$G(s, p, K) = \frac{Q(s)}{P(s)}, \tag{29}$$

where $Q(s)$ and $P(s)$ belong to the families of real interval polynomials $\mathbf{Q}(s)$ and $\mathbf{P}(s)$,

respectively.

$$\mathbf{Q}(s) = \left\{ Q(s) : Q(s) = q_0 + q_1 s + \cdots + q_\tau s^\tau, \quad and \ q_i \in \left[ q_i^-, q_i^+ \right], \quad for \ all \ i = 0, \cdots, \tau \right\},$$

and $\mathbf{P}(s) = \left\{ P(s) : P(s) = p_0 + p_1 s + \cdots + p_n s^n, \quad and \ p_j \in \left[ p_j^-, p_j^+ \right], \quad for \ all \ j = 0, \cdots, n \right\}.$ (30)

$K_Q^i(s)$, $i = 1, 2, 3, 4$ and $K_P^j(s)$, $j = 1, 2, 3, 4$ represent the Kharitonov polynomials associated with $\mathbf{Q}(s)$ and $\mathbf{P}(s)$, respectively. The Kharitonov systems associated with $G(s, p, K)$ are defined as the 16 plants of the following set,

$$G_K(s) := \left\{ \frac{K_Q^i(s)}{K_P^j(s)} : i, j \in \{1, 2, 3, 4\} \right\},$$ (31)

where

$$K_Q^1(s) = q_0^- + q_1^- s + q_2^+ s^2 + q_3^+ s^3 + q_4^- s^4 + q_5^- s^5 + q_6^+ s^6 + \cdots;$$

$$K_Q^2(s) = q_0^+ + q_1^+ s + q_2^- s^2 + q_3^- s^3 + q_4^+ s^4 + q_5^+ s^5 + q_6^- s^6 + \cdots;$$

$$K_Q^3(s) = q_0^+ + q_1^- s + q_2^- s^2 + q_3^+ s^3 + q_4^+ s^4 + q_5^- s^5 + q_6^- s^6 + \cdots;$$

$$K_Q^4(s) = q_0^- + q_1^+ s + q_2^+ s^2 + q_3^- s^3 + q_4^- s^4 + q_5^+ s^5 + q_6^+ s^6 + \cdots;$$

$$K_P^1(s) = p_0^- + p_1^- s + p_2^+ s^2 + p_3^+ s^3 + p^- s^4 + p_5^- s^5 + p_6^+ s^6 + \cdots;$$

$$K_P^2(s) = p_0^+ + p_1^+ s + p_2^- s^2 + p_3^- s^3 + p_4^+ s^4 + p_5^+ s^5 + p_6^- s^6 + \cdots;$$

$$K_P^3(s) = p_0^+ + p_1^- s + p_2^- s^2 + p_3^+ s^3 + p_4^+ s^4 + p_5^- s^5 + p_6^- s^6 + \cdots;$$

$$K_P^4(s) = p_0^- + p_1^+ s + p_2^+ s^2 + p_3^- s^3 + p_4^- s^4 + p_5^+ s^5 + p_6^+ s^6 + \cdots.$$

A P type fuzzy control system is absolutely stable in sector $[0, k]$ for all $G(s) \in G(s, p, K)$, if a real $v_o$ can be obtained by verifying the robust Popov condition for $G(s) \in G_K(s)$ to satisfy inequality (28).

**Remark 3.4:**

(1) The previous descriptions imply that only 16 Popov plots need to be drawn from family $G_K(s)$ to check that the P type fuzzy logic control system is stable when the robust

Popov condition (28) holds for the whole family $G(s)$.

(2) The P type fuzzy control systems of Lur'e type can be tested by the parametric robust Popov criterion. By [51], [53], [54], the criterion incorporated with Kharitonov for interval Lur'e systems can be considered here for parametric absolute stability analysis of P type fuzzy control systems.

## 3.4 Transformation SFLC from PD to P Type

In the following, the SFLC is transformed from PD to P type, so that the equilibrium point and stability can be analyzed by the transformed special P type fuzzy logic control system.

From Fig. 2.4, the factor $\dfrac{1}{\sqrt{1+\lambda^2}}$ of SFLC is integrated into both the proportional and derivative factors. The $\alpha$ and $\beta$ in Fig. 2.7 are then defined as

$$\alpha = \frac{\lambda}{\sqrt{1+\lambda^2}}, \quad \text{and} \quad \beta = \frac{1}{\sqrt{1+\lambda^2}}. \tag{32}$$

**Assumption 3.2:** $CB = 0$.

According to Assumption 3.2 and Fig 2.7, the following derivation can be obtained.

$$e = r - y = r - Cx. \tag{33}$$

By differentiating both sides, then

$$\dot{e} = -C\dot{x} = -C(Ax + Bu_f) = -CAx. \tag{34}$$

From (33) and (34), then

$$\rho = \alpha e + \beta \dot{e} = \alpha(r - Cx) + \beta(-CAx) = r' - C_1 x, \tag{35}$$

where $C_1 = (\alpha C + \beta CA)$, and $r' = \alpha r$.

After transformation, the transformed plant in Fig. 3.1 can be obtained

$$G_{PD}(s, p, K) = C_1(p)[sI - A(p)]^{-1}B(p, K). \tag{36}$$

From Fig. 3.1, the special P type transformation from the SFLC system can be described as:

$$\dot{x} = A(p)x + B(p,K)u_f,$$

$$y' = C_1(p)x, \tag{37}$$

where the control input $u_f = \sigma(\rho)$, and control error $\rho = r' - y'$.

The transfer function $H_{PD}(s,p)$ of the transformed plant in Fig. 3.1 can be described as

$$H_{PD}(s,p) = C_1(p)\left[sI - A(p)\right]^{-1} B'(p), \tag{38}$$

## 3.5 Equilibrium Point Analysis for PD Type Fuzzy Control Systems with Linear Plants

From Fig. 3.1, the equilibrium point can be analyzed

$$\dot{x} = A(p)x + B(p,K)\sigma(\rho). \tag{39}$$

Let $\dot{x} = 0$,

$$0 = A(p)x + B(p,K)\sigma(\rho). \tag{40}$$

If $A^{-1}(p)$ exists, then

$$x + A^{-1}(p)B(p,K)\sigma(\rho) = 0. \tag{41}$$

By multiplying the result of (40) by $C$ and using (35), then

$$-C(p)x - C(p)A^{-1}(p)B(p,K)\sigma(\alpha e + \beta \dot{e}) = 0 \tag{42}$$

When $t \to \infty$, $\dot{x} = 0$ and $\dot{e} = 0$ are implied.

By $\dot{e} = 0$,

$$e^e - r - C(p)A^{-1}(p)B(p,K)\sigma(\alpha e^e) = 0. \tag{43}$$

**Remark 3.5**: The error equilibrium point of the PD type fuzzy control system is

$$e^e = -e_d^e. \tag{44}$$

## 3.6 Stability Analysis for PD Type Fuzzy Control Systems with Linear Plants

The transformed P type of SFLC in Fig. 3.1 can be employed to analyze the stability of SFLC for a given $(r, p, K)$.

### 3.6.1 Frequency domain approach

Consider the error dynamic system in Fig. 3.1 for the given parameter vector $(r, p, K)$.

$$\dot{\tilde{x}} = A(p)\tilde{x} + B(p, K)\tilde{\sigma}(-C_1(p)\tilde{x}),$$ (45)

where $\tilde{x} = x - \breve{x}^e(r, p, K)$, $\tilde{\sigma}(-C_1(p)\tilde{x}) = \sigma\left[-C_1(p)\tilde{x} + \breve{e}^e(r, p, K)\right] - \sigma\left[\breve{e}^e(r, p, K)\right]$,

and $\breve{e}^e(r, p, K) = r' - C_1(p)\breve{x}^e(r, p, K)$. (46)

The error dynamic system is also of Lur'e type. The function $\tilde{\sigma}$ satisfies the following sector condition, if $\breve{e}^e(r, p, K) \in \mathbf{O}$:

$$0 \le \tilde{e}\tilde{\sigma}(\tilde{e}) \le k[\breve{e}^e(r, p, K)]\tilde{e}^2, \quad \forall \tilde{e} \in \Re,$$ (47)

where $\tilde{e} = e - \breve{e}^e(r, p, K)$, and $k > 0$.

From the Popov criterion, (39) is absolutely stable for a given $(r, p, K)$, if a real number $\tilde{v}_0 = \tilde{v}_0(r, p, K)$ satisfying

$$\text{Re}[(1 + j\omega\tilde{v}_0)G_{PD}(j\omega, p, K)] + \frac{1}{k[e^e(r, p, K)]} > 0, \quad \forall \omega \in \Re.$$ (48)

### 3.6.2 Time domain approach

Consider an arbitrary parameter vector $(r, p, K)$ in SFLC. Suppose that an equilibrium state $x^e(r, p, K)$ of the system exists. The stability can be determined by the linearization of

(37) near the error equilibrium point.

## 3.7 Stability Analysis for PD Type Fuzzy Control Systems with Uncertain Linear Plants

Since the transformed SFLC is a special P type fuzzy control system as shown in Fig. 3.1, the parametric Popov criterion [51] incorporated with Kharitonov theorem is adopted to analyze the stability of PD type fuzzy control systems with uncertainties.
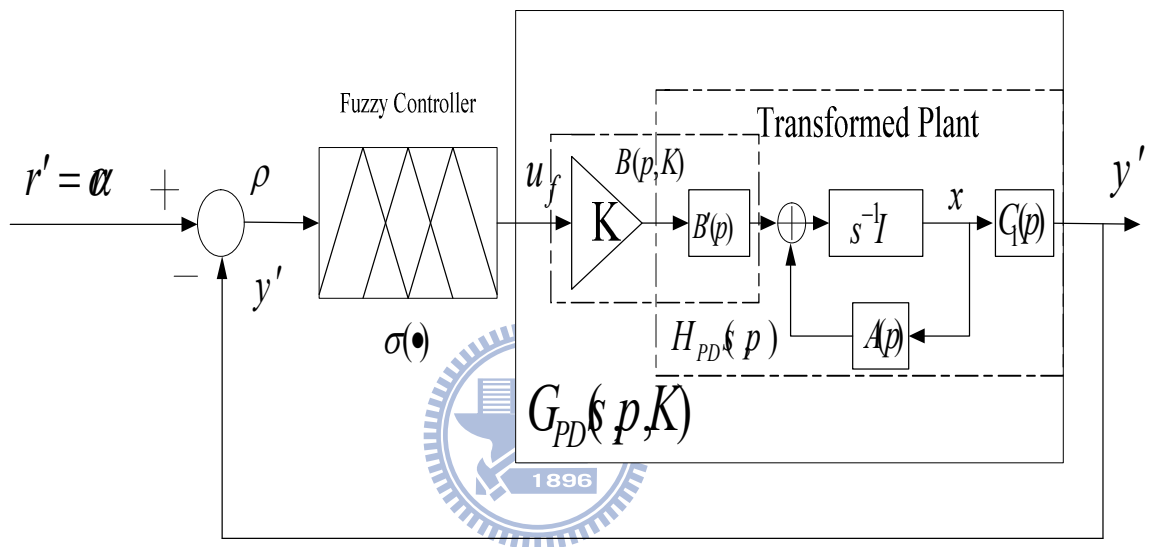
Fig. 3.1 The transformed SFLC with the special P type fuzzy control system formation.

# Chapter 4

# Fuzzy Current Control RC Circuit System Design

The temperature control is an important issue in many industrial processes or medical applications. The temperature controls systems are analogous to RC electrical circuits and are governed by the following third-order equation (49) [75]. In our design, FLC is applied to control the RC electrical circuits to reach the specified output voltage. In other words, it is similar to regulate the temperature to desired set point. This chapter specifies fuzzy current control RC circuit systems of P and PD types for verifying the theoretical analysis using PSPICE simulation.

In this chapter, the circuit structure is specified first. The fuzzy logic controller is then designed to construct the fuzzy control function, which is mapping I/O relation of the fuzzy controller. Finally, some components of the overall structure of the fuzzy logic control system are introduced.

## 4.1 The Block Diagram of the Fuzzy Current Control RC Circuit System

Figure 4.1 depicts the block diagram of a fuzzy current control RC circuit. The control objective of this system is to track a dc constant reference voltage $r$. To avoid the loading

effect from the circuit of the next stage, the voltage buffer is utilized to feed the output voltage $v_3$ back into the controller to generate the control error voltage $v_e$. The core of this system is the fuzzy controller. Both P and PD type fuzzy controllers are designed in the circuit system. The control voltage $v_{of}$ is transformed into the control current $i_{ovc}$ with a voltage controlled current circuit.

Finally, the amplified current $u(t)$ from the current amplifier is injected into circuit plant to let output voltage $v_3$ to track a reference voltage r.

## 4.2 Circuit Plant

The circuit plant in Fig. 4.2 [75] is composed of RC circuits and external current source control input $u(t)$. The output voltage is $v_3$. Consider the transfer function of circuit plant

$$H(s) = \frac{Y(s)}{U(s)} = \frac{R_3 C_1}{\Delta}, \tag{49}$$

where

$$\Delta = R_1 R_2 R_3 C_1 C_2 C_3 s^3 + C_1 (R_1 R_2 C_1 C_2 + R_2 R_3 C_2 C_3 + R_2 R_3 C_1 C_3 + R_1 R_3 C_1 C_2 + R_1 R_3 C_1 C_3) s^2$$
$$+ C_1 (R_2 C_2 + R_2 C_1 + R_3 C_1 + R_1 C_1 + R_3 C_2 + R_3 C_3) s + C_1.$$

## 4.3 Fuzzy Logic Controller Circuit

The circuit of a fuzzy logic controller is shown in Fig. 4.3. This circuit is designed to construct the control function of the fuzzy controller. Figure 4.4 illustrates the relationship between the circuit parameters and the control function [76], [77].

## 4.4 The Overall Design Circuit

Figure 4.3 shows the overall design circuit. For simplification, the voltage controlled

current circuit, current amplifier and PD type signal generator are introduced in [78].

## 4.4.1 Voltage controlled current circuit

Fig. 4.3 displays the voltage controlled current circuit. If the following equalities (50) stand, then

$$\frac{R_{vc4}}{R_{vc3}} = \frac{R_{vc2}}{R_{vc1}}, \tag{50}$$

and

$$i_{ovc} = \frac{V_{of}}{R_{vc1}}. \tag{51}$$

## 4.4.2 Current amplifier

The current amplifier is designed to normalize the signal from voltage controlled current circuit and amplifies it. The control input $u(t)$ from the current amplifier for the circuit plant is given by
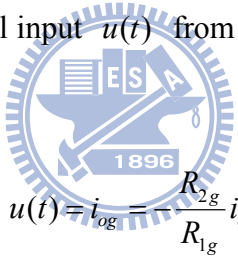
$$u(t) = i_{og} = -\frac{R_{2g}}{R_{1g}} i_{ovc}. \tag{52}$$

## 4.4.3 PD type signal generation

The derivative and proportional signals are generated by OP amplifier differentiator and OP inverting amplifier as illustrated in Fig. 4.3.

The OP amp differentiator is designed as

$$v_d = -R_{12}C_4 \frac{dv_e}{dt}. \tag{53}$$

The value $R_{12}C_4$ is chosen to meet $\beta$.

Conversely, the OP inverting amplifier is given by

$$v_p = -\frac{R_{10}}{R_8} v_e. \tag{54}$$

where $\alpha = \dfrac{R_{10}}{R_8}$ .

In Fig. 4.3, a P type fuzzy control system is chosen when two switches open at P positions. Conversely, a PD type fuzzy control system is selected when two switches close at PD.
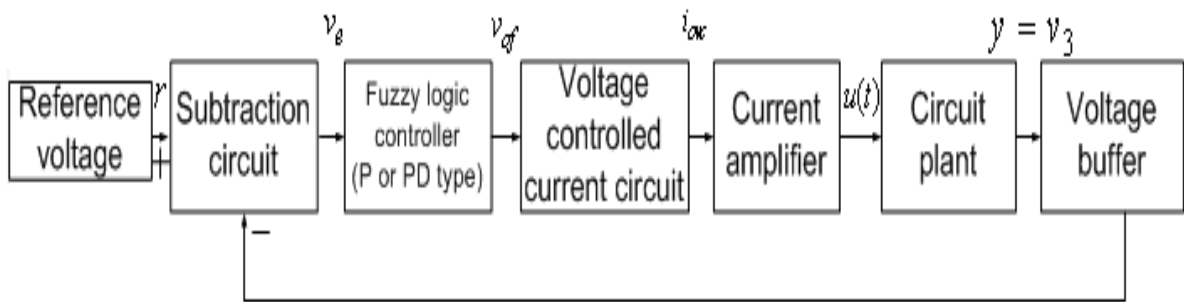
Fig. 4.1 The block diagram of a fuzzy current control RC circuit system.
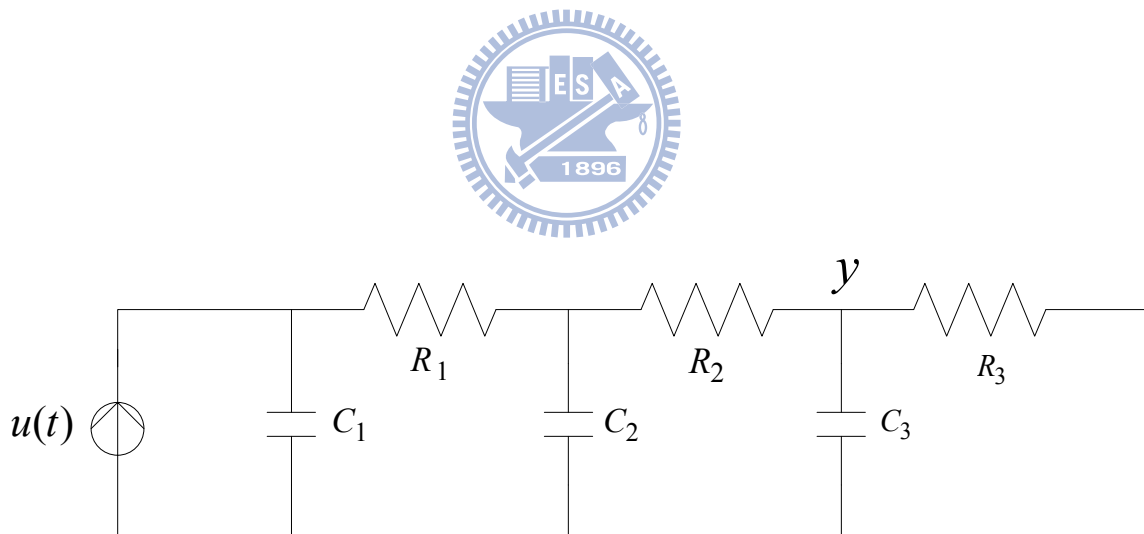


Fig. 4.2 The RC circuit plant [75].
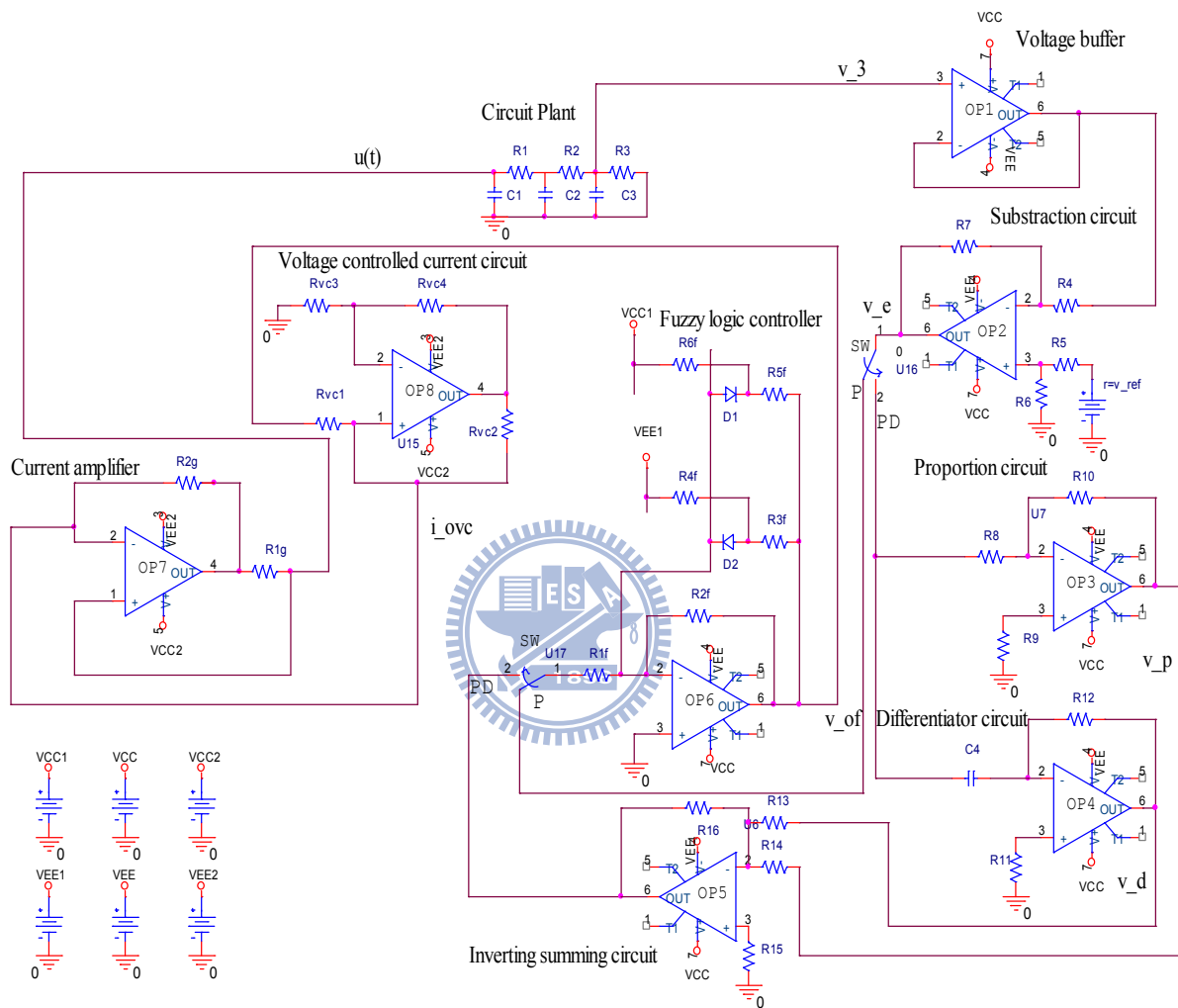
Fig. 4.3 The designed fuzzy current control RC circuit system.
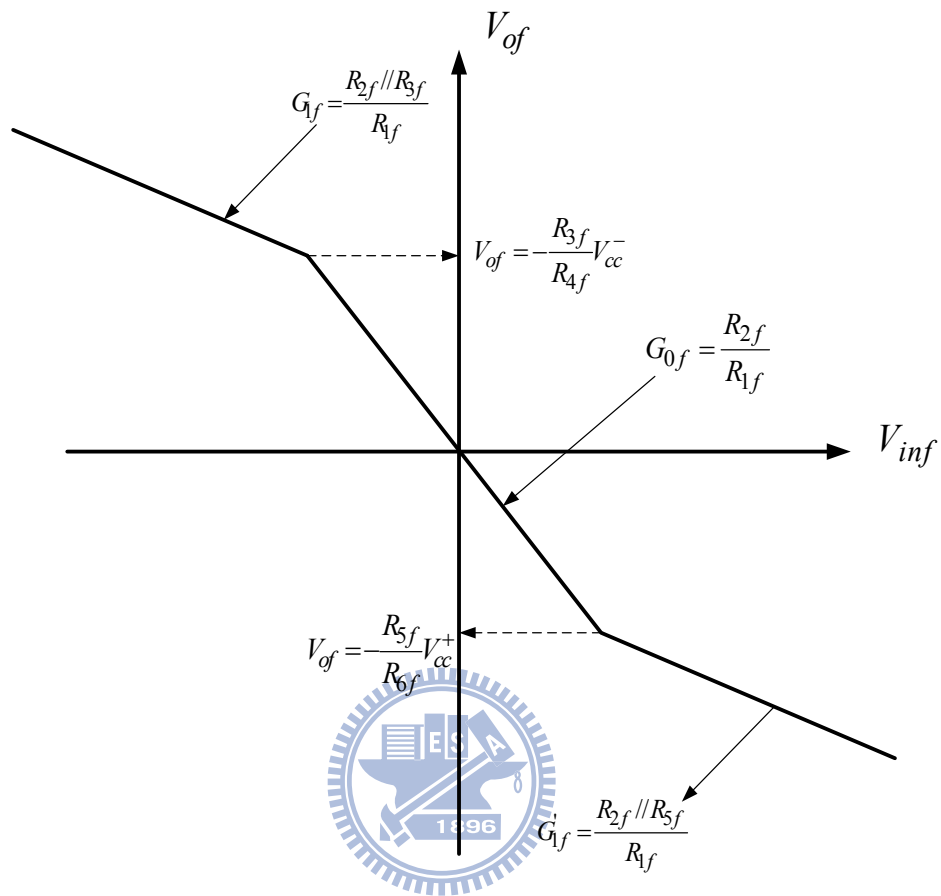
Fig. 4.4 The control function of a fuzzy controller with circuit design parameters.

# Chapter 5

# Simulation Results

In this chapter, a fuzzy control RC circuit plant as shown in Fig. 4.2 is utilized to investigate the parametric equilibrium points and stability when the circuit plant is certain or uncertain with P and PD type fuzzy logic controllers, respectively. The varying parameters include reference input $r$, an adjustable parameter $K$ and an interval circuit plant parameters $p$.

For the analysis of certain plants, the equilibrium points under the $(r, K)$ parameter space with stable notation are given. The phase plane and time waveforms are given to verify the analytical results. The design circuit with PSPICE simulation is also provided to check theoretical analysis. On the other hand, the parametric robust Popov criterion is employed to test the stability of the parameter vector $(r, p, K) \in R_{ref} \times \boldsymbol{P} \times \mathbf{K}$. From this point of view, the effect of $K$ can be combined into plant parameters by the previous introduction.

Let $R_1 = R_2 = R_3 = 1\Omega$, and $C_1 = C_2 = C_3 = 1F$ in (49), the third-order transfer with form

$$H(s) = \frac{q_0}{p_3 s^3 + p_2 s^2 + p_1 s + p_0} , \tag{55}$$

where $q_0 = 1$, $p_0 = 1$, $p_1 = 6$, $p_2 = 5$ and $p_3 = 1$.

From Fig. 2.1, combining the adjustable parameter $K$, the transfer function is given by

$$G(s, K) = \frac{q_0 K}{p_3 s^3 + p_2 s^2 + p_1 s + p_0} . \tag{56}$$

The state space representation for $G(s, K)$ can be derived

$$A(p) = \begin{bmatrix} 0 & 1 & 0 \\ 0 & 0 & 1 \\ -p_0/p_3 & -p_1/p_3 & -p_2/p_3 \end{bmatrix}, \quad B(K) = \begin{bmatrix} 0 \\ 0 \\ (q_0K)/p_3 \end{bmatrix},$$

and $C(p) = \begin{bmatrix} 1 & 0 & 0 \end{bmatrix}$. (57)

The fuzzy rules are adapted in this simulation as follows:

$Rule\ \mathbf{1:}$ If $e$ is $NBE$, then $u_f$ is $NBU$;

$Rule\ \mathbf{2:}$ If $e$ is $NSE$, then $u_f$ is $NSU$;

$Rule\ \mathbf{3:}$ If $e$ is $ZRE$, then $u_f$ is $ZRU$; (58)

$Rule\ \mathbf{4:}$ If $e$ is $PSE$, then $u_f$ is $PSU$;

$Rule\ \mathbf{5:}$ If $e$ is $PBE$, then $u_f$ is $PBU$.

Figure 5.1 illustrates the membership functions. Table 5.1 shows the fuzzy control system parameters. Fig. 2.3 shows the control function, where $k_0 = 6$, $k_1 = 4/9$ and $c_1 = 5/9$. Consider the following simulation with $K = 1 \sim 20$, $r = -1 \sim 1$ and the initial condition $x(0) = \begin{bmatrix} 0 & 0 & 0 \end{bmatrix}'$. Table 5.2 lists the circuit components in Fig. 4.3. For practical considerations, the parameters of the fuzzy controller are selected as Table 5.2 in order to approach the ideal control function depicted in Fig. 5.2.

## 5.1 P Type Example Demonstrations

## 5.1.1 Certain linear circuit plant

Under Assumptions 3.1, the equilibrium points of the fuzzy control systems in each segment can be calculated using (18).

$$e^e = \begin{cases} \text{segment } 1: \dfrac{rp_0 - q_0 K c_1}{p_0 + qKk_1}, & e^e \in [a_1, a_2], \\[3mm] \text{segment } 2: \dfrac{rp_0}{p_0 + q_0 K k_0}, & e^e \in [-a_1, a_1], \\[3mm] \text{segment } 3: \dfrac{rp_0 + q_0 K c_1}{p_0 + q_0 K k_1}, & e^e \in [-a_2, -a_1]. \end{cases} \tag{59}$$

The equilibrium point of one segment is $e^e$ when $t \to \infty$ and $e \to e^e$.

Equation (60) can be solved by linearizing (9) and using (57)

$$\hat{A}(r, p) = \begin{bmatrix} 0 & 1 & 0 \\ 0 & 0 & 1 \\ -(1 + K\zeta(r, p, K)) & -6 & -5 \end{bmatrix}. \tag{60}$$

The stability can be determined by $\hat{A}$. $\zeta \in \{k_0, k_1\}$ denotes the slope of $e^e$ in the control function, and $\zeta$ is determined by $e^e$ from (18). In (18), the reference $r$ and actuator gain $K$ affect $e^e$. Figure 5.3 depicts the analysis of the stability of equilibrium points. The reason for the formation of unstable oscillations is discussed in the following subchapter. Figures 5.4 and 5.5 display the verification of the analysis in Fig. 5.3, with respect to P1 (unstable) and P2 (stable point).

## 5.1.2 Mechanism of oscillations in the fuzzy control system

In this example, the P type fuzzy control system is a piecewise-linear system with three segments. An equilibrium $(e^e, \dot{e}^e = 0)$ exists in every segment for a specific $(r, K)$ pair. Figure 5.4 (a) shows the three error equilibriums of every piecewise segment in the phase plane of $(e, \dot{e})$ when $(r, K) = (0.2, 5)$. Three equilibrium points are represented as '*' (stable equilibrium point for segment 1), x (unstable equilibrium point for segment 2) and '$\triangledown$' (stable equilibrium point for segment 3), for segments 1–3, respectively. Assume that $(e, \dot{e})$ locates in segment 1 initially. $(e, \dot{e})$ is pulled into the equilibrium point '*' of segment 1 located in segment 3. When $(e, \dot{e})$ enters segment 2, $(e, \dot{e})$ is pushed away from

equilibrium point x of segment 2. After $(e, \dot{e})$ is pushed away from segment 2 and enters segment 3, $(e, \dot{e})$ is pulled back to the equilibrium point '$\nabla$' of segment 3. The limit cycle is formulated by pushing and pulling.

Conversly $(e, \dot{e})$ crosses the segments 1, 2, and 3, is all pulled into equilibrium points and finally $(e, \dot{e})$ achieves the global equilibrium point of segment 2. The authors discuss in detail the stability under different design parameters [79].

## 5.1.3 Alternative control function

In Fig. 5.3, the effect of reference for stability is not obvious. Therefore, the different fuzzy controllers in Table 5.3 are designed with different control functions. The results in Fig. 5.6 specify how the different controllers will influence the equilibrium points and stability besides $r$ and $K$.

## 5.1.4 Uncertain linear circuit plant

In this part, the stability of the fuzzy control system with interval plant is checked by (28) incorporated with Kharitonov theorem. In the following simulations, $r \in [-1,1]$, $K = 2$, $R_1 \sim R_3$ and $C_1 \sim C_3$ in circuit plant listed in Table 5.2 with tolerance $\pm 5\%$ and $k_R^* = 6$ in (28) are selected. The plant (56) for P type fuzzy control system can be rewritten as

$$G(s, K) = \frac{[q_0^-, q_0^+]K}{[p_3^-, p_3^+]s^3 + [p_2^-, p_2^+]s^2 + [p_1^-, p_1^+]s + [p_0^-, p_0^+]}, \tag{61}$$

where $[q_0^-, q_0^+] = [0.9, 1.1]$, $[p_3^-, p_3^+] = [0.74, 1.34]$, $[p_2^-, p_2^+] = [3.87, 6.14]$, $[p_1^-, p_1^+] = [5.14, 6.95]$, and $[p_0^-, p_0^+] = [0.95, 1.05]$.

It should be noted that the effect of interval actuator gain can be considered into $[q_0^-, q_0^+]$, so we just choose $K = 2$ in this example.

By (28) incorporated with Kharitonov theorem, the absolute stability can be tested as shown in Fig. 5.7. Because the parameter in numerator is just one, only eight Popov curves

are plotted enough to indicate the stability in such a case.

## 5.2 PD Type Example Demonstrations

In the following simulation, $\lambda = 10$ is selected in PD type fuzzy control system.

## 5.2.1 Certain linear circuit plant

In this subchapter, Fig. 3.1 demonstrates the PD type fuzzy control system. Under the Assumptions 3.1, and 3.2, the error equilibrium points of the fuzzy control systems in every segment can be obtained by (43).

$$e^e = -e_d^e = \begin{cases} \text{segment } 1: \dfrac{(rp_0 - qKc_1)\sqrt{1+\lambda^2}}{\lambda qKk_1 + p_0\sqrt{1+\lambda^2}}, & e^e \in [a_1, a_2], \\[4mm] \text{segment } 2: \dfrac{rp_0\sqrt{1+\lambda^2}}{\lambda qKk_0 + p_0\sqrt{1+\lambda^2}}, & e^e \in [-a_1, a_1], \\[4mm] \text{segment } 3: \dfrac{(rp_0 + qKc_1)\sqrt{1+\lambda^2}}{\lambda qKk_1 + p_0\sqrt{1+\lambda^2}}, & e^e \in [-a_2, -a_1]. \end{cases} \tag{62}$$

By linearizing (39) and using (57), (63) can be carried out, and Fig. 5.8 can be obtained.

$$\tilde{A}(r, p, K) = A - \chi(r, p, K)B(K)C_1$$

$$= \begin{bmatrix} 0 & 1 & 0 \\ 0 & 0 & 1 \\ -(1 + K\chi(r, p, K)) & -6 & -5 \end{bmatrix}. \tag{63}$$

where $\chi \in \{k_0, k_1\}$ denotes the slope of $e^e$ in the control function, and $\chi$ is determined by $e^e$ from (18).

In the following, Figs. 5.9 and 5.10 verify the analysis in Fig. 5.8 with respect to P1 (unstable) and P2 (stable point).

## 5.2.2 Alternative control function

The alternative controller in Table 5.3 obviously influences the equilibrium point and

stability, when the reference is varying. Figure 5.11 shows the analytical results.

## 5.2.3 Uncertain linear circuit plant

In this subchapter, Fig. 3.1 is adopted to demonstrate the parametric stability of the PD type fuzzy control system. Following transformation, the analytic new plant for PD type fuzzy systems is given by (38):

$$H_{PD}(s) = \frac{R_2 R_3^2 C_1 C_3 (s + \lambda)}{\Upsilon} \tag{64}$$

where

$$\Upsilon = \sqrt{1+\lambda^2} \left[ R_1 R_2^2 R_3^2 C_1 C_2 C_3^2 s^3 + R_2 R_3 C_1 C_3 (R_1 R_2 C_1 C_2 + R_2 R_3 C_2 C_3 + C_1 C_3 R_2 R_3 + R_1 R_3 C_1 C_2 + R_1 R_3 C_1 C_3) s^2 \right.$$
$$\left. + R_2 R_3 C_1 C_3 (R_2 C_2 + R_2 C_1 + R_3 C_1 + R_1 C_1 + R_3 C_2 + R_3 C_3) s + R_2 R_3 C_3 C_1) \right].$$

In the following simulation, $r \in [-1,1]$, $K = 1$, $R_1 \sim R_3$ and $C_1 \sim C_3$ in circuit plant, as listed in Table 5.2 with tolerance $\pm 5\%$ and $k_R^* = 6$ in (28), are specified to evaluate the stability of a PD type fuzzy control system. From (36), the analytic new plant for PD type fuzzy control system can be recast as

$$G_{PD}(s,K) = \frac{K([\tilde{q}_1^-, \tilde{q}_1^+] s + [\tilde{q}_0^-, \tilde{q}_0^+])}{[\tilde{p}_3^-, \tilde{p}_3^+] s^3 + [\tilde{p}_2^-, \tilde{p}_2^+] s^2 + [\tilde{p}_1^-, \tilde{p}_1^+] s + [\tilde{p}_0^-, \tilde{p}_0^+]}, \tag{65}$$

where $[\tilde{q}_1^-, \tilde{q}_1^+] = [0.77, 1.28]$, $[\tilde{q}_0^-, \tilde{q}_0^+] = [7.74, 12.76]$, $[\tilde{p}_3^-, \tilde{p}_3^+] = [6.02, 16.37]$, $[\tilde{p}_2^-, \tilde{p}_2^+] = [33.34, 74.24]$, $[\tilde{p}_1^-, \tilde{p}_1^+] = [44.33, 80.81]$, and $[\tilde{p}_0^-, \tilde{p}_0^+] = [8.19, 12.22]$. The total of sixteen Popov curves illustrated in Fig. 5.12 are plotted to verify that the PD type fuzzy control system is stable according to (28) incorporated with Kharitonov theorem.

Table 5.1

Parameters of the fuzzy logic controller in simulations

| $e$ (or $\rho$) | NBE | NSE | ZRE | PSE | PBE |
|---|---|---|---|---|---|
| | −1 | −0.1 | 0 | 0.1 | 1 |
| $u_f$ | NBU | NSU | ZRU | PSU | PBU |
| | −1 | −0.6 | 0 | 0.6 | 1 |
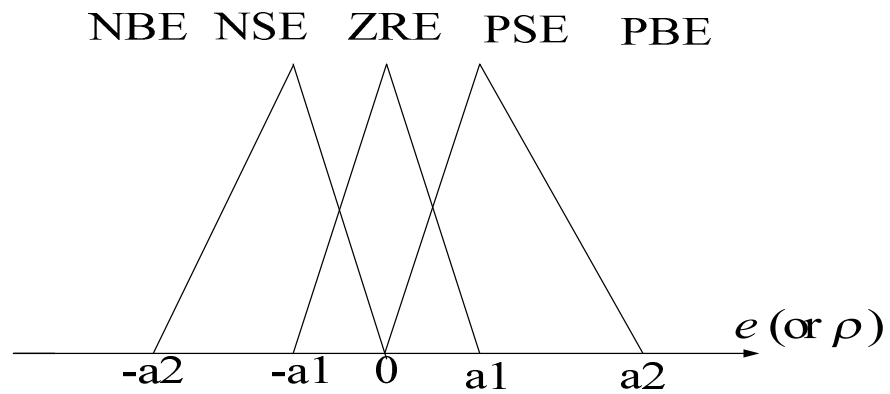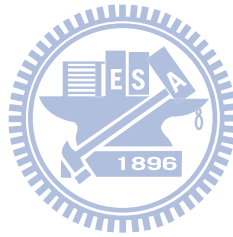


(a)
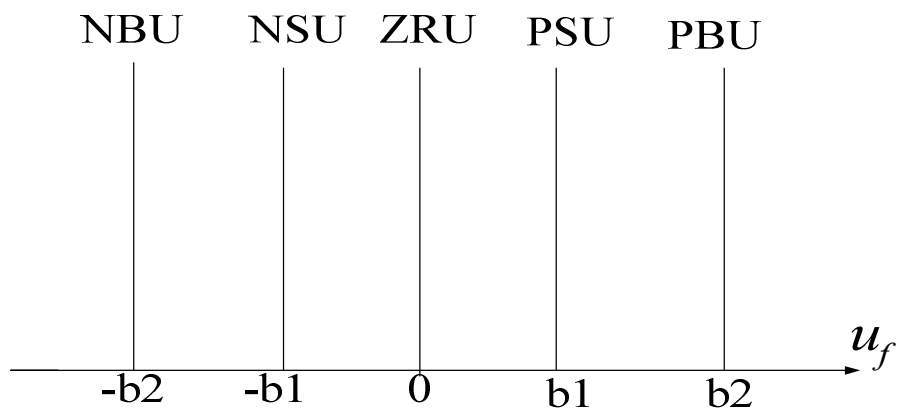
(b)

Fig. 5.1 The membership functions of the fuzzy control system.
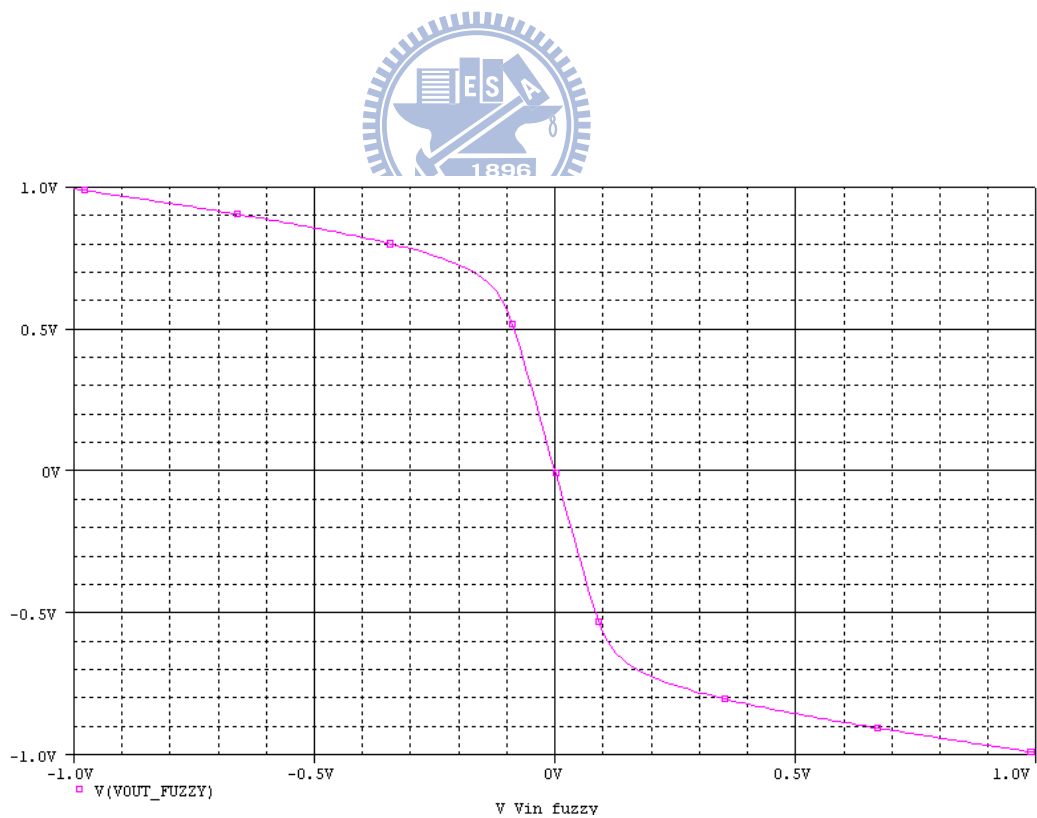


Fig. 5.2 The fuzzy control function with PSPICE simulation by Table 5.2 parameters.

Table 5.2
Parameters of the fuzzy current control RC circuit system

| Circuit Blocks | Circuit components |
|---|---|
| Circuit plant | $R_1 = R_2 = R_3 = 1\Omega$, and $C_1 = C_2 = C_3 = 1F$. |
| Subtraction circuit | $R_4 = R_5 = R_6 = R_7 = 25k\Omega$, and $v_{ref} = 0.2\,\text{V}$. |
| Proportion circuit | $R_8 = 1k\Omega$, $R_9 = 10k\Omega$, and $R_{10} = 1k\Omega$. |
| Differentiator circuit | $R_{11} = 10k\Omega$, $R_{12} = 0.9k\Omega$, and $C_4 = 100\ \mu F$. |
| Inverting summing circuit | $R_{13} = R_{14} = R_{15} = R_{16} = 10k\Omega$. |
| Fuzzy controller | $R_{1f} = 2k\Omega$, $R_{2f} = 12k\Omega$, $R_{3f} = R_{5f} = 400\Omega$, $R_{4f} = R_{6f} = 13k\Omega$, and D1 and D2: 1N4148. |
| Voltage controlled current circuit | $R_{vc1} = R_{vc2} = R_{vc3} = R_{vc4} = 10k\Omega$. |
| Current amplifier | $R_{1g}$ and $R_{2g}$ are chosen to meet the selected *K* with voltage controlled current circuit design.<br>P type design:<br>    Stable: $R_{1g} = 1\Omega$ and $R_{2g} = 50k\Omega$.<br>    Unstable $R_{1g} = 1\Omega$ and $R_{2g} = 40k\Omega$.<br>PD type design:<br>    Stable: $R_{1g} = 1\Omega$ and $R_{2g} = 90k\Omega$.<br>    Unstable: $R_{1g} = 1\Omega$ and $R_{2g} = 100k\Omega$. |
| Power source | VCC=15V, VEE=-15V, VCC1=8V, VEE1=-8V, VCC2=30V, and VEE2=-30V. |
| Operational amplifiers in design | P type design:<br>    OP amps 1~6 with OPA602, and OP amps 7~8 with LM675 (Power op amp).<br>PD type design:<br>    OP amps 1~6 with OPA602, OP amps 7 with OPA501 (Power op amp) and OP amps 8 with LM675. |
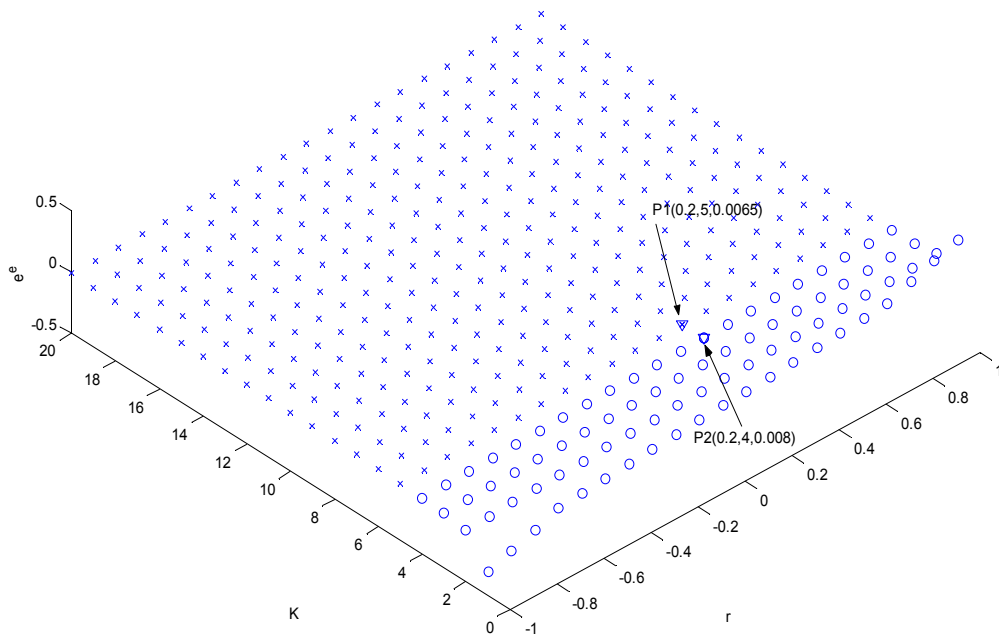
Fig. 5.3 The equilibrium stability of the P type fuzzy control system by Table 5.1 for $(r, K)$, where o indicates a stable equilibrium, and × denotes an unstable equilibrium.



(a)

(b)
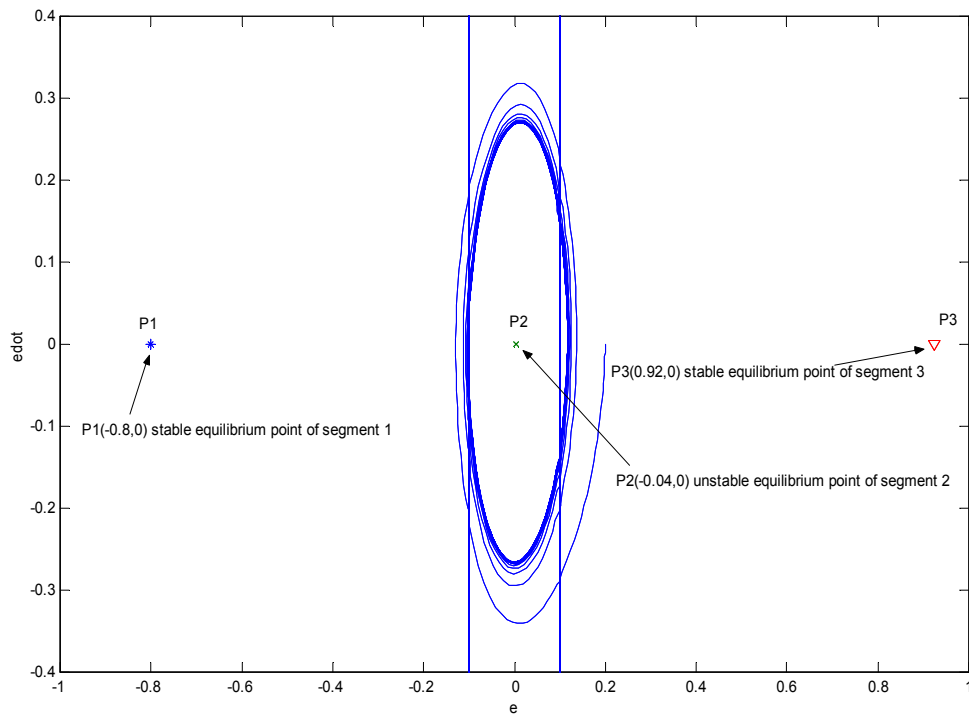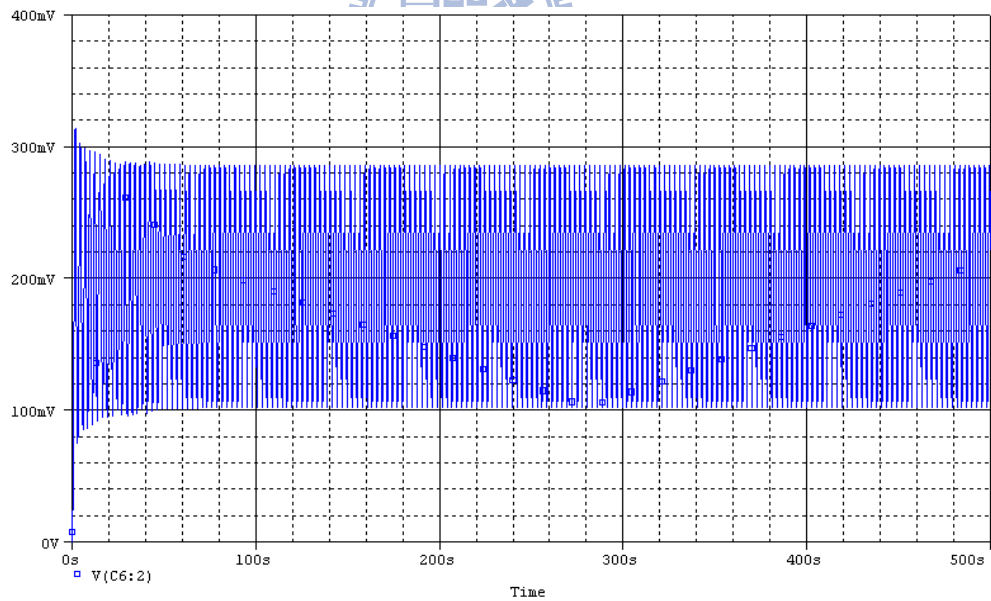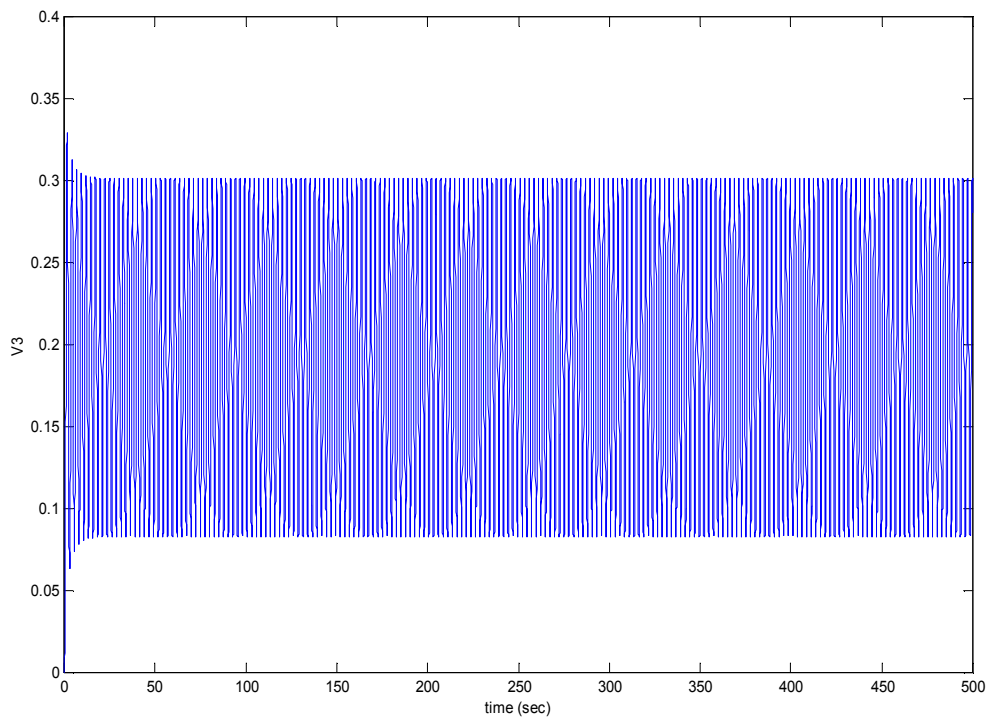


(c)

Fig. 5.4 (a) The phase plane of $(e, \dot{e})$ when $(r, K) = (0.2, 5)$; (b) The time waveform when $(r, K) = (0.2, 5)$; (c) PSPICE waveform when $(r, K) = (0.2, 5)$.

P1

P1(-0.73,0) unstable equilibrium point of segment 1

P2

P3

P3(0.87,0) stable equilibrium point of segment 3

P2(0.005,0) stable equilibrium point of segment 2

(a)



(b)

(c)
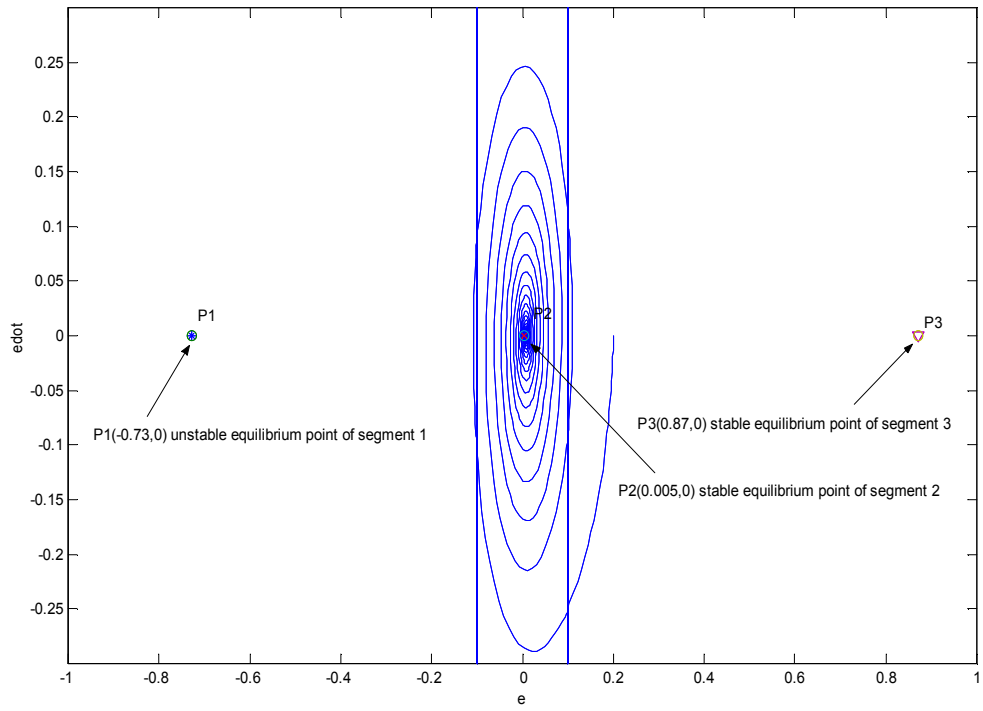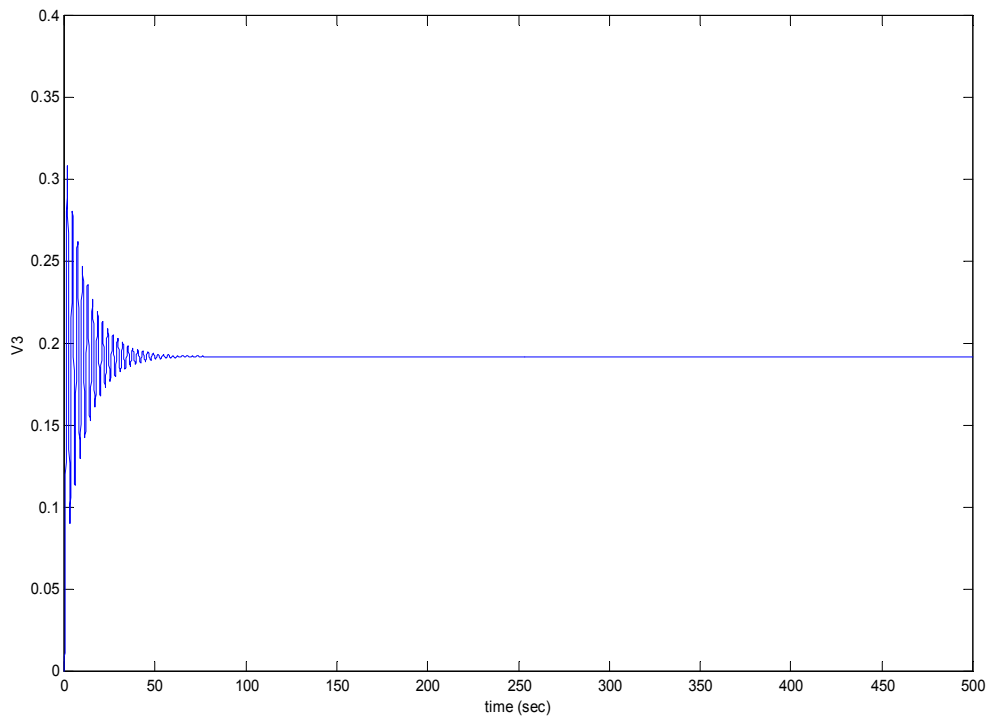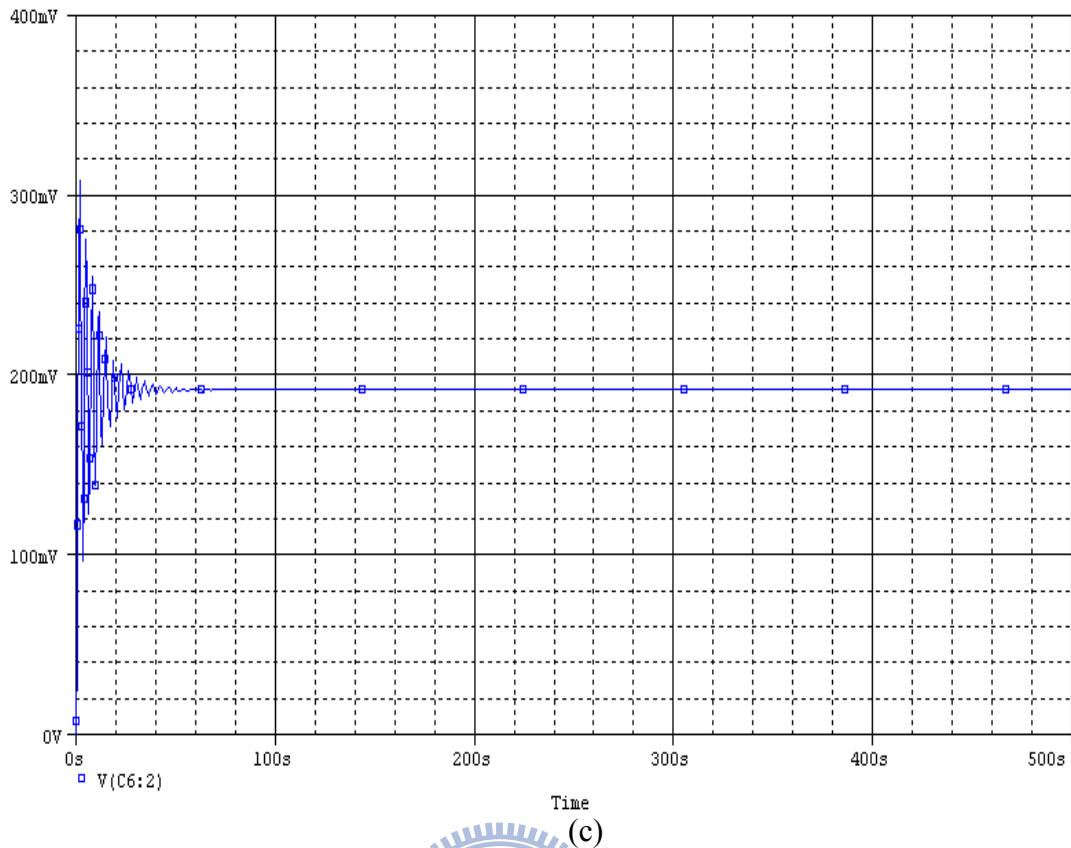
Fig. 5.5 (a) The phase plane of $(e, \dot{e})$ when $(r, K) = (0.2, 4)$; (b) The time waveform when $(r, K) = (0.2, 4)$; (c) PSPICE waveform when $(r, K) = (0.2, 4)$.
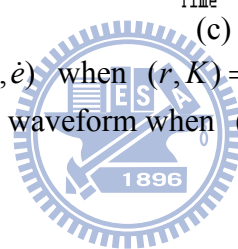
Table 5.3
Alternative parameters of the fuzzy logic controller

| $e$ (or $\rho$) | NBE | NSE | ZRE | PSE | PBE |
|---|---|---|---|---|---|
| | $-1$ | $-0.01$ | 0 | 0.01 | 1 |
| $u_f$ | NBU | NSU | ZRU | PSU | PBU |
| | $-1$ | $-0.1$ | 0 | 0.1 | 1 |

50
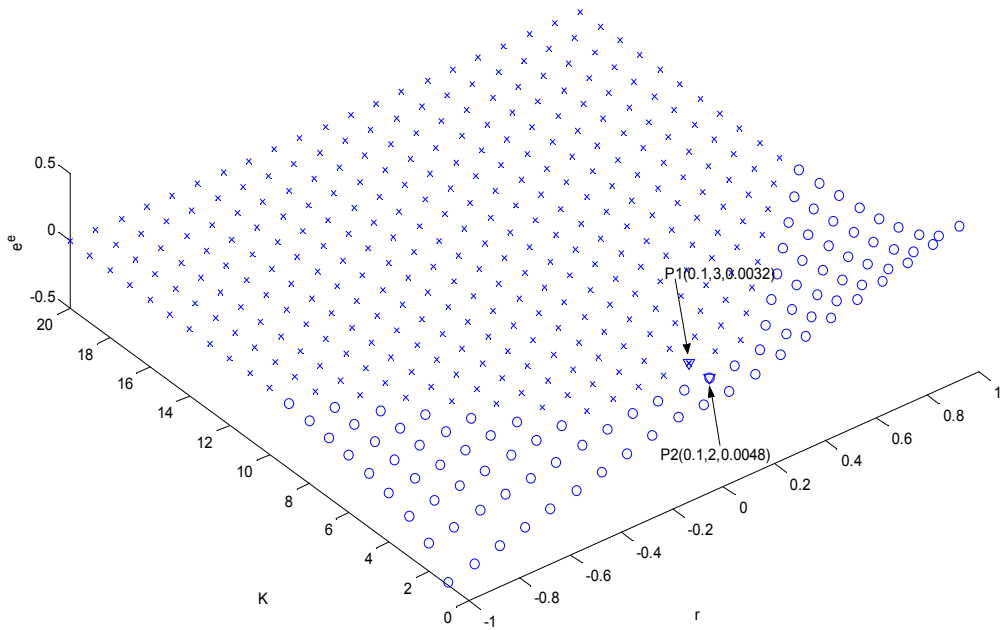
Fig. 5.6 The equilibrium with the stability of the alternative fuzzy controller by Table 5.3 for $(r, K)$, where o denotes a stable equilibrium, and × indicates an unstable equilibrium.
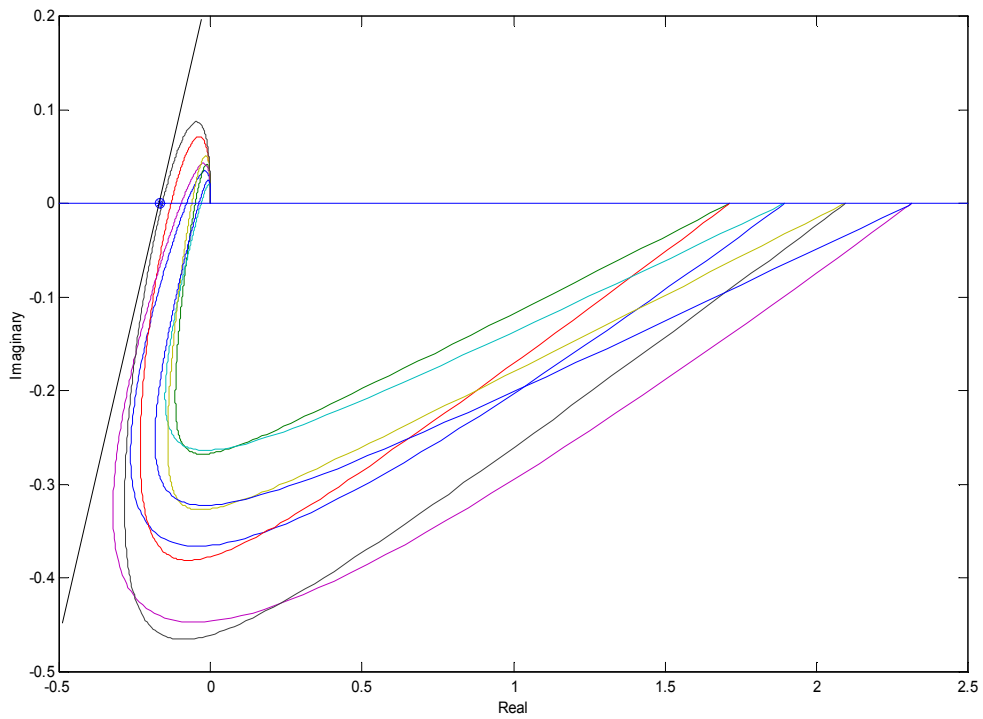


Fig. 5.7 The Popov plots for the P type fuzzy control system with uncertain circuit plant.
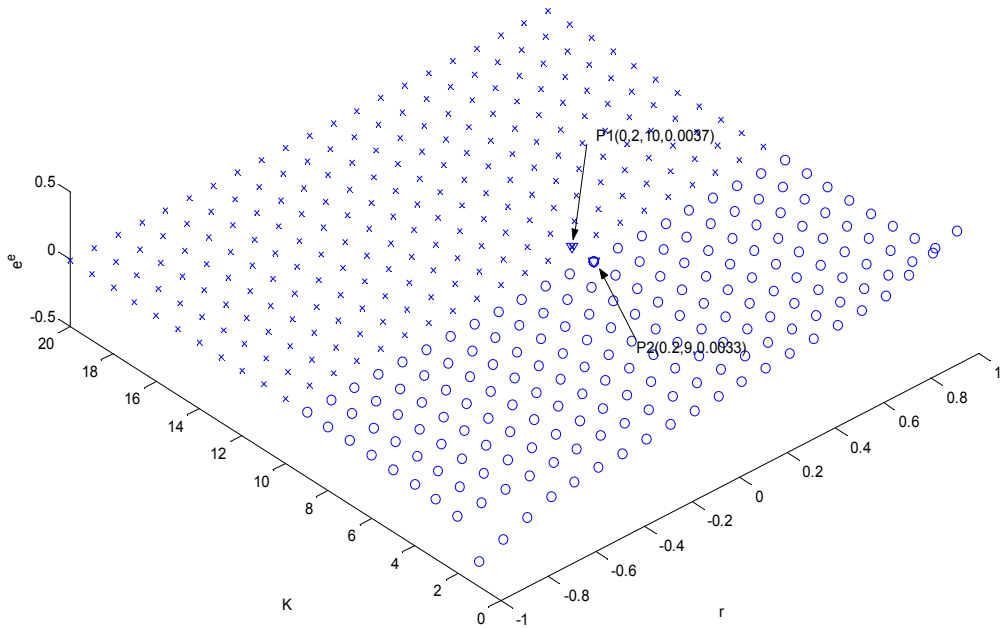
Fig. 5.8 The equilibriums with the stability of the PD type fuzzy control system by Table 5.1
for $(r, K)$, where o indicates a stable equilibrium, and × denotes an unstable
equilibrium.
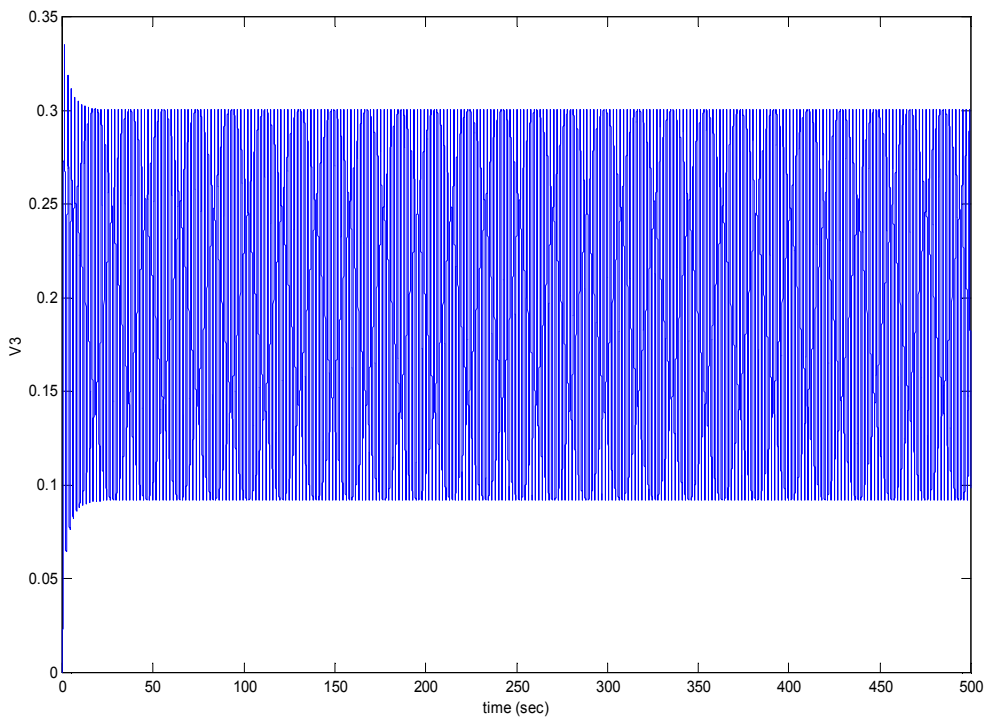


(a)
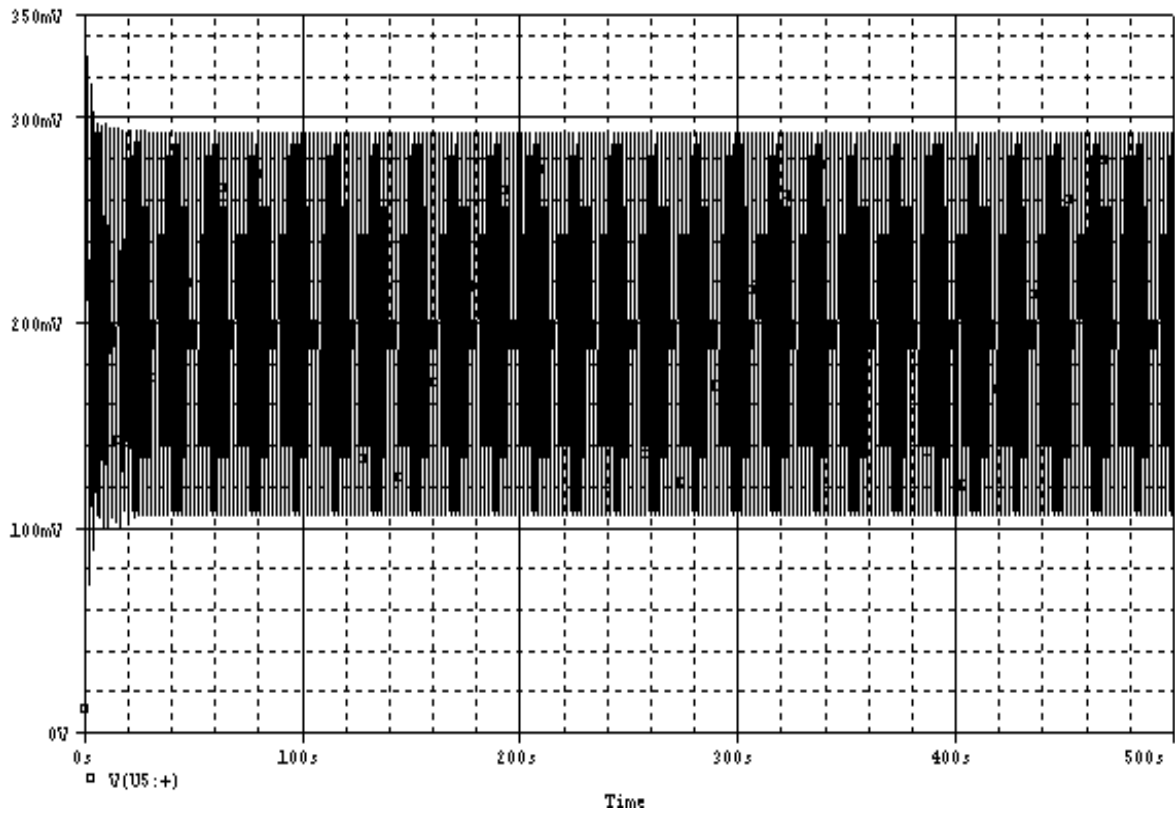
Fig. 5.9 (a) The time waveform when $(r, K) = (0.2, 10)$ (b) PSPICE waveform when $(r, K) = (0.2, 10)$.



(a)

(b)
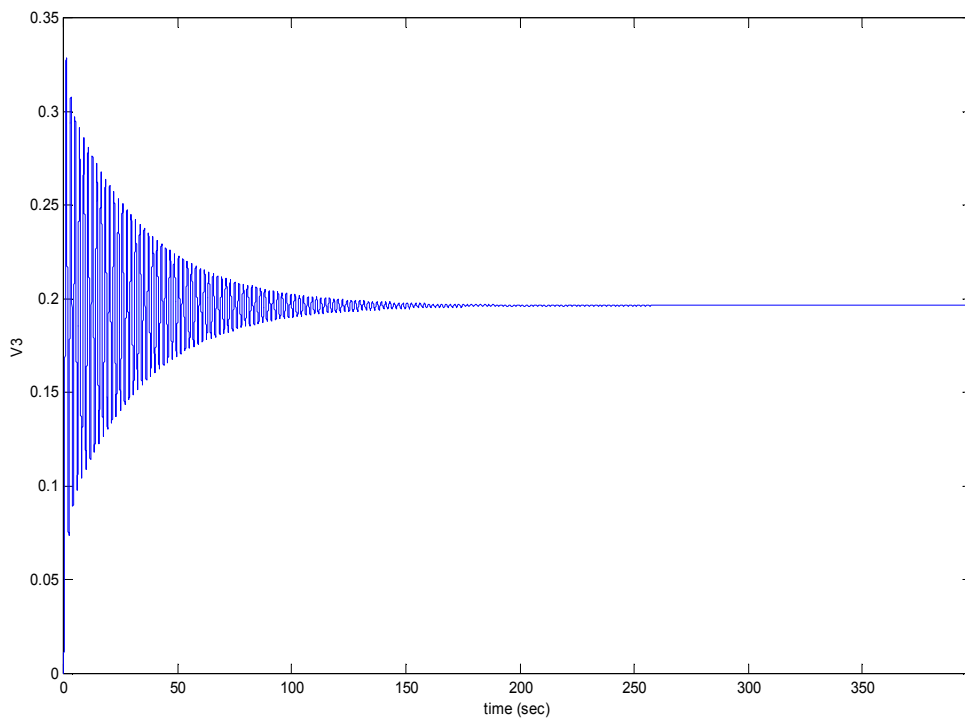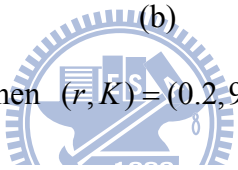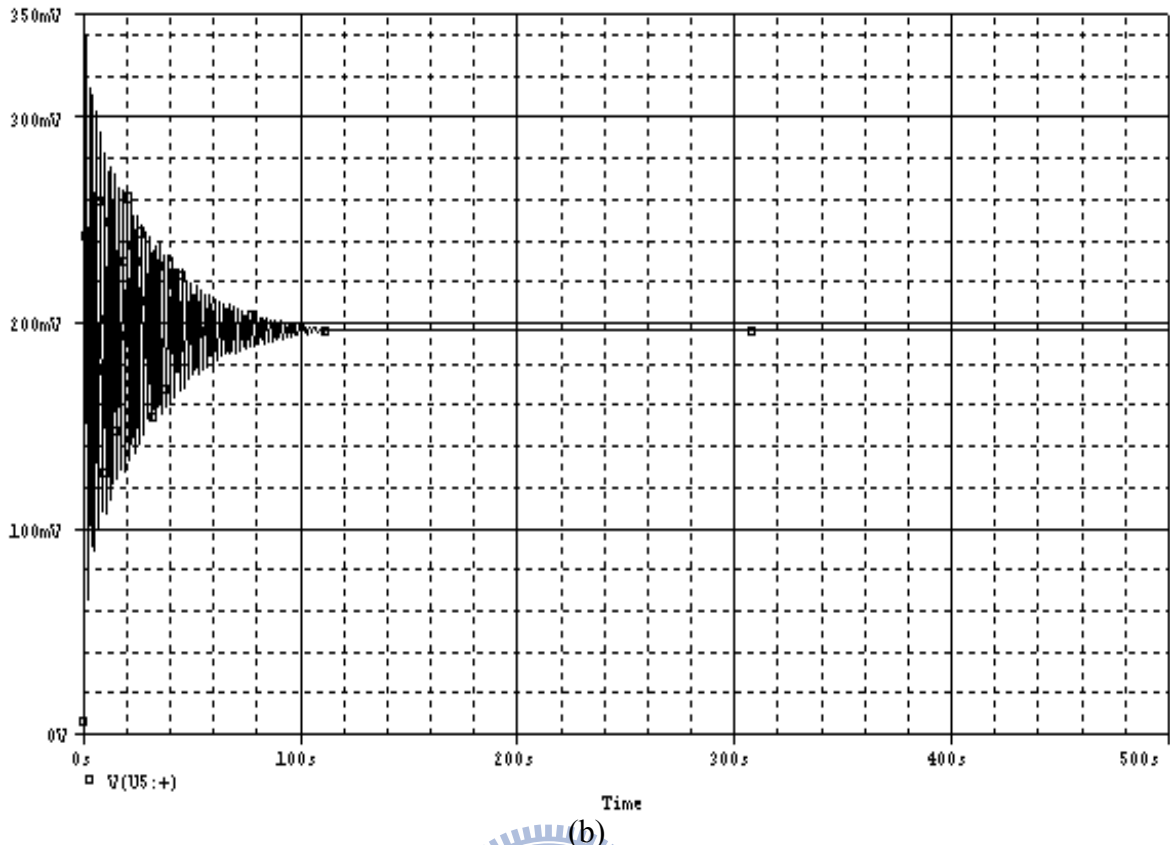
Fig. 5.10 (a)The time waveform when $(r,K)=(0.2,9)$; (b) PSPICE waveform when $(r,K)=(0.2,9)$.
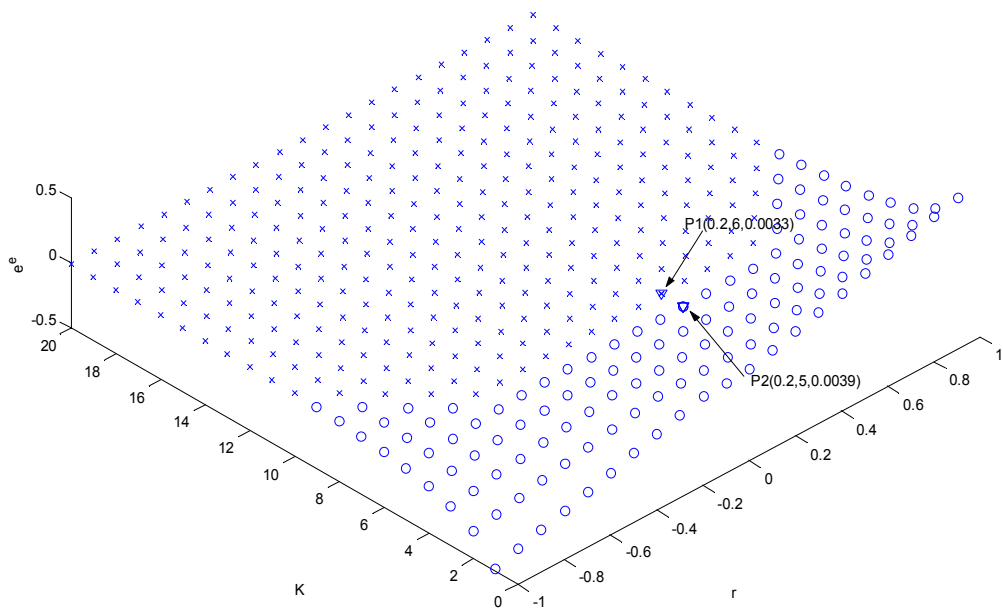


Fig. 5.11 Equilibrium with the stability of the PD type fuzzy control systems in Table 5.3 for $(r,K)$, where o denotes a stable equilibrium, and $\times$ indicates an unstable equilibrium.
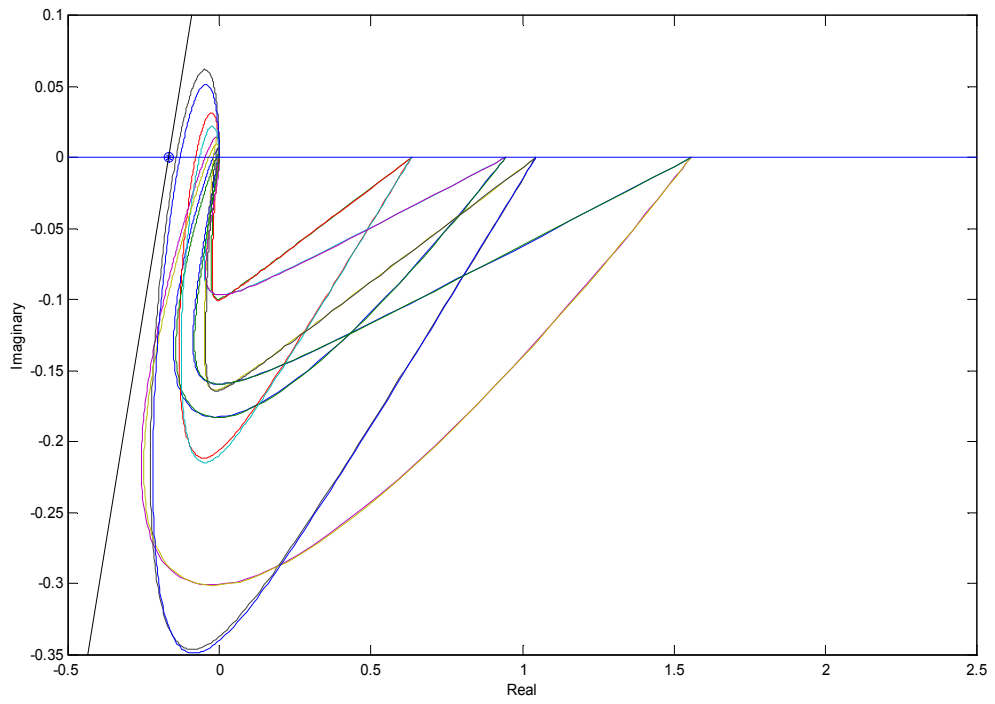
Fig. 5.12 The Popov plots for the PD type fuzzy control systems with the uncertain circuit plant.

# Chapter 6

# Comparisons with Other Approaches

In this chapter, we will illustrate the stability of uncertain fuzzy control systems which are considered as stable by compared methods will crash under the effect of the reference inputs. On the other hand, the stability can be tested with our applied method and guaranteed under the effect of the reference inputs. It should be noted that the applied parametric robust Popov criterion will be comprised with the robust Lur'e test [54], the robust circle criterion [54], and the robust Popov criterion [54]. In the following, we consider the P type fuzzy control system in Fig. 2.1 to demonstrate the comparisons. Because the PD type fuzzy control systems can be transformed into P type ones, we will not exhibit the PD cases additionally.

## 6.1 Robust Lur'e Test

Consider the stable interval plant [54] in Fig. 2.1:

$$G(s,K) = \frac{K([q_1^-, q_1^+]s + [q_0^-, q_0^+])}{s^4 + [p_3^-, p_3^+]s^3 + [p_2^-, p_2^+]s^2 + [p_1^-, p_1^+]s + [p_0^-, p_0^+]}, \tag{66}$$

where $[q_0^-, q_0^+] = [3,\ 3.3]$ , $[q_1^-, q_1^+] = [3,\ 3.2]$ , $[p_0^-, p_0^+] = [3,\ 4]$ , $[p_1^-, p_1^+] = [2,\ 3]$ , $[p_2^-, p_2^+] = [24,\ 25]$, and $[p_3^-, p_3^+] = [1,\ 1.2]$. For the following stability test demonstrations, the default values in the parameters are chosen: $q_0 = 3.2$ , $q_1 = 3.1$ , $p_0 = 3.5$ , $p_1 = 2.5$ , $p_2 = 24.5$, and $p_3 = 1.1$. The parameters in membership functions of the fuzzy logic controller can be chosen such Table 6.1. The actuator gain $K = 1$. The total sixteen robust Lur'e curves

will be illustrated to test the stability of the fuzzy control systems.

From Fig. 6.1, $-1/k_L \approx -1.60$ is obtained. Therefore, the control surface $\sigma(\bullet)$ of fuzzy logic controller should belong to sector bound $[0, k_L \approx 0.63]$ as shown in Fig. 6.2, and the fuzzy logic control system is robust absolutely stable.

If the parameters in membership functions of the fuzzy logic controller are chosen such Table 6.1, then the fuzzy control system is stable. The stable and unstable test cases respect to the robust Lur'e test are with a pulse reference input for testing $r = 0$ and a constant input $r = 1300$, respectively. The stable and unstable output waveforms are shown in Figs. 6.3 and 6.4, respectively. In this case, we can find that if the reference input is increased, the stability of the fuzzy control system which is considered as stable will crash.

## 6.2 Robust Circle Criterion
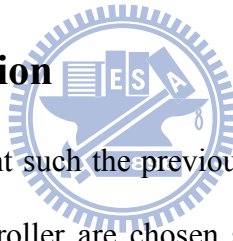
Suppose the stable interval plant such the previous test and the parameters in membership functions of the fuzzy logic controller are chosen such Table 6.2. The total sixteen robust circle curves will be illustrated to test the stability too. From Fig. 6.5, the circle center located on $(-1, 0)$, and radian is 0.6138. The circle cut the negative real axis at two points $-1/k_{C1} \approx -1.61$ and $-1/k_{C2} \approx -0.39$. Therefore, the control surface $\sigma(\bullet)$ of the fuzzy logic controller should belong to the sector bound $[k_{C1} \approx 0.62, k_{C2} \approx 2.59]$ as shown in Fig. 6.6, and the fuzzy logic control system is robust absolutely stable.

If the parameters in membership functions of the fuzzy logic controller are chosen such Table 6.2, then the fuzzy control system is stable. The stable and unstable test cases respect to the robust circle criterion are with a pulse reference input and a constant input $r = 2000$, respectively. The stable and unstable output waveforms are shown in Figs. 6.7 and 6.8, respectively. In this case, we can find that if the reference input is increased the stability of

the fuzzy control system which is considered as stable will crash, too.

## 6.3 Robust Popov Criterion

Let's consider the stable interval plant such the previous test and the parameters in membership functions of the fuzzy logic controller are chosen such Table 6.1. The total sixteen robust Popov plots will be plotted to test the stability too. From Fig. 6.9, the Popov line cut the negative real axis at $-1/k_p \approx -0.62$ point. Therefore, the control surface $\sigma(\bullet)$ of the fuzzy logic controller should belong to the sector bound $[0, k_p \approx 1.61]$ as shown in Fig. 6.10, and the fuzzy logic control system is robust absolutely stable.

If the parameters in membership functions of the fuzzy logic controller are chosen such Table 6.1, then the fuzzy control system is stable. The stable and unstable test cases respect to the robust Popov criterion are with a pulse reference input and a constant input $r = 1300$, respectively. The stable and unstable output waveforms are identical the results as shown in Figs. 6.3 and 6.4, respectively. In this case, we also find that if the reference input is increased, the stability of the fuzzy control system which is considered as stable will crash.

## 6.4 Parametric Robust Popov Criterion

Let's suppose the stable interval plant such the previous test and the parameters in membership functions of the fuzzy logic controller are chosen such Table 6.1. If we consider the reference inputs $r = [-990, \ 990]$, (28) incorporated with Kharitonov theorem is applied to test the absolute stability of this fuzzy logic control system. By (28), $-1/k_R^* = -1/0.1 = -10$ is chosen. The total sixteen parametric robust Popov curve will be illustrated to test the robust stability with the reference input in Fig. 6.11. From Fig. 6.11, the fuzzy control system is robust absolutely stable. Figures 6.12~6.14 show the output

waveforms for different reference inputs: a bounded pulse reference, $r = 990$ and $r = -990$, respectively. These time waveforms show that the applied parametric robust Popov criterion is valid. In other words, by the applied parametric robust Popov criterion, the stability of the fuzzy control systems with uncertain interval plants can be guaranteed under the reference inputs in certain interval range.

## 6.5 A Brief Summary on Comparisons

The following Table 6.3 is made for the comparisons with other robust criterions. It shows the applied parametric robust Popov criterion can deal with fuzzy logic control systems with the uncertain interval plants and the constant reference inputs cases. The other three approaches: the robust Lur'e test, the robust circle criterion and the robust Popov criterion just can deal with the uncertain interval plants and the zero reference inputs cases. In previous demonstrated examples, the stability will crash due to reference input shift. On the other hand, the stability of the fuzzy control systems with uncertain interval plants can be assured under the interval range reference inputs by the applied parametric robust Popov criterion.
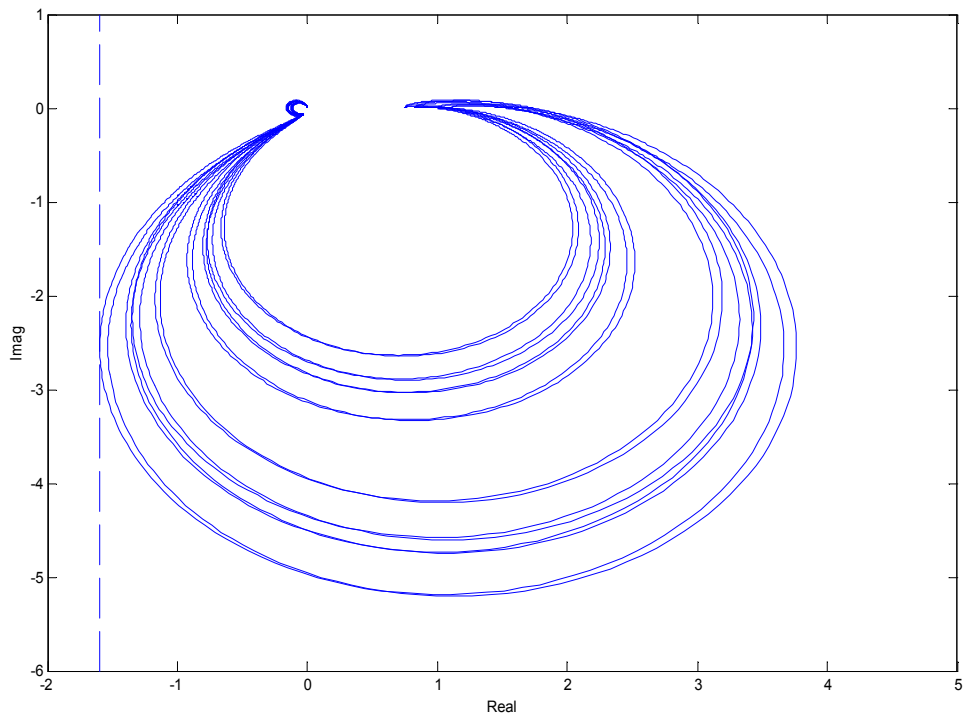
Fig. 6.1 The robust Lur'e test.
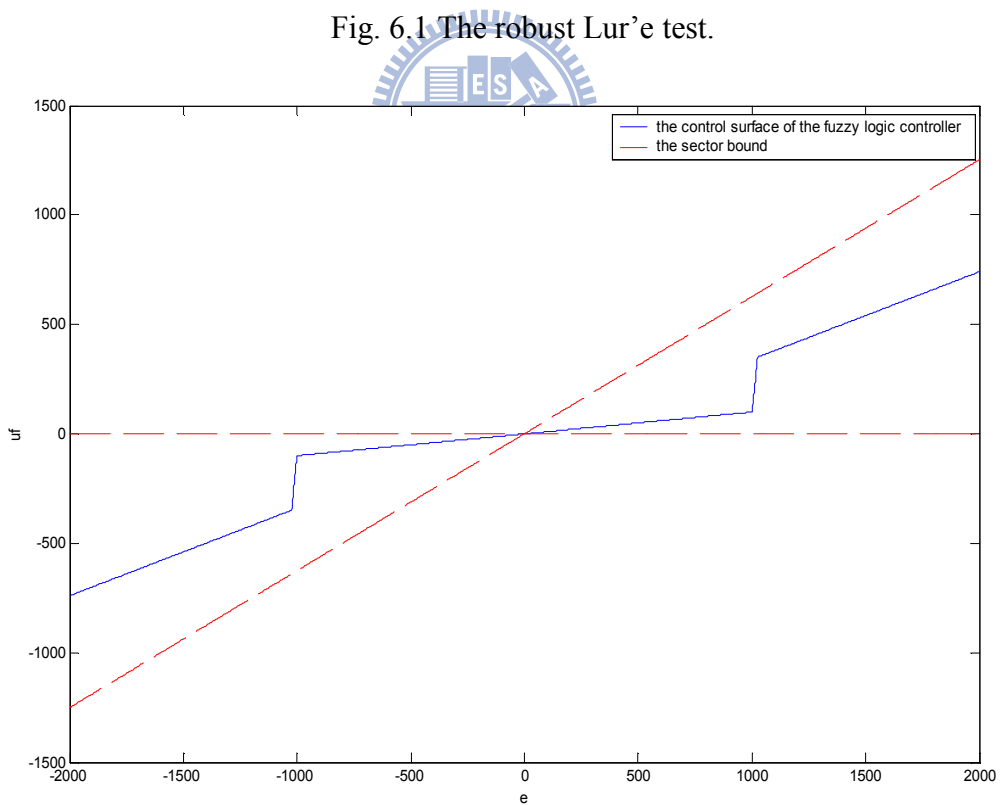


Fig. 6.2 The sector bound from the robust Lur'e test and the control surface of the fuzzy logic controller.

Table 6.1

Parameters of fuzzy logic controller for the robust Lur'e test

|   | nbe | nme | nse | zre | pse | pme | pbe |
|---|-----|-----|-----|-----|-----|-----|-----|
| $e$ | -2000 | -1025 | -1000 | 0 | 1000 | 1025 | 2000 |
|   | nbu | nmu | nsu | zru | psu | pmu | pbu |
| $u_f$ | -740 | -350 | 100 | 0 | 100 | 350 | 740 |
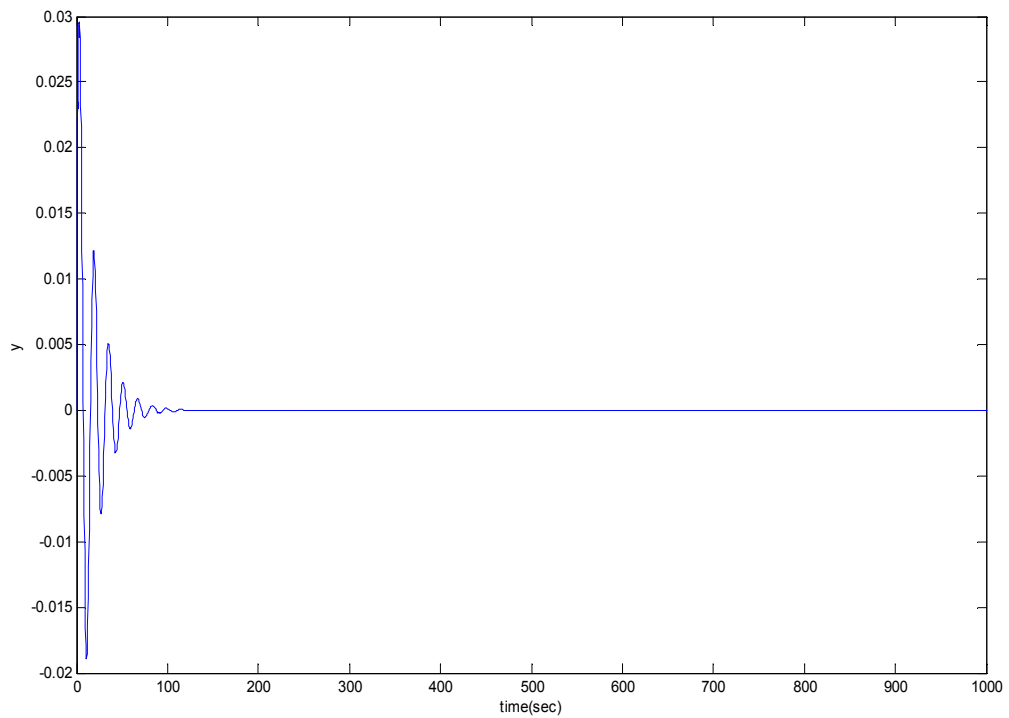


Fig. 6.3 The time waveform of the stable test case respect to the robust Lur'e test.
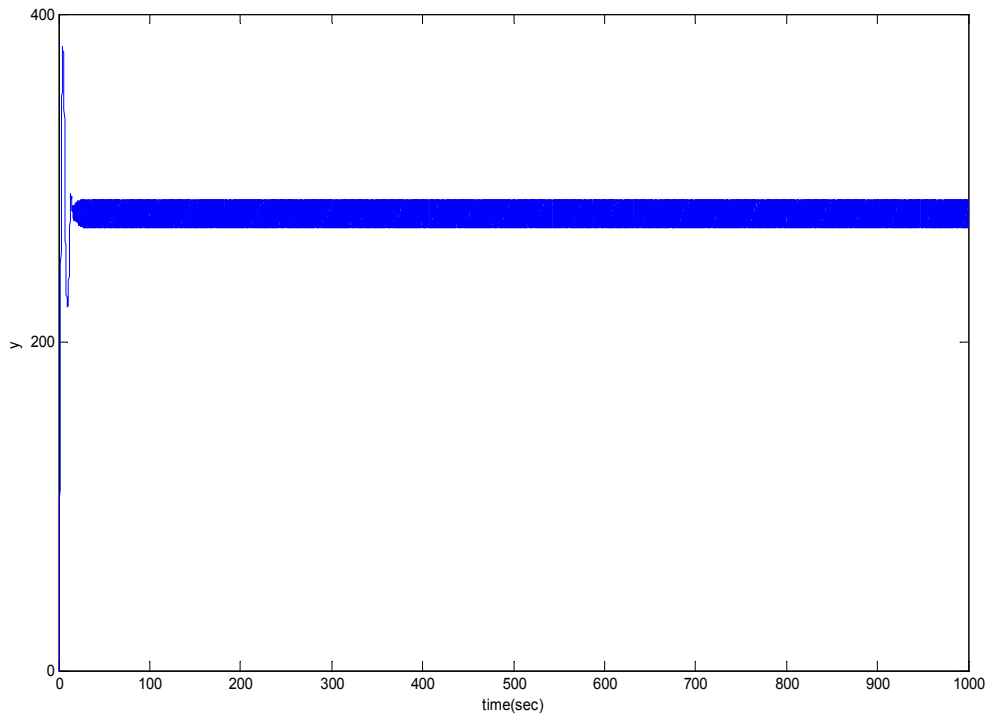
Fig. 6.4 The time waveform of the unstable test case respect to the robust Lur'e test.
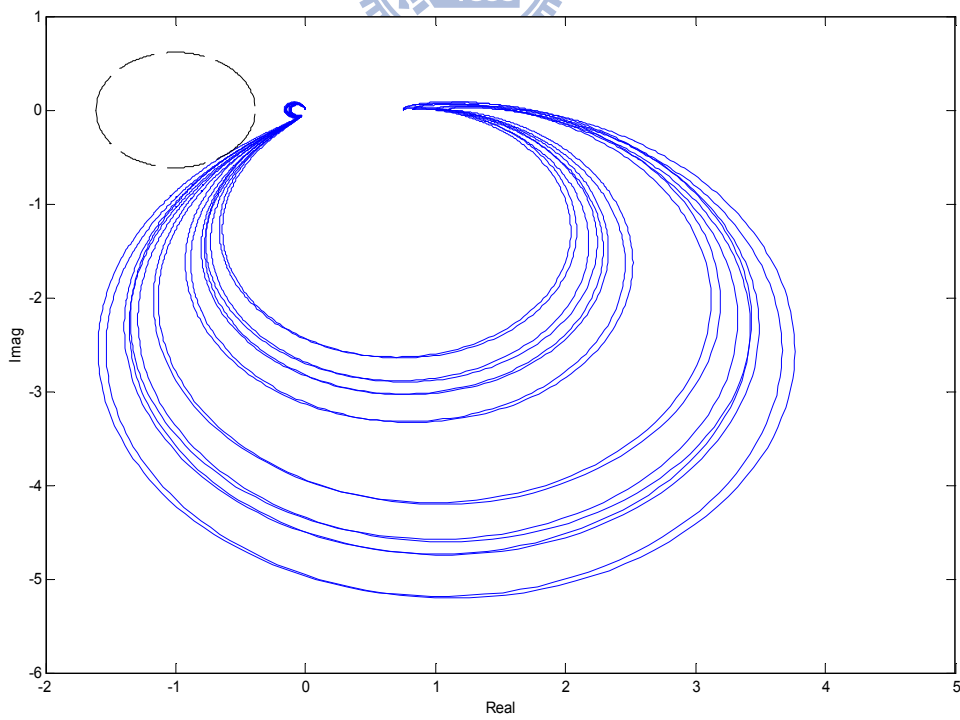


Fig. 6.5 Robust circle criterion.
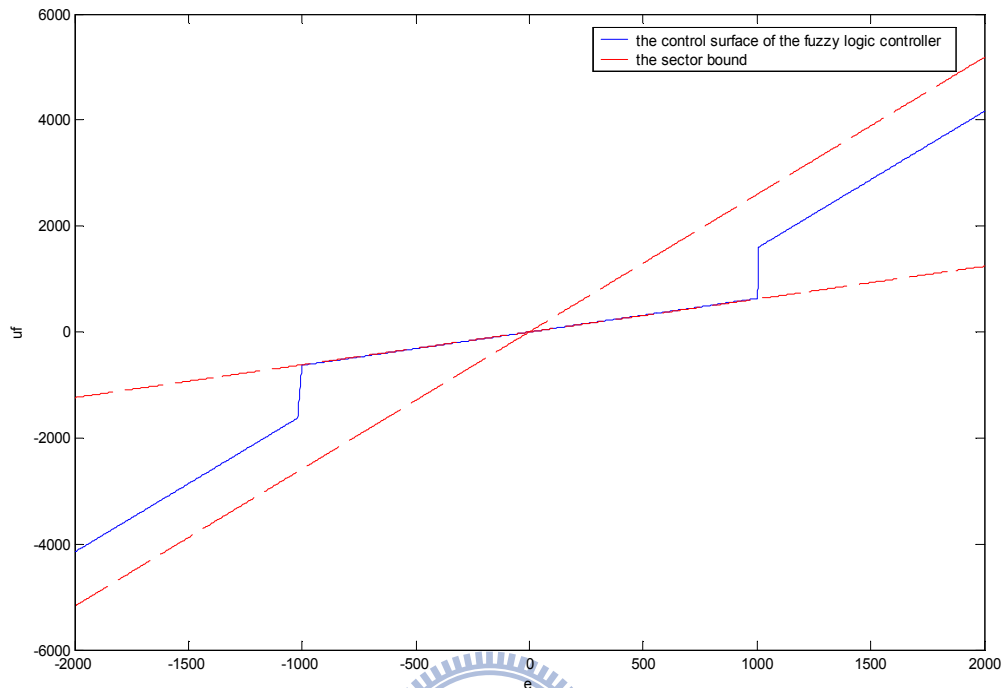
Fig. 6.6 The sector bound from the robust circle criterion and control surface of fuzzy logic controller.
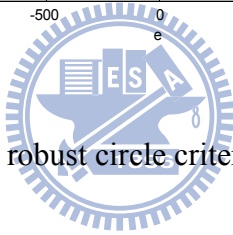
Table 6.2

Parameters of fuzzy logic controller for the robust circle criterion

| $e$ | nbe | nme | nse | zre | pse | pme | pbe |
|---|---|---|---|---|---|---|---|
| | -2000 | -1020 | -1000 | 0 | 1000 | 1020 | 2000 |
| $u_f$ | nbu | Nmu | nsu | zru | psu | pmu | pbu |
| | -4158.4 | -1630 | -630 | 0 | 630 | 1630 | 4158.4 |
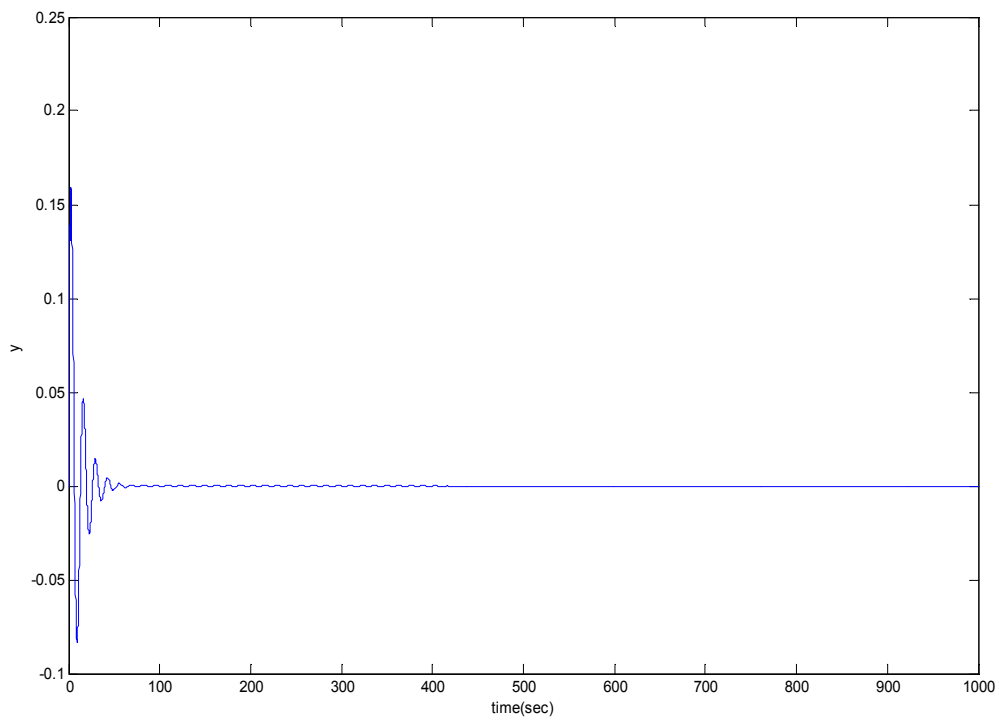
Fig. 6.7 The time waveform of the stable test case respect to the robust circle criterion.
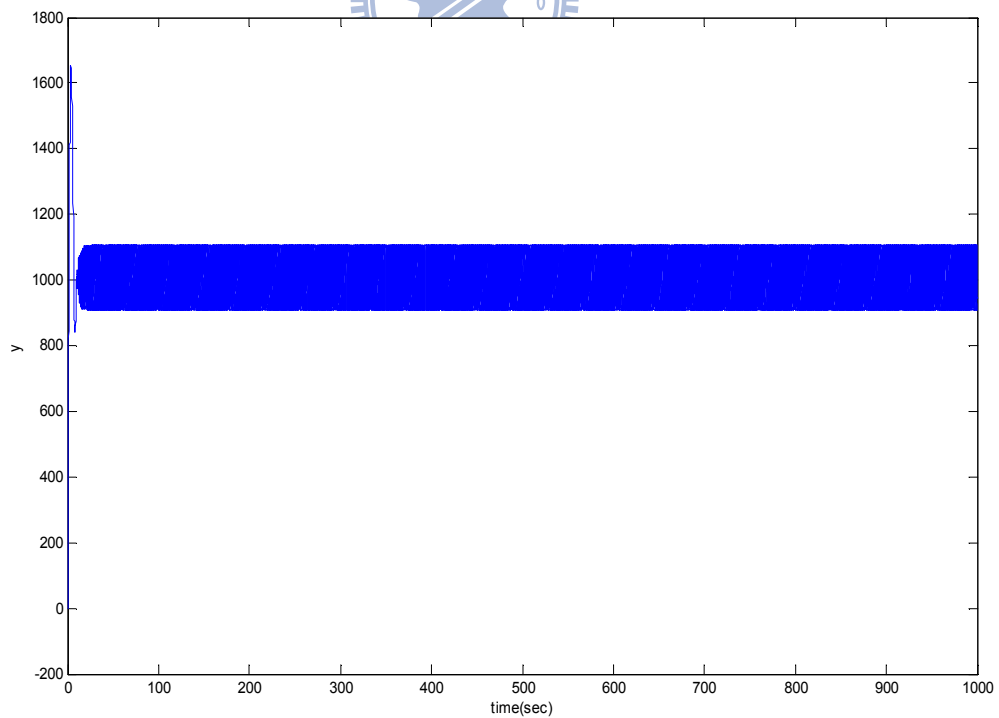


Fig. 6.8 The time waveform of the unstable test case respect to the robust circle criterion.
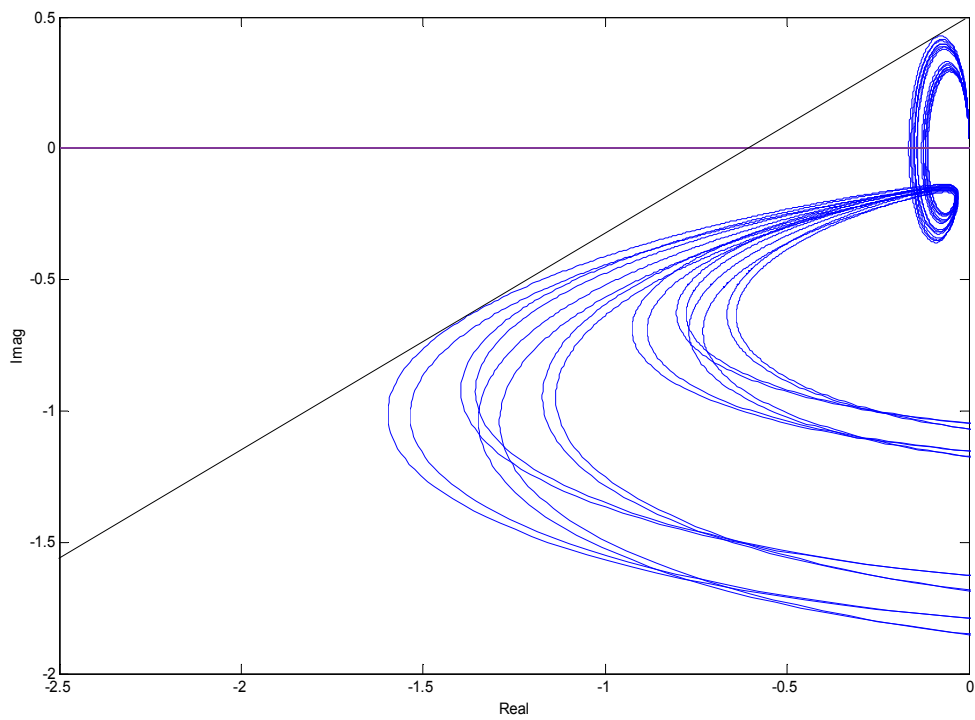
Fig. 6.9 Robust Popov criterion.
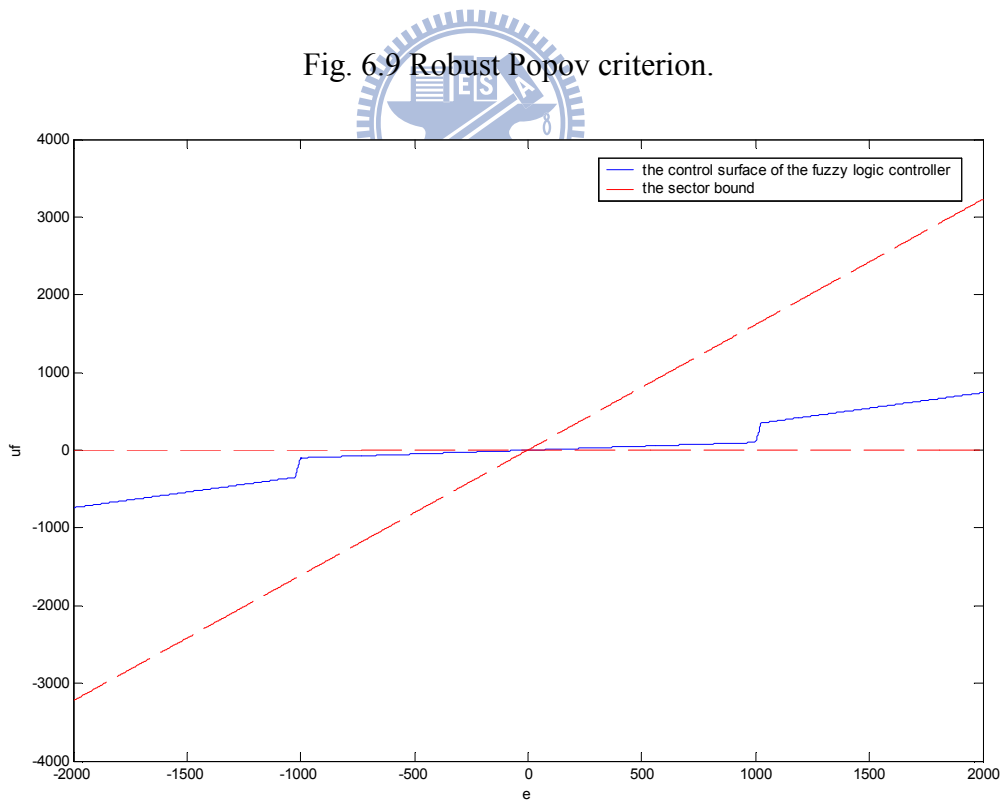


Fig. 6.10 The sector bound from the robust Popov criterion and control surface of fuzzy logic controller.
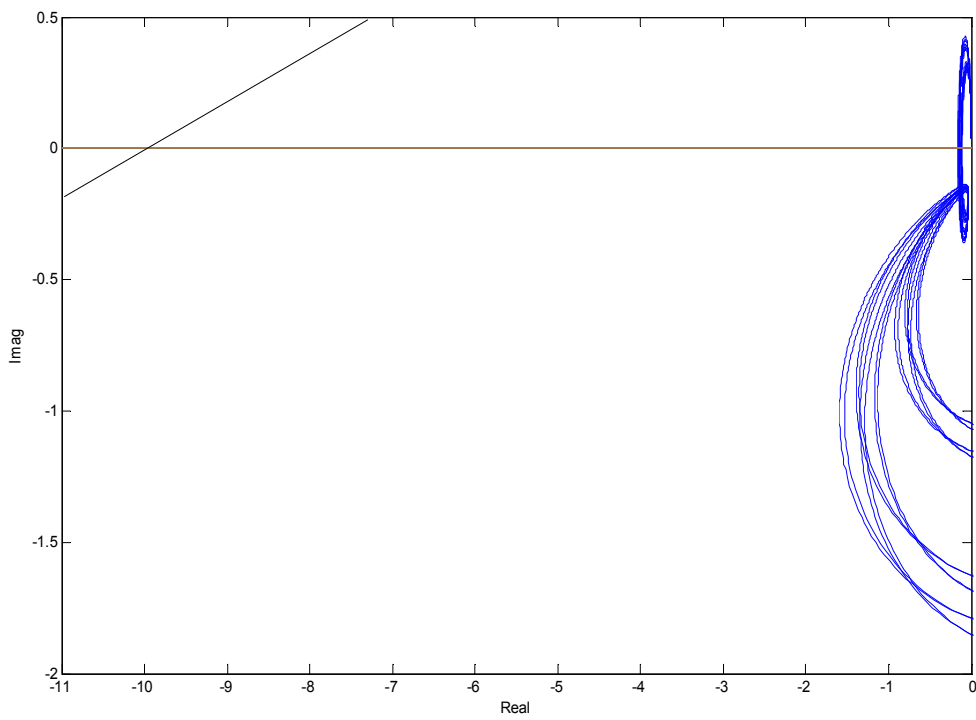
Fig. 6.11 Parametric robust Popov criterion for the reference inputs.
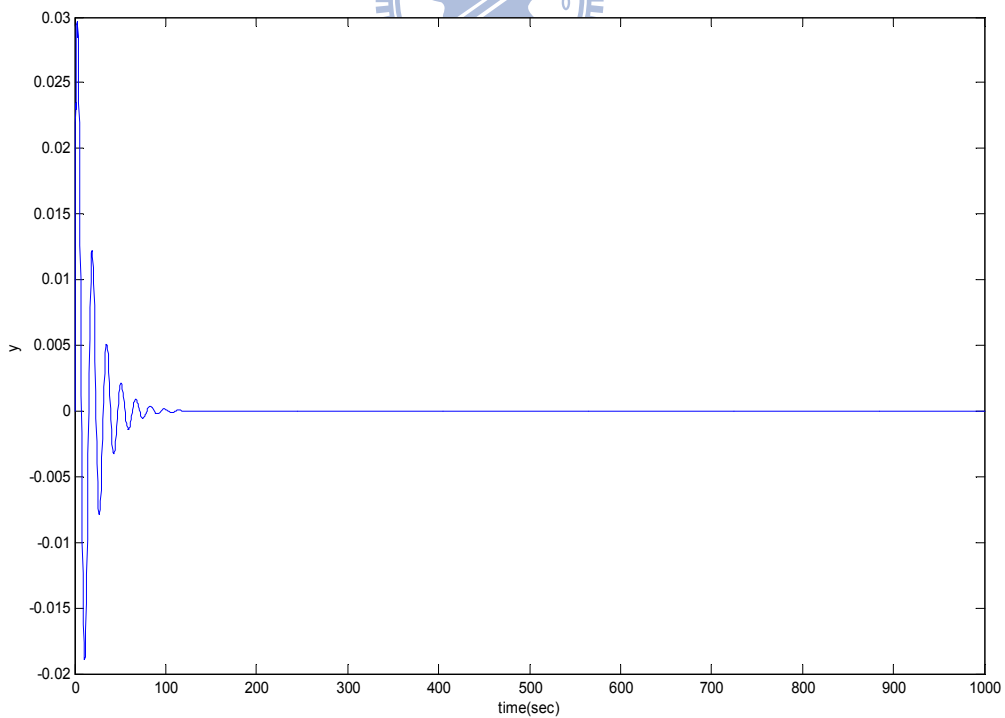


Fig 6.12 The time waveform of the stable test case respect to the parametric robust Popov
criterion with a bounded pulse reference.
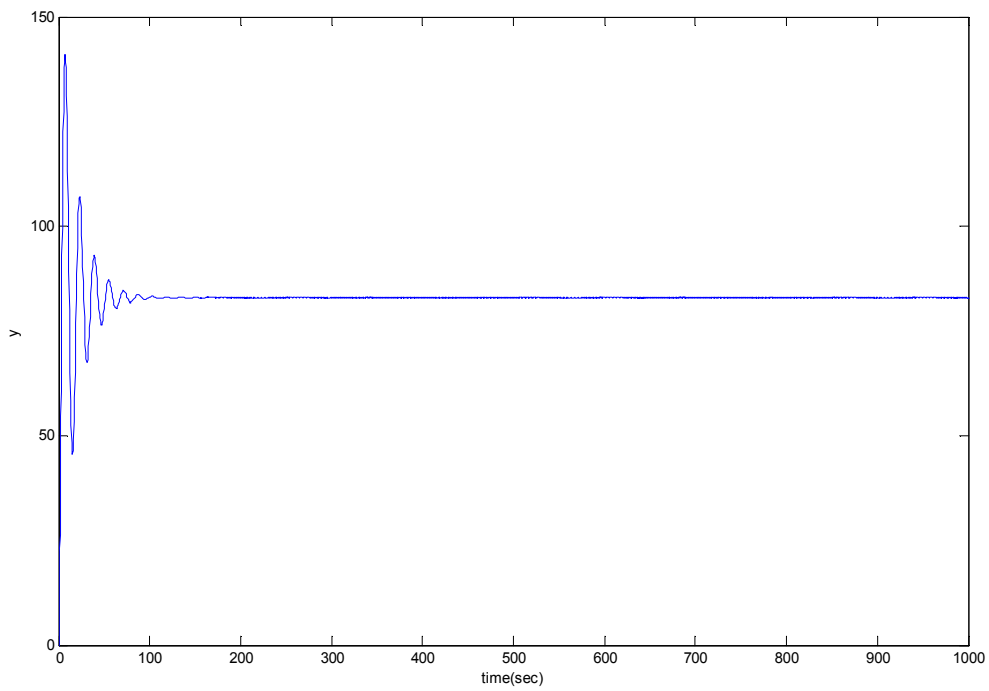
Fig. 6.13 The time waveform of the stable test case respect to the parametric robust Popov
criterion with the reference input $r = 990$.
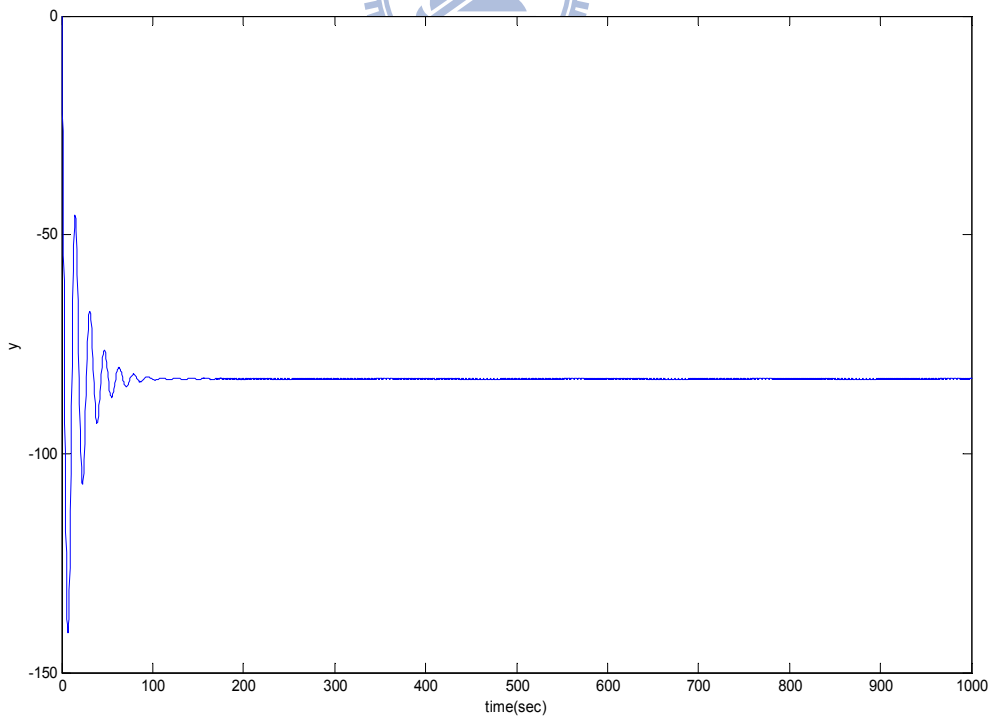


Fig. 6.14 The time waveform of the stable test case respect to the parametric robust Popov
criterion with the reference input $r = -990$.

Table 6.3

The validity of the different robust stability tests

|  | *Parametric robust Popov criterion* | *Robust Lur'e test* | *Robust circle criterion* | *Robust Popov criterion* |
|---|---|---|---|---|
| *Zero reference inputs* | *Yes* | *Yes* | *Yes* | *Yes* |
| *Constant reference inputs* | *Yes* | *No* | *No* | *No* |
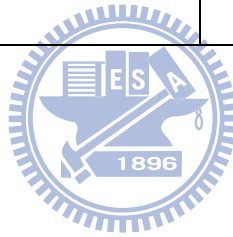
# Chapter 7

# Application: Observer-Based Synchronization for a Class of Unknown Chaotic Systems with Adaptive Fuzzy-Neural Network

## 7.1 Overview

The study of the synchronization for a class of unknown chaotic systems with adaptive fuzzy-neural network is based on the concepts of AFNO, Brunowsky canonical form and Lur'e systems. The proposed synchronization system contains chaos master with the canonical form and the soft-computing slave with AFNO. The AFNO is composed of a FNN and a linear observer. In this design, the AFNO in the slave should synchronize with all states in the master by a scale transmitted signal only. The FNN in the AFNO is utilized to model the nonlinear function in the master end adaptively. The linear observer estimates the all states at the slave end with three inputs including a transmitted state, output of the FNN, and robust compensation input for counteracting the effect of the external disturbance. When all states in the master end are estimated at slave end, the synchronization is achieved. Simulation results confirm that the AFNO is applied to chaos synchronization is valid.

## 7.2 Overall Structure of Adaptive Synchronization with Fuzzy-Neural Observer Design

### 7.2.1 Introduction of Overall Structure

Assume that the master and slave are all Lur'e type. Figure 7.1 illustrates the overall structure of adaptive synchronization with AFNO, which is synthesized with an FNN and a linear observer. In this design, only a scalar transmitted signal $x_{M1}$ is sent to the slave from the master. By the observed state $\hat{\underline{x}}_S$, $f_S(\hat{\underline{x}}_S)$ can be computed to approximate $f_M(\underline{x}_M)$ with FNN. The adaptive laws update the weights in FNN when the error exists between $x_{M1}$ and $\hat{x}_{s1}$. The linear observer inputs are $u_S = f_S(\hat{\underline{x}}_S)$, the transmission signal $x_{M1}$, and the robust input $u_r$. The synchronization is achieved when $\underline{x}_M = \hat{\underline{x}}_S$.

### 7.2.2 Dynamics of the Master and Slave Ends

Master End:

$$\dot{\underline{x}}_M = A_M \underline{x}_M + B_M (f_M(\underline{x}_M) + d)$$
$$y_{M1} = x_{M1} = C_M \underline{x}_M,$$

(67)

Slave End: [73,80]

$$\dot{\hat{\underline{x}}}_S = A_S \hat{\underline{x}}_S + B_S (\hat{f}_S(\hat{\underline{x}}_S) - u_r) + K_o e_o$$
$$y_{S1} = \hat{x}_{S1} = C_S \hat{\underline{x}}_S,$$

(68)

where

$$A_M = A_S = \begin{bmatrix} 0 & 1 & 0 & \cdots & 0 \\ 0 & 0 & 1 & \cdots & 0 \\ \cdots & \cdots & \cdots & \cdots & \cdots \\ 0 & 0 & 0 & \cdots & 1 \\ 0 & 0 & 0 & \cdots & 0 \end{bmatrix} ; B_M = B_S = \begin{bmatrix} 0 \\ 0 \\ \vdots \\ 0 \\ 1 \end{bmatrix} ;$$

$C_M = C_S = \begin{bmatrix} 1 & 0 & \cdots & 0 & 0 \end{bmatrix}$; $d$ denotes an bounded external disturbance;

$$\underline{x}_M = [x_M \quad \dot{x}_M \quad \cdots \quad x_M^{(n-1)}]^T = [x_{M1} \quad x_{M2} \quad \cdots \quad x_{Mn}]^T \in \Re^n ,$$

and $\underline{x}_S = [x_S \quad \dot{x}_S \quad \cdots \quad x_S^{(n-1)}]^T = [x_{S1} \quad x_{S2} \quad \cdots \quad x_{Sn}]^T \in \Re^n$; observer gain $K_o^T = [k_1 \quad k_2 \quad \cdots \quad k_n]$ is designed to satisfy $A_S - K_o C_S$ strictly Hurwitz, where $(C_S, A_S)$ represents observer pair; $e_o = x_{M1} - \hat{x}_{S1}$; $u_r$ is designed to enhance the robustness caused by $d$; $f_M(\underline{x}_M)$ is approximated by adaptive FNN with $\hat{f}_S(\hat{\underline{x}}_S)$. $f_M(\underline{x}_M)$ is unknown (uncertain) but bounded continuous functions. [81,82]
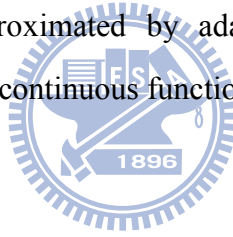
Synchronization Error:

The synchronization error can be defined as:

$$\underline{e}_{syn} = \underline{x}_M - \hat{\underline{x}}_S , \tag{69}$$

where $\underline{e}_{syn} = [e_{syn} \quad \dot{e}_{syn} \quad \cdots \quad e_{syn}^{(n-1)}]^T = [e_{syn1} \quad e_{syn2} \quad \cdots \quad e_{synn}]^T \in \Re^n$.

The master and slave achieve synchronization when all states are estimated at the slave.

## 7.3 Adaptive Fuzzy-Neural Network Observer Design

In this subchapter, AFNO is introduced. Under an assumption, the designed AFNO can estimate the master's states to achieve synchronization. AFNO can then be synthesized by an

FNN and a linear observer.

## 7.3.1 Fuzzy-Neural Network [73,80]

The FNN is designed to model the nonlinear function $f_M(\underline{x}_M)$ with $f_S(\hat{\underline{x}}_S)$. The FNN depicted in Fig. 7.2 is utilized as an approximator to model the nonlinear functions such as $f(\underline{x})$. The FNN [83,84], which consists of fuzzy IF-THEN rules and a fuzzy inference engine, is adopted as a function approximator. The fuzzy inference engine employs the IF-THEN rules to generate a mapping from an input linguistic vector $\underline{x} = [x_1 \quad x_2 \quad \cdots \quad x_n]^T \in \Re^n$ to an output linguistic variable $y(\underline{x}) \in \Re$. Fuzzy IF-THEN rule $i$ th is thus written as:

$$R^{(i)}: \text{if } x_1 \text{ is } A_1^i \text{ and } \ldots \text{and } x_n \text{ is } A_n^i, \text{ then } y \text{ is } B^i,$$

where $A_1^i$, $A_2^i, \cdots, A_n^i$ and $B^i$ are fuzzy sets with membership functions $\mu_{A_i^i}(x_j)$ and $\mu_{B^i}(\bar{y}^i)$, respectively. By using product inference, center-average, and singleton fuzzifier, output $y(\underline{x})$ from the fuzzy-neural approximator can be written as

$$y(\underline{x}) = \frac{\sum_{i=1}^{h} \bar{y}^i (\prod_{j=1}^{n} \mu_{A_j^i}(x_j))}{\sum_{i=1}^{h} (\prod_{j=1}^{n} \mu_{A_j^i}(x_j))} = \underline{\theta}_f^T \Gamma(\underline{x}), \tag{70}$$

where $\mu_{A_j^i}(x_j)$ denotes the membership function value of fuzzy variable $x_j$; $h$ is the total number of IF-THEN rules, and $\bar{y}^i$ is the point at which $\mu_{B^i}(\bar{y}^i) = 1$. $\underline{\theta}_f = [\bar{y}^1 \quad \bar{y}^2 \quad \cdots \quad \bar{y}^h]^T$ denotes an adjustable parameter vector, and $\Gamma = [\tau^1 \quad \tau^2 \quad \cdots \quad \tau^h]^T$ represents a fuzzy basic vector, where $\tau^i$ is given by

$$\tau^i(\underline{x}) = \frac{(\prod_{j=1}^{n} \mu_{A_j^i}(x_j))}{\sum_{i=1}^{h} (\prod_{j=1}^{n} \mu_{A_j^i}(x_j))}. \tag{71}$$

By adjusting the parameter vector $\underline{\theta}_f$ in (70) with adaptive laws, the uncertain nonlinear

function $f(\underline{x})$ can be approximated by $\hat{f}(\underline{x})$ generated in (72). By using the fuzzy-neural approximator, the estimated functions $\hat{f}(\underline{x})$ can be determined from the outputs of the fuzzy-neural approximator, which is defined as follows:

$$\hat{f}(\underline{x}|\underline{\theta}_f) = \underline{\theta}_f^T \Gamma(\underline{x}),\tag{72}$$

where $\underline{\theta}_f$ is an adjustable parameter vector.

In summary, (72) can describe the input-output relation of the FNN. The overall structure of the FNN is divided into four layers as shown in Fig. 7.2. The physical meanings of (72) can be interpreted by Fig. 7.2 in the following. The input nodes in Layer I represent input linguistic vectors. Nodes in Layer II denote values of the membership function of total linguistic variables. Each node in Layer III excuses a fuzzy rule. The output of Layer IV is the output signal modeling the nonlinear function. The connection parameters between layer III and layer IV are adjusted by using adaptive laws. The number of fuzzy rules can be dependent on complex level of nonlinear systems. In general, the more complex the systems are, the more numerous rules are demand. Of course, the computing load is heavy with more numerous rules. On the other hands, when the rules are less, the computing load is slight. This is a trade off problem.

## 7.3.2 Adaptive Fuzzy-Neural Network Observer

**Assumption 7.1** [73,80]:

The master state vector $\underline{x}_M$ and the slave state vector $\hat{\underline{x}}_S$ belong to compact sets $S_M$ and $S_S$ respectively, where

$$S_M = \left\{ \underline{x}_M \in \Re^n : \|\underline{x}_M\| \le \varepsilon_{\underline{x}_M} < \infty \right\},\tag{73}$$

$$S_S = \left\{ \hat{\underline{x}}_S \in \Re^n : \|\hat{\underline{x}}_S\| \le \varepsilon_{\hat{\underline{x}}_S} < \infty \right\},\tag{74}$$

and $\varepsilon_{\underline{x}_M}$ and $\varepsilon_{\hat{\underline{x}}_S}$ are designed parameters.

The optimal parameter vector $\underline{\theta}_f^*$ falls in some convex region with constant radius $\varepsilon_{\underline{\theta}_f}$. The convex region can be specified as shown in (75).

$$R_{\underline{\theta}_f} = \left\{ \underline{\theta}_f \in \mathfrak{R}^h : \left\| \underline{\theta}_f \right\| \le \varepsilon_{\underline{\theta}_f} \right\}. \tag{75}$$

The optimal parameter vector $\underline{\theta}_f^*$ can be described as:

$$\underline{\theta}_f^* = \arg \min_{\underline{\theta}_f \in R_{\underline{\theta}_f}} \left\{ \sup_{\underline{x}_M \in S_M, \hat{\underline{x}}_S \in S_S} \left| f_M(\underline{x}_M) - \hat{f}_S(\hat{\underline{x}}_S \mid \underline{\theta}_f) \right| \right\}. \tag{76}$$

**Remark 7.1**: The optimal $\underline{\theta}_f^*$ is possible in an ideal situation. In our applications, the adaptive laws will be applied to tune $\underline{\theta}_f$ to approach $\underline{\theta}_f^*$.

The adaptive fuzzy-neural nonlinear observer with respect to a class of nonlinear systems (67) can be designed under assumption 7.1. AFNO can be designed [73,80]:

$$\begin{aligned} \dot{\hat{\underline{x}}}_S &= A_S \hat{\underline{x}}_S + B_S(\underline{\theta}_f^T \Gamma(\hat{\underline{x}}_S) - u_r) + K_o e_o \\ y_{S1} &= \hat{x}_{S1} = C_S \hat{\underline{x}}_S, \end{aligned} \tag{77}$$

where $\underline{\theta}_f^T \Gamma(\hat{\underline{x}}_S)$ is calculated by FNN to approximate the nonlinear functions $f_M(\underline{x}_M)$ in dynamical systems, and $u_r$ denotes the robust input to compensate the effect due to external disturbance and the approximated modeling error by FNN. Based on [73,80], $u_r$ can be designed as follows:

$$u_r = -\frac{1}{\gamma} \lambda_{\min}(Q) e_o, \tag{78}$$

where $Q = Q^T > 0$, and $\gamma$ is a positive constant. In general, $\gamma$ should be proper designed. The small gamma will cause large $u_r$ to attenuate the effect of disturbance. Indeed, the better attenuation performance will be obtained when the small $\gamma$ is chosen. Additionally, $Q = Q^T > 0$ will make the Riccati-like equation satisfied in stability and adaptive law derivation with Lyapunove function [80].

The adaptive laws in FNN are as follows:

$$
\dot{\underline{\theta}}_f = \begin{cases} \gamma_1 e_o \phi(\hat{\underline{x}}_S), & \text{if } \left\| \underline{\theta}_f \right\| < \varepsilon_{\underline{\theta}_f} \text{ or } (\left\| \underline{\theta}_f \right\| = \varepsilon_{\underline{\theta}_f}, \\ & \text{and } e_o \underline{\theta}_f^T \phi(\hat{\underline{x}}_S) \leq 0) \\ \Pr_f(\gamma_1 e_o \phi(\hat{\underline{x}}_S)), & \text{if } \left\| \underline{\theta}_f \right\| = \varepsilon_{\underline{\theta}_f} \text{ and } e_o \underline{\theta}_f^T \phi(\hat{\underline{x}}_S) > 0, \end{cases} \tag{79}
$$

where $\phi(\hat{\underline{x}}_S) = L^{-1}(s)\Gamma(\hat{\underline{x}}_S)$; $L^{-1}(s)$ denotes a proper stable transfer function to transform $H(s)L(s)$ into a proper strictly-positive real (SPR) transfer function, and $\gamma_1$ denotes the designed parameter. The function $H(s)$ is represented as follows:

$$
H(s) = C_S(sI - (A_S - K_o C_S))^{-1} B_S. \tag{80}
$$

$\Pr_f(\gamma_1 e_o \phi(\hat{\underline{x}}_S))$ in (81) is the operator of projection for achieving minimal modeling error for $f_M(\underline{x}_M)$.

$$
\Pr_f(\gamma_1 e_o \phi(\hat{\underline{x}}_S)) = \gamma_1 e_o \phi(\hat{\underline{x}}_S) - \gamma_1 \frac{e_o \underline{\theta}_f^T(\hat{\underline{x}}_S)\phi(\hat{\underline{x}}_S)}{\left\| \underline{\theta}_f \right\|^2} \underline{\theta}_f. \tag{81}
$$

The design procedure, stability proof and adaptive laws (79) can be referred in [73,80]

## 7.4 Simulation Results

This subchapter verifies the feasibility of AFNO for synchronization using two examples.

## 7.4.1 Example 1

In this example, AFNO is applied to synchronize a master Chua's circuit under modeling error, different initial conditions and external bounded disturbances .The results will demonstrate the adaptability and robustness of AFNO.

The master Chua's circuit is reformed as a canonical form [85].

$$
\begin{bmatrix} \dot{x}_{M1} \\ \dot{x}_{M2} \\ \dot{x}_{M3} \end{bmatrix} = \begin{bmatrix} 0 & 1 & 0 \\ 0 & 0 & 1 \\ 0 & 0 & 0 \end{bmatrix} \begin{bmatrix} x_{M1} \\ x_{M2} \\ x_{M3} \end{bmatrix} + \begin{bmatrix} 0 \\ 0 \\ 1 \end{bmatrix} (f_M(\underline{x}_M) + d),
\tag{82}
$$

where $\quad f_M(\underline{x}_M) = \dfrac{14}{1805} x_{M1} - \dfrac{168}{9025} x_{M2} + \dfrac{1}{38} x_{M3} - \dfrac{2}{45} \times \left( \dfrac{28}{361} x_{M1} + \dfrac{7}{95} x_{M2} + x_{M3} \right)^3$

The adaptive laws tune FNN to approach $f_M(\underline{x}_M)$. The observer is designed to place poles

of $A_S - K_o C_S$ in -30 i.e. linear observer gain vector is $K_o^T = \begin{bmatrix} 90 & 2700 & 27000 \end{bmatrix}$.

Other parameters of AFNO are $\gamma = 10$, $\gamma_1 = 0.01$, $Q$ is $3 \times 3$ identity matrix, and

$L^{-1} = \dfrac{1}{s+2}$. The membership functions for $\hat{x}_{Si}$, $i = 1, 2, 3$ in FNN are given as follows:

$\mu_{A_j^1}(\hat{x}_{Si}) = 1/(1 + \exp(5 \times (\hat{x}_{Si} + 0.75)))$,

$\mu_{A_j^2}(\hat{x}_{Si}) = \exp(-(\hat{x}_{Si} + 0.5)^2)$,

$\mu_{A_j^3}(\hat{x}_{Si}) = \exp(-(\hat{x}_{Si} + 0.25)^2)$,

$\mu_{A_j^4}(\hat{x}_{Si}) = \exp(-(\hat{x}_{Si})^2)$,

$\mu_{A_j^5}(\hat{x}_{Si}) = \exp(-(\hat{x}_{Si} - 0.25)^2)$, $\tag{83}$

$\mu_{A_j^6}(\hat{x}_{Si}) = \exp(-(\hat{x}_{Si} - 0.5)^2)$,

$\mu_{A_j^7}(\hat{x}_{Si}) = 1/(1 + \exp(-5 \times (\hat{x}_{Si} - 0.75)))$.

In this example, three states should be estimated, accounting for why the fuzzy rules in

process are 343. The initially adjustable parameters in adaptive FNN are chosen to be

$\underline{\theta}_f(0) = \underline{0}$ to demonstrating modeling error. The weights of FNN are turned by the adaptive

laws to form $f_M(\underline{x}_M)$.

Different initial conditions of the master and slave are listed in Table 7.1. Furthermore, the

distinct disturbances are listed in Table 7.2.

Figures 7.3~7.5 summarize the simulation results of different initial conditions for three states in AFNO. In Figs. 7.3~7.5, the distinct initial conditions for each state in AFNO are listed in Table 7.1 and a type of disturbance in the master end is set as Case 1 in Table 7.2. Figure 7.3 illustrates that the first state $\hat{x}_{S1}$ in AFNO with three different initial conditions synchronizes $x_{M1}$ in Chua's circuit. Figures 7.4 and 7.5 illustrate that $\hat{x}_{S2}$ and $\hat{x}_{S3}$ synchronize $x_{M2}$ and $x_{M3}$, respectively. Although the initial conditions differ from each other, AFNO synchronizes with Chua's circuit quickly, well, and adaptively. Moreover, the synchronization error approaches zero as time goes to infinity. The robustness of AFNO can be also specified from Figs. 7.6~7.8 with various intensity disturbances in the master end. In Figs. 7.6~7.8, the initial conditions of three states are selected as Case1 in Table 7.1 and the different disturbances are chosen as Table 7.2. Figure 7.6 demonstrates that the first state $\hat{x}_{S1}$ in the slave synchronizes $x_{M1}$ in the master end immediately and well under three different disturbances. Figures 7.7 and 7.8 reveal that $\hat{x}_{S2}$ and $\hat{x}_{S3}$ synchronize $x_{M2}$ and $x_{M3}$, individually. Even if the different disturbances are added in the master Chua's circuit, AFNO synchronizes with the master robustly.

## 7.4.2 Example 2

Example 2 demonstrates the adaptability of the utilized method by switched master between Chua's circuit and Rössler system as shown in Fig. 7.9. When the master is switched to another system, the slave follows to synchronize another chaotic system soon and well. The similar different initial conditions and disturbances listed in Tables 7.1 and 7.2 are considered in simulations for demonstrating the robustness of AFNO.

The original Rössler system can be presented as [62]:

$$\dot{z}_1 = z_2 + az_1$$

$$\dot{z}_2 = -z_1 - z_3 \tag{84}$$

$$\dot{z}_3 = b - cz_3 + z_2z_3,$$

where $\underline{z} = [z_1 \quad z_2 \quad z_3]^T$.

Let

$$\underline{x}_M = T^{-1}\underline{z}, \tag{85}$$

where $T = \begin{bmatrix} -1 & 0 & 0 \\ a & -1 & 0 \\ 1 & -a & 1 \end{bmatrix}$.

The Rössler system is reformed as the canonical form with

$$f_M(\underline{x}_M) = -cx_{M1} + (ac-1)x_{M2} + (a-c)x_{M3} + ax_{M1}^2 - (a^2+1)x_{M1}x_{M2} + ax_{M1}x_{M3} + ax_{M2}^2$$
$$-x_{M2}x_{M3} + b,$$

where $a = 0.2$, $b = 0.2$, and $c = 6.3$. Notably, $f_M(\underline{x}_M)$ is revised from [62].

The parameters of AFNO at the slave resemble those in Example 1. The initial condition of

Rössler system is set $[0 \quad 0 \quad 0]^T$.

Figures 7.10~7.12 indicate the simulation results with respect to each state for diverse

initial conditions in AFNO and switched masters. The distinct initial conditions for each state

in AFNO are shown in Table 7.1 and a kind of disturbance in the master end is set as Case 1

in Table 7.2. Figure 7.10 illustrates that the first state $\hat{x}_{S1}$ in AFNO with three different

initial conditions synchronizes $x_{M1}$ in the   master end, even if the switched masters exist at

the third second (Chua's circuit to Rössler system) and the sixth second (Rössler system to

Chua's circuit). Figures 7.11 and 7.12 exhibit that $\hat{x}_{S2}$ and $\hat{x}_{S3}$ synchronize $x_{M2}$ and $x_{M3}$,

respectively. Although the initial conditions differ from each other and the switched masters

exist, AFNO synchronizes with the switched masters fast, well, and adaptively. On the other

hand, simulation results in Figs. 7.13~7.15 verify the robustness of AFNO for the different

disturbances and the switched systems in the master end. In Figs. 7.13~7.15, the initial

conditions of three states are chosen as Case1 in Table 7.1 and the different disturbances are selected as Table 7.2. Figure 7.13 displays that the first state $\hat{x}_{S1}$ synchronizes $x_{M1}$ immediately and well under three different disturbances, even thought the switched masters exist at the third second (Chua's circuit to Rössler system) and the sixth second (Rössler system to Chua's circuit). Figures 7.14 and 7.15 reveal that $\hat{x}_{S2}$ and $\hat{x}_{S3}$ synchronize $x_{M2}$ and $x_{M3}$, separately. In spite of the different disturbances and the switched systems are considered in the master end, AFNO synchronizes with the master robustly.

It is noted that Figs 7.10~7.15 display the simulation results indicating AFNO synchronizes with Chua's circuit at 0~3 sec. The Rössler system also runs dynamically from the initial condition. AFNO synchronizes with Rössler at 3~6 sec, while Chua's circuit runs simultaneously.

From these simulation results, AFNO can synchronize with a class of unknown chaotic systems adaptively and robustly.
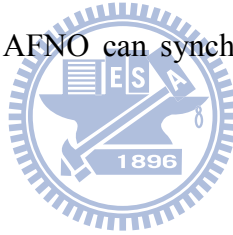
## 7.5 Conclusion Remarks

This work has applied AFNO for synchronization with respect to a class of unknown chaotic systems via a scalar transmitted signal only. Once the nonlinear chaotic systems could be transformed into the canonical form of Lur'e system type by the differential geometric method, the AFNO method can be utilized for synchronization. In this approach, the nonlinear term in the master end was modeled by the adaptive fuzzy-neural network (FNN) in AFNO on line. Furthermore, the states in the master end were observed from a scale transmitted signal by observer design. When states in the master and slave ends were identical, we said the synchronization was reached. By this scheme, the AFNO could estimate the unknown master's states adaptively, even though the master was altered into another chaotic system. On the other hand, AFNO could deal with the modeling error, and external bounded

disturbance to demonstrate its robustness advantage. Simulation results showed that the adaptive and robust AFNO was suitable for chaos synchronization with respect to a class unknown chaotic systems.

Fig. 7.1 The overall structure of synchronization with AFNO.
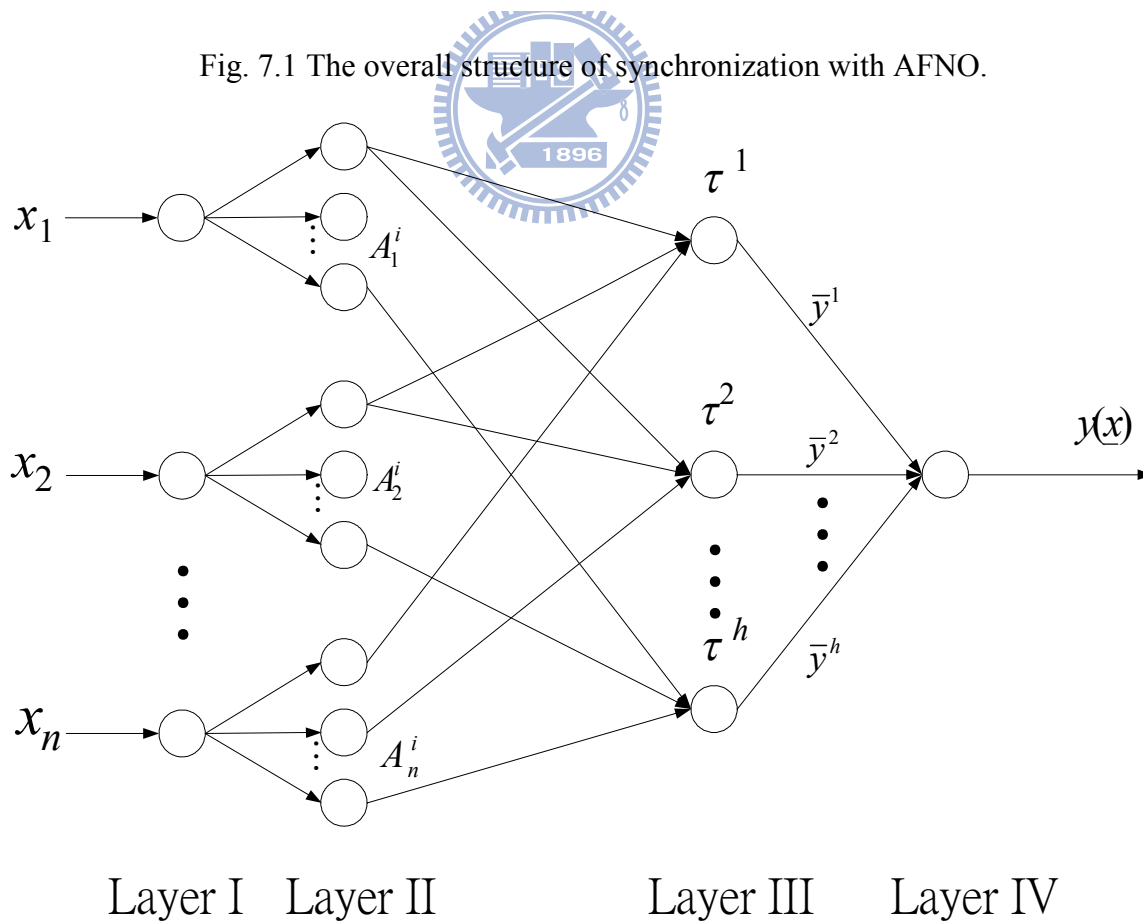


Fig. 7.2 The fuzzy-neural approximator [73,80].

Table 7.1

Three cases of the initial conditions

| Cases | Initial conditions |
|---|---|
| Case 1 | $\underline{x}_M(0) = [0 \quad 0 \quad 0]^T$, and $\underline{x}_S(0) = [1 \quad 1 \quad 1]^T$ |
| Case 2 | $\underline{x}_M(0) = [0 \quad 0 \quad 0]^T$, and $\underline{x}_S(0) = [2 \quad 2 \quad 2]^T$ |
| Case3 | $\underline{x}_M(0) = [0 \quad 0 \quad 0]^T$, and $\underline{x}_S(0) = [3 \quad 3 \quad 3]^T$ |

Note: In the simulations, the disturbances in the master end are set as Case 1 in Table 7.2 in three cases.

Table 7.2

Three cases of the disturbances

| Cases | Disturbance ($d$) |
|---|---|
| Case 1 | $\pm 0.5$ with period $2\pi$ |
| Case 2 | $\pm 0.8$ with period $2\pi$ |
| Case3 | $\pm 1$ with period $2\pi$ |

Note: In the simulations, the initial conditions are chosen as Case1 in Table 7.1 in three cases.
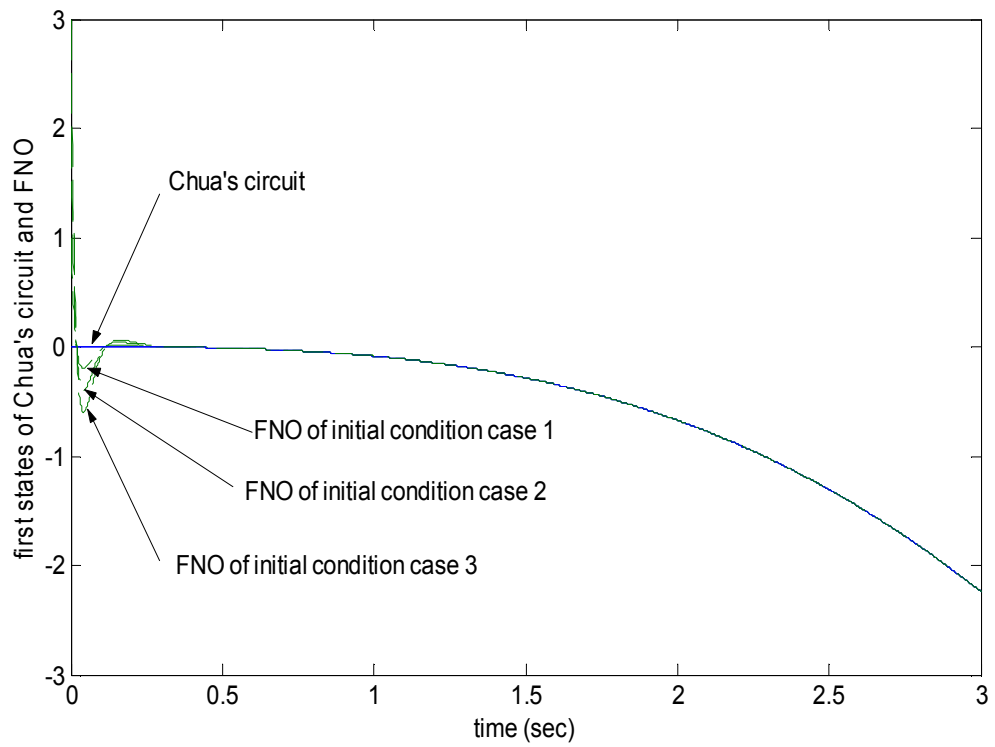
Fig. 7.3 The first states $x_{M1}$ and $\hat{x}_{S1}$ in Chua's circuit and AFNO under different initial conditions.
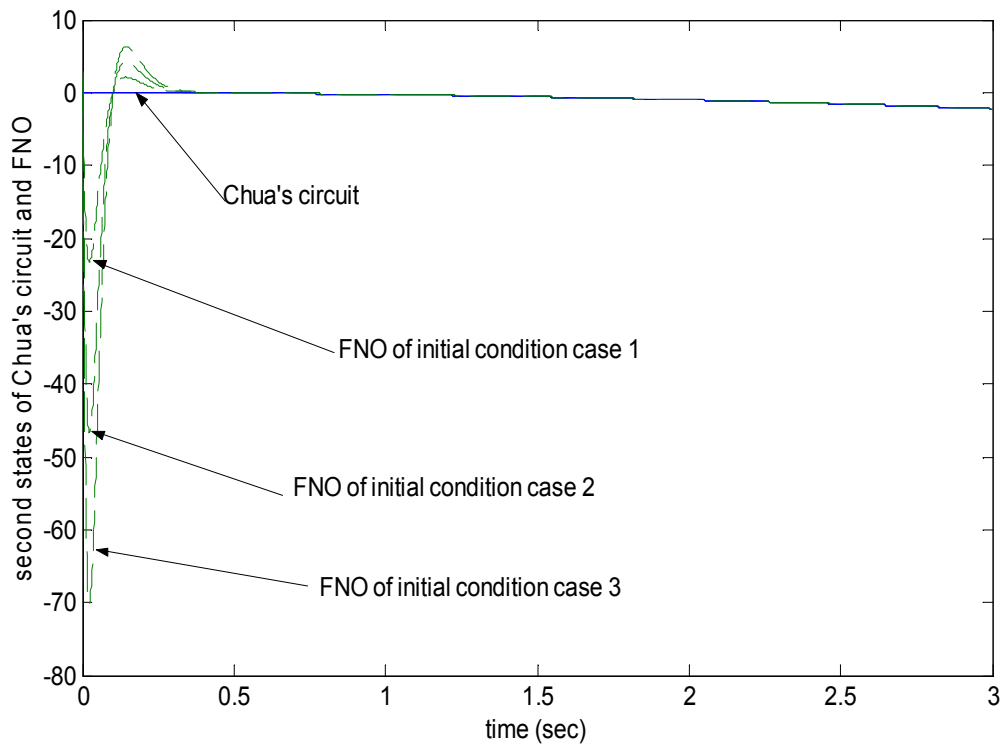


Fig. 7.4 The second states $x_{M2}$ and $\hat{x}_{S2}$ in Chua's circuit and AFNO under different initial conditions.
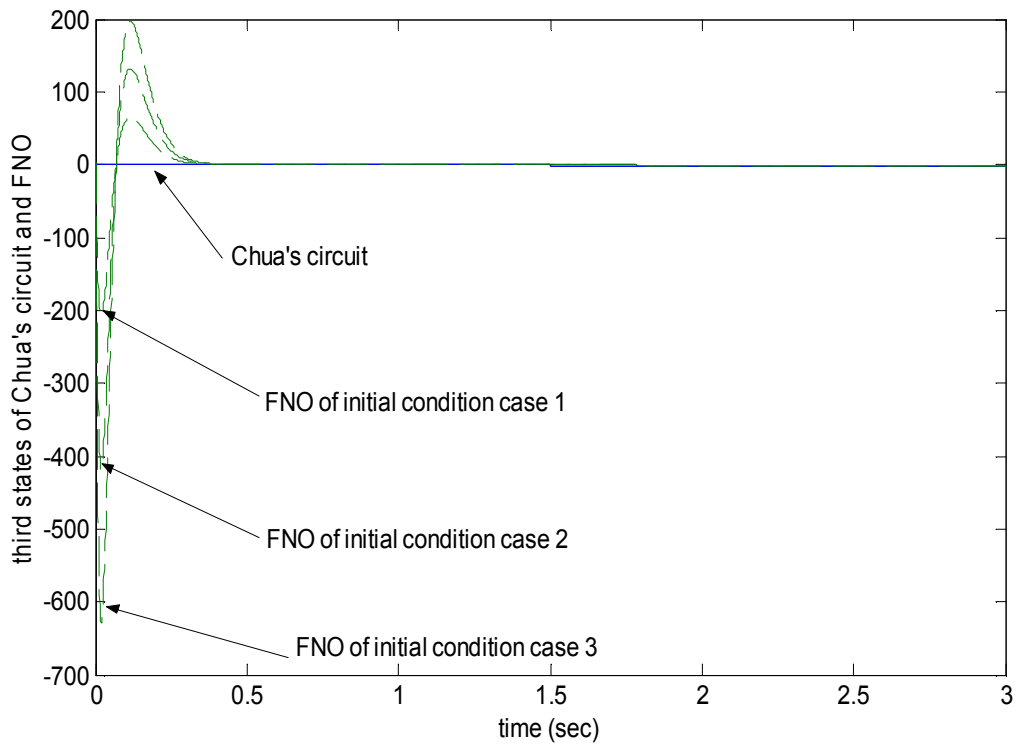
Fig. 7.5 The third states $x_{M3}$ and $\hat{x}_{S3}$ in Chua's circuit and AFNO under different initial conditions.
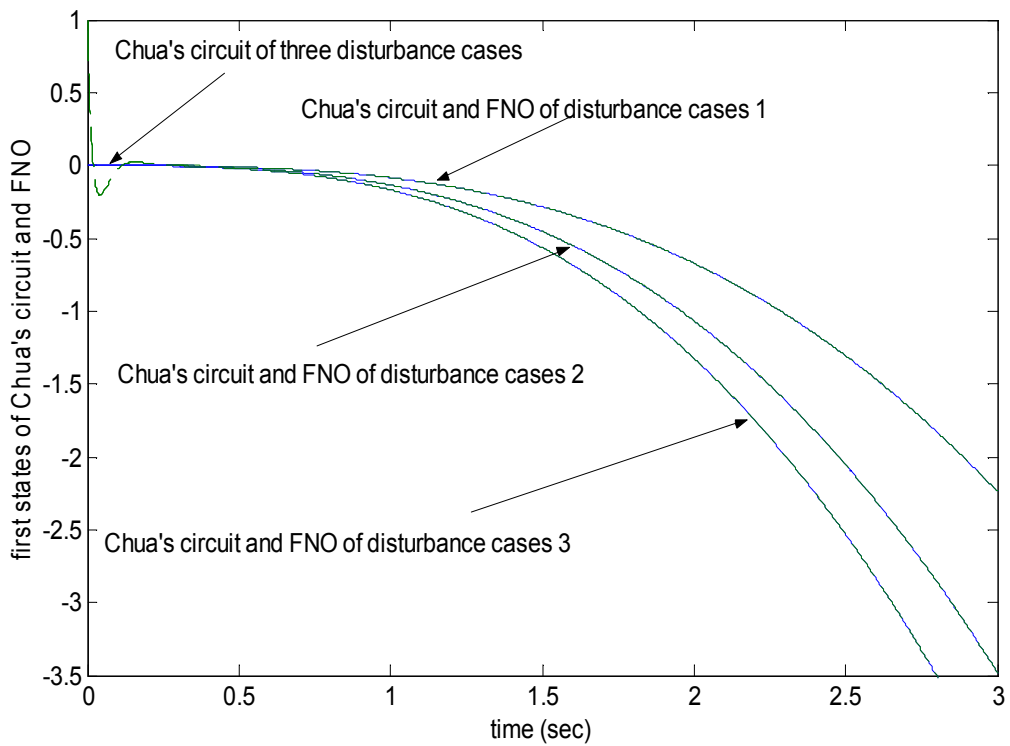


Fig. 7.6 The first states $x_{M1}$ and $\hat{x}_{S1}$ in Chua's circuit and AFNO under different disturbances.
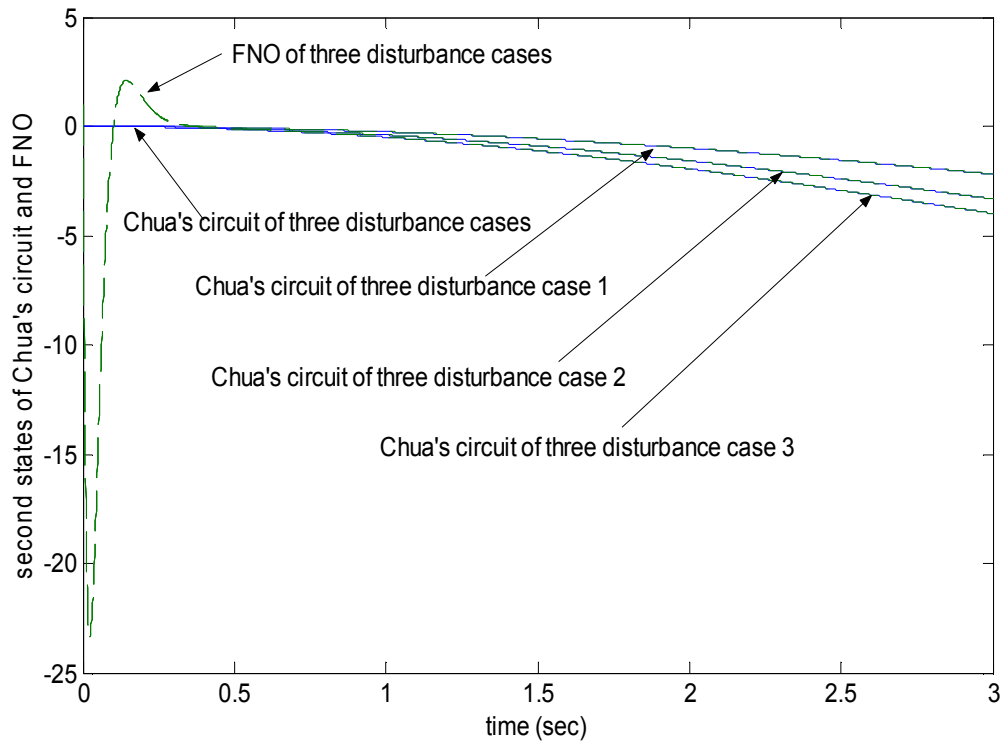
Fig. 7.7 The second states $x_{M2}$ and $\hat{x}_{S2}$ in Chua's circuit and AFNO under different
disturbances.
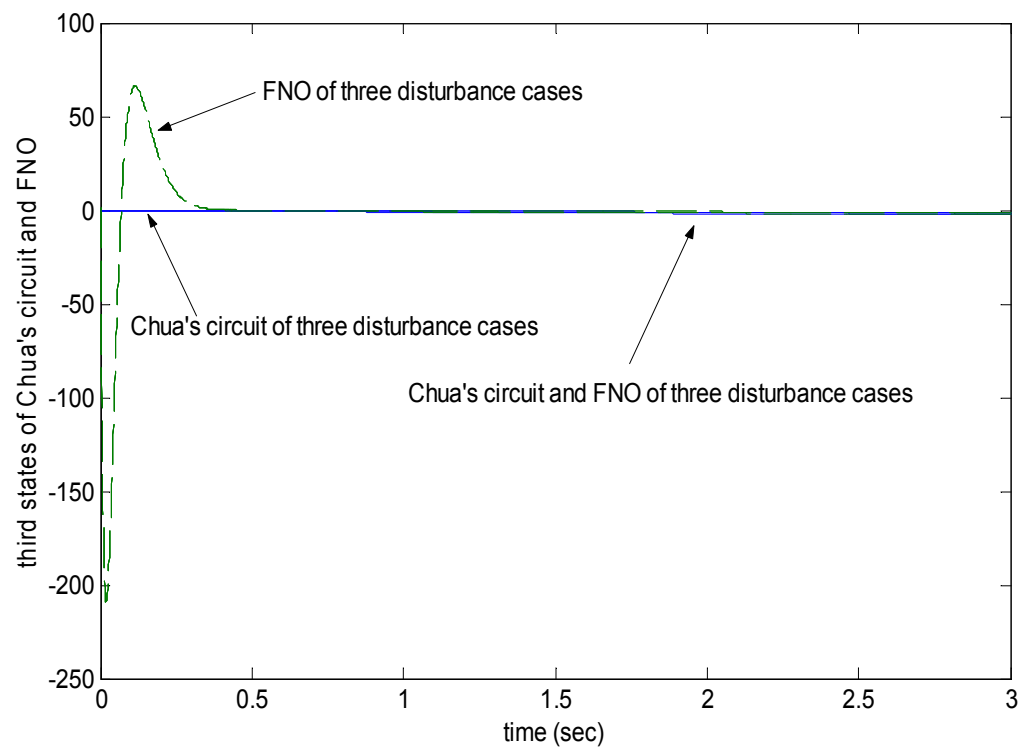


Fig. 7.8 The third states $x_{M3}$ and $\hat{x}_{S3}$ in Chua's circuit and AFNO under different
disturbances.
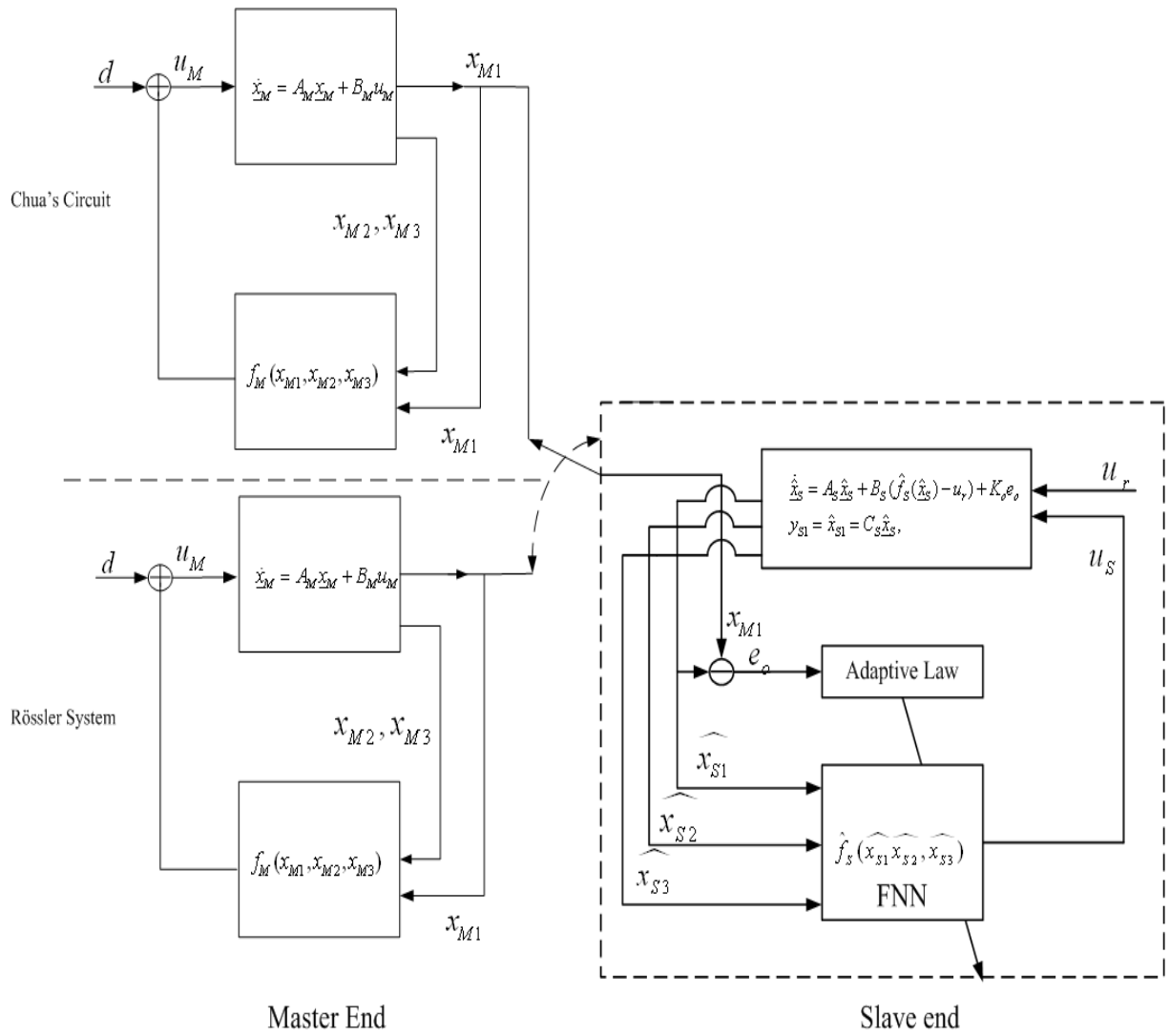
Fig. 7.9 The structure of synchronization with the switched masters.
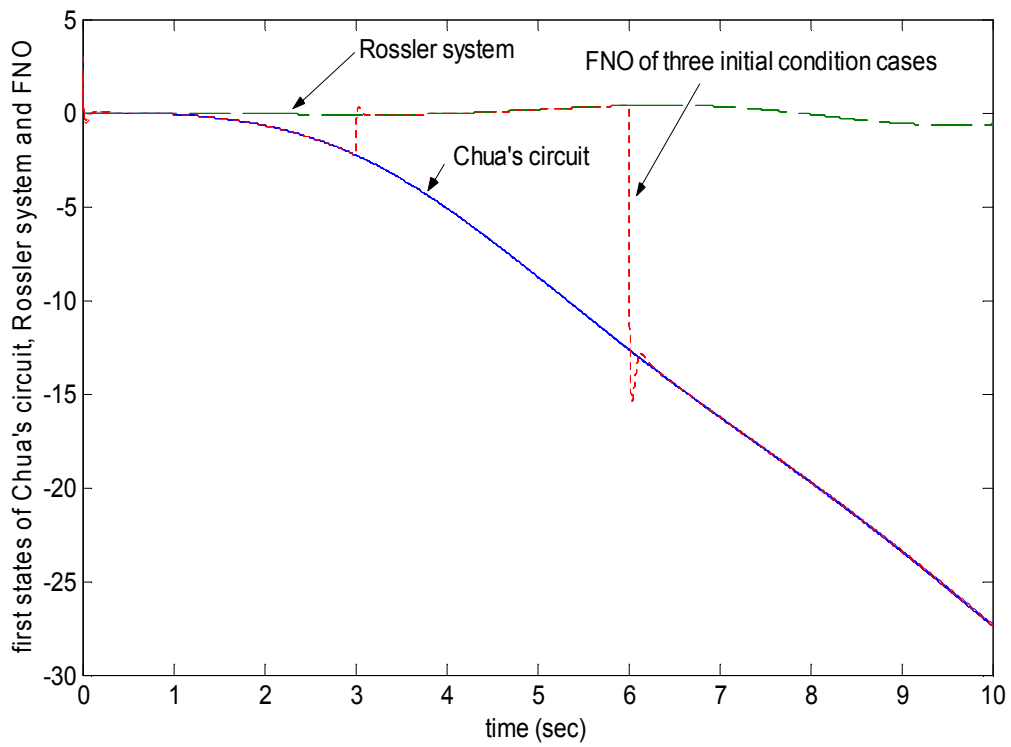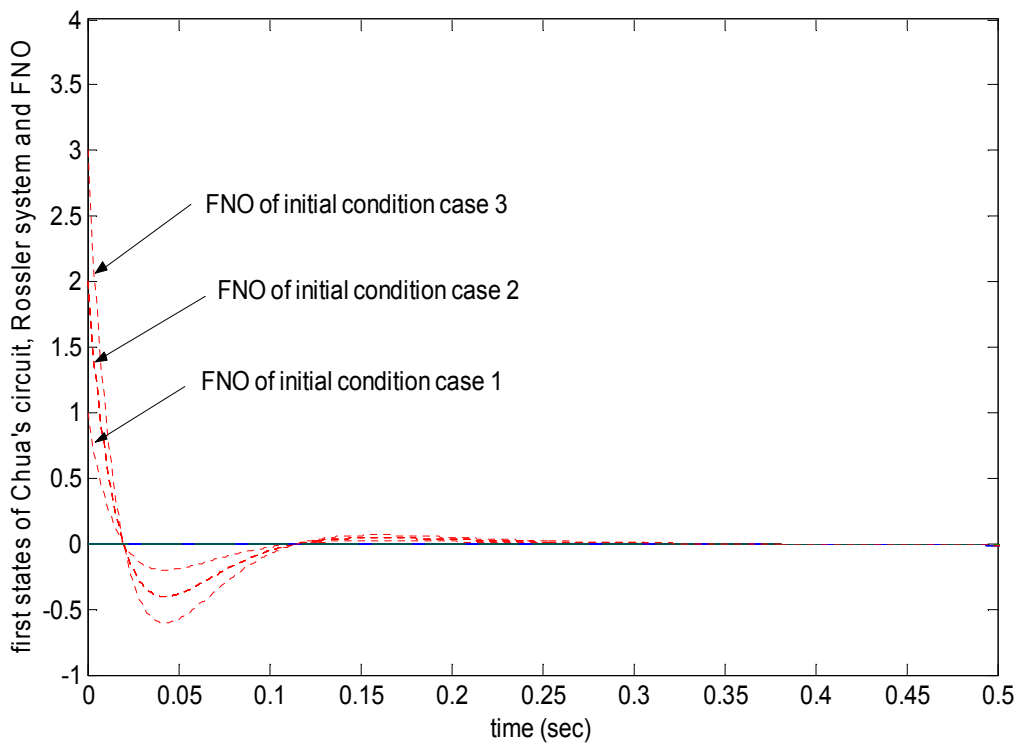
Fig. 7.10 The first states in Chua's circuit, Rössler system and AFNO under different initial conditions and switched masters: (a) actual figure size (b) enlarged figure size of local region.
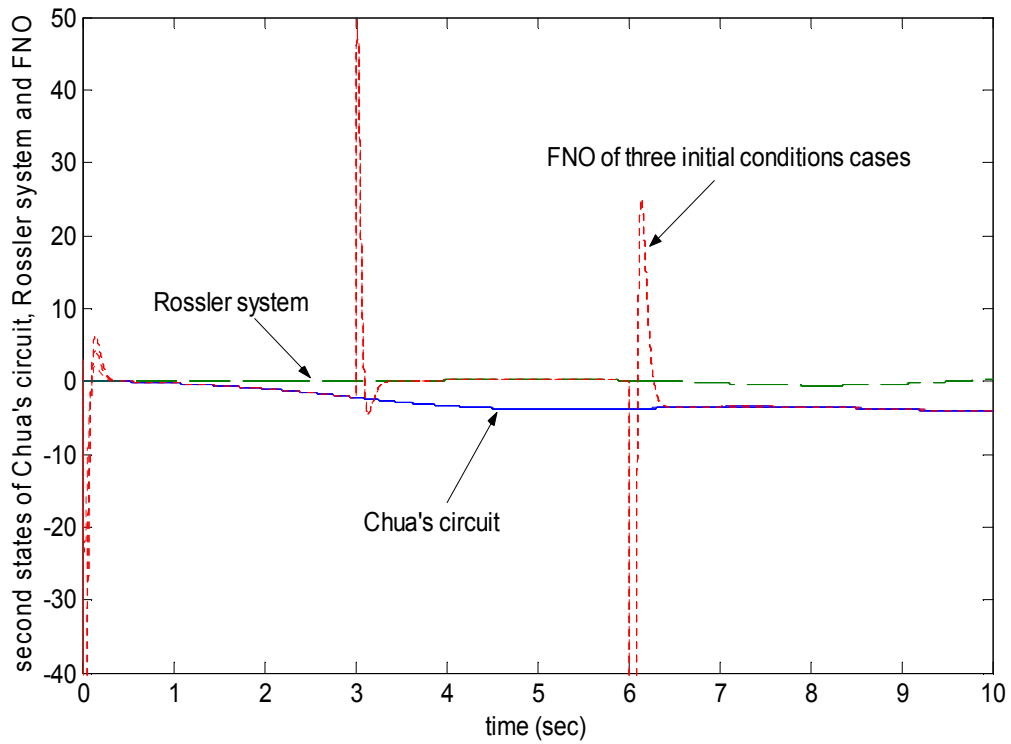
Fig. 7.11 The second states in Chua's circuit, Rössler system and AFNO under different initial conditions and switched masters.
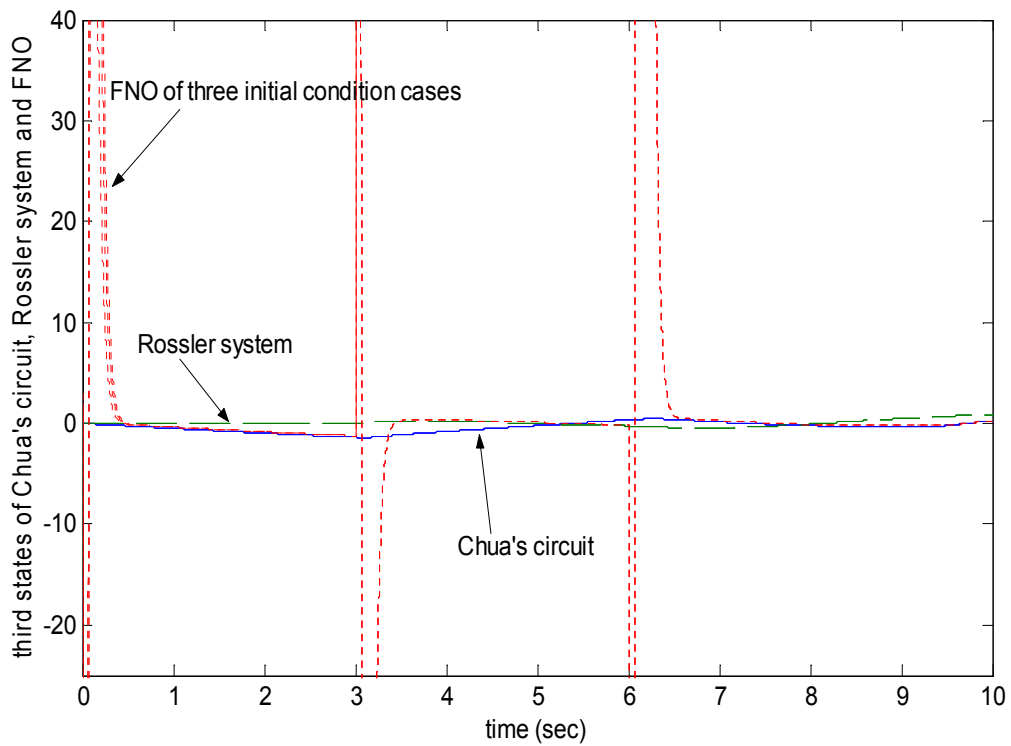


Fig. 7.12 The third states in Chua's circuit, Rössler system and AFNO under different initial conditions and switched masters.
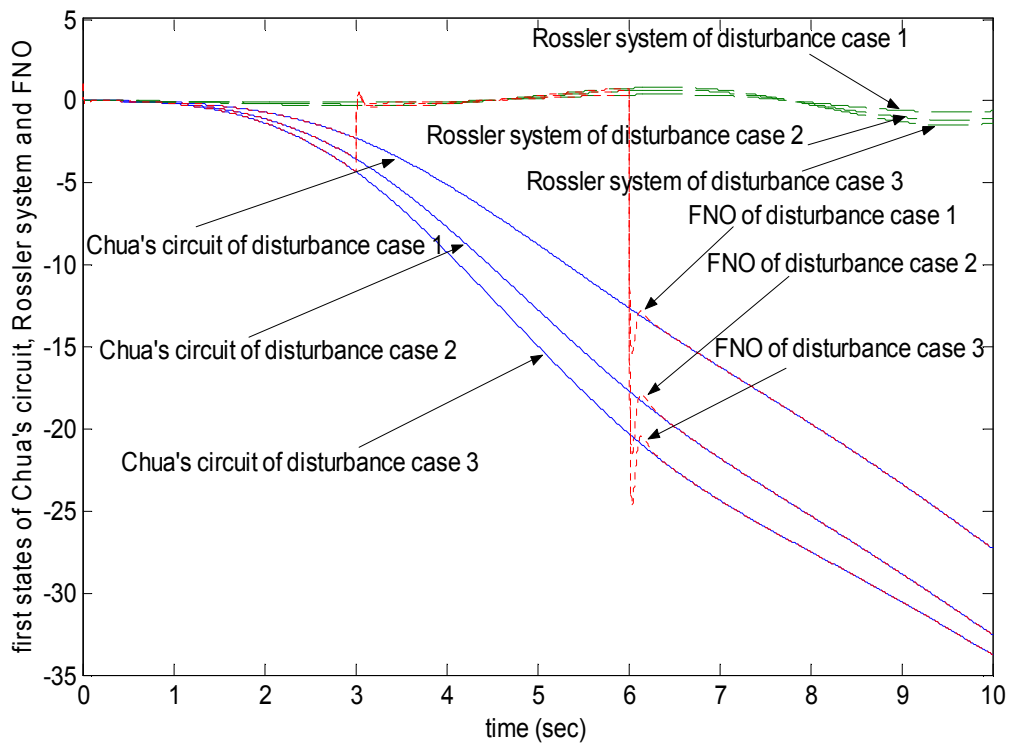
Fig. 7.13 The first states in Chua's circuit, Rössler system and AFNO under different disturbances and switched masters.
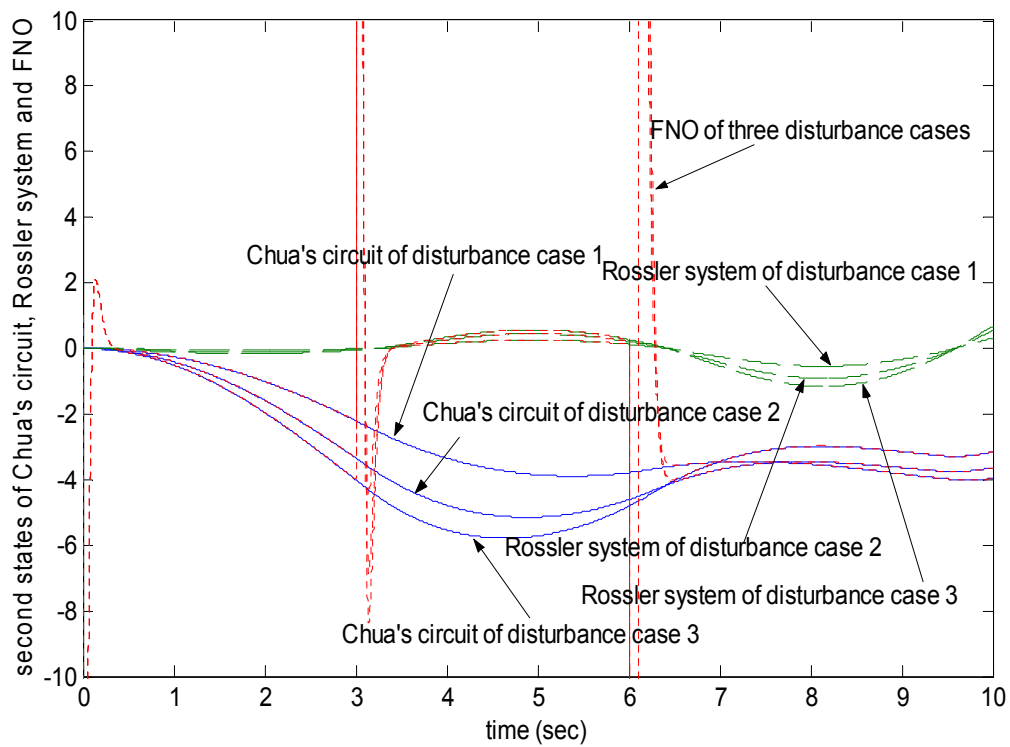


Fig. 7.14 The second states in Chua's circuit, Rössler system and AFNO under different disturbances and switched masters.
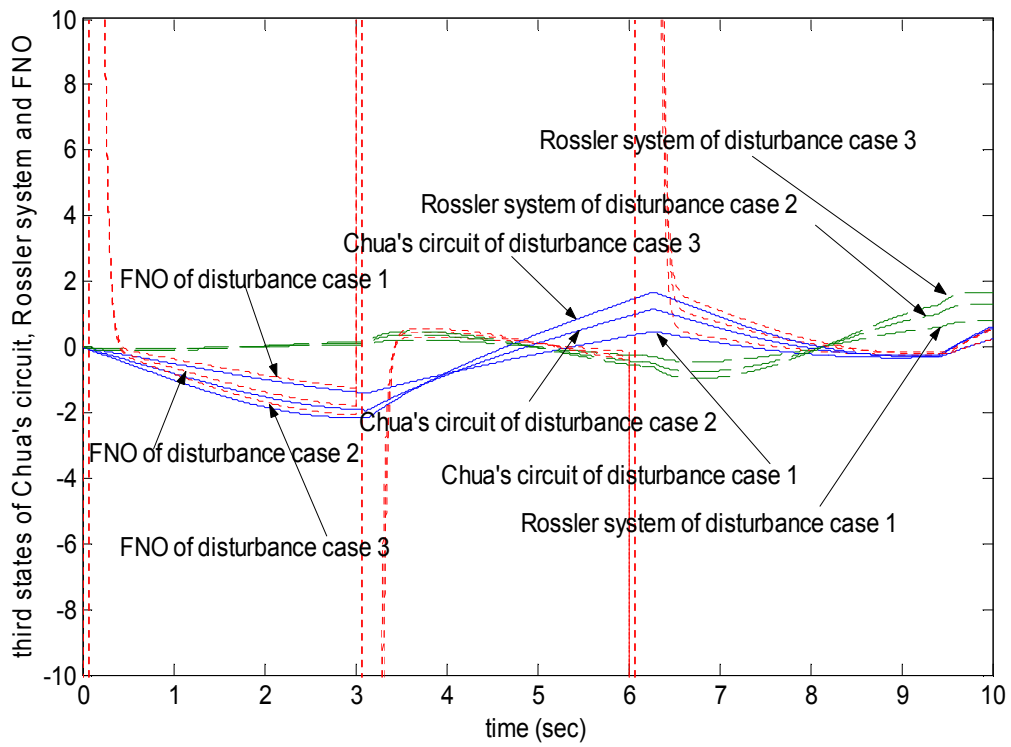
Fig. 7.15 The third states in Chua's circuit, Rössler system and AFNO under different disturbances and switched masters.
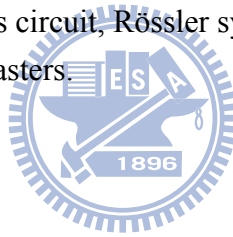
# Chapter 8

## Conclusions

In this dissertation, the parametric absolute stability in P and PD type fuzzy logic control systems with both certain and uncertain linear plants with parameters such as the reference input, actuator gain and interval plan have been analyzed. The adaptive AFNO has been also applied to synchronize a class of unknown chaotic systems via a scalar transmitted signal only. In the stability analysis, for certain linear plants, the Popov and linearization methods are applied to analyze the stability in both P and PD type fuzzy control systems under different reference inputs and actuator gains. The steady state errors of the fuzzy control systems are also analyzed. For uncertain plants, the parametric robust Popov criterion based on the Lur'e system is applied to the stability analysis of P and PD type fuzzy control systems. Moreover, a fuzzy current controlled RC circuit is designed to compare theoretical analyses with PSPICE simulation results. Furthermore, the oscillation phenomena in fuzzy control systems are interpreted from the point of view of the equilibriums in this simulation example. Finally, the parametric robust Popov criterion is compared with the other approaches to show the effectiveness respect to non-zero reference inputs.

About application with the fuzzy control system, AFNO has been applied for synchronization with respect to a class of unknown chaotic systems via a scalar transmitted signal only. Once the nonlinear chaotic systems could be transformed into the canonical form of Lur'e system type by the differential geometric method, the AFNO method can be utilized for synchronization. In this approach, the nonlinear term in the master end was modeled by

the adaptive fuzzy-neural network (FNN) in AFNO on line. Furthermore, the states in the master end were observed from a scale transmitted signal by observer design. When states in the master and slave ends were identical, we said the synchronization was reached. By this scheme, the AFNO could estimate the unknown master's states adaptively, even though the master was altered into another chaotic system. On the other hand, AFNO could deal with the modeling error, and external bounded disturbance to demonstrate its robustness advantage. Simulation results showed that the adaptive and robust AFNO was suitable for chaos synchronization with respect to a class unknown chaotic systems.

# References

[1] C. C. Lee, "Fuzzy Logic in Control Systems: Fuzzy Logic Control—Parts I and II," *IEEE Transaction on Systems, Man Cybernetics*, vol. 20, no.2, pp. 404–435, 1990.

[2] E. H. Mamdani, "Applications of Fuzzy Algorithms for Control of Simple Dynamic Plant," *Proceedings of the IEEE*, vol. 121, no.2, pp. 1585–1588, 1974.

[3] K. Tanaka and M. Sugeno, "Stability Analysis and Design of Fuzzy Control Systems," *Fuzzy Sets and Systems*, vol. 45, pp. 135-156, 1992.

[4] S. G. Cao, N. W. Rees and G. Feng, "Stability Analysis of Fuzzy Control Systems," *IEEE Transaction on Systems, Man Cybernetics B*, vol. 26 , no. 1, pp. 201–204, Feb. 1996.

[5] J. Joh, Y. H. Chen, and R. Langari, "On the Stability Issues of Linear Takagi-Sugeno Fuzzy Models," *IEEE Transaction on Fuzzy Systems*, vol. 6, no. 3, pp. 402–410, Aug. 1998.

[6] S. G. Cao, N. W. Rees, and G. Feng, "Analysis and Design of Fuzzy Control Systems Using Fuzzy-State Space Models," *IEEE Transaction on Fuzzy Systems*, vol. 7, no. 2, pp. 192–200, Apr. 1999

[7] M. Sugeno, "On Stability of Fuzzy Systems Expressed by Fuzzy Rules with Singleton Consequents," *IEEE Transaction on Fuzzy Systems*, vol. 7, no. 2, pp. 201–224, Apr. 1999.

[8] G. Feng, "Approaches to Quadratic Stabilization of Uncertain Fuzzy Dynamic Systems," *IEEE Transaction Circuits and Systems I*, vol. 48, no. 6, pp. 760–769, June 2001.

[9] G. Feng, "Stability Analysis of Discrete-time Fuzzy Dynamic Systems Based on Piecewise Lyapunov Functions," *IEEE Transaction on Fuzzy Systems*, vol. 12, no. 1, pp. 22–28, Feb. 2004.

[10] F. H. Hsiao, C. W. Chen, Y. W. Liang, S. D. Xu, W. L. Chiang, "T-S Fuzzy Controller for Nonlinear Interconnected Systems with Multiple Time Delays," *IEEE Transaction Circuits and Systems I*, vol. 52, no. 9, pp. 1883–1893, Sep. 2005.

[11] C. C. Fuh and P. C. Tung, "Robust Stability Analysis of Fuzzy Control Systems," *Fuzzy Sets and Systems*, vol. 88, no.3, pp. 289-298, 1997.

[12] J. C. Lo, and Y. M. Chen, "Stability Issues on Takagi-Sugeno Fuzzy Model-Parametric Approach," *Fuzzy Sets and Systems*, vol. 7, no. 5, pp. 597-607, 1999.

[13] H. K. Lam, and Lakmal D. Seneviratne, "Stability Analysis of Interval Type-2 Fuzzy-Model-Based Control Systems," *IEEE Transaction on Systems, Man Cybernetics B*, vol. 38, no. 3, pp. 617–628, June 2008.

[14] H. H. Choi, "Robust Stabilization of Uncertain Fuzzy Systems Using Variable Structure System Approach," *IEEE Transaction on Fuzzy Systems*, vol. 16, no. 3, pp. 715–724, June 2008.

[15] T. H. S. Li, S. H. Tsia, J. Z. Lee, M. Y. Hsiao, and C. H. Chao, "Robust $H_\infty$ Fuzzy Control for a Class of Uncertain Discrete Fuzzy Bilinear Systems," *IEEE Transaction on Systems, Man Cybernetics B*, vol. 38, no. 2, pp. 510–527, April 2008.

[16] C. T. Pang and Y. Y. Lur, "On the Stability of Takagi-Sugeno Fuzzy Systems with Time Varying Uncertainties," *IEEE Transaction on Fuzzy Systems*, vol. 16, no. 1, pp. 162–170, Feb. 2008.

[17] S. Xu, B. Song, J. Lu, and J. Lam, "Robust Stability of Uncertain Discrete-Time Singular Fuzzy Systems," *Fuzzy Sets and Systems*, vol. 158, no. 20, pp. 2306-2316, 2007.

[18] H. K. Lam, and Lakmal D. Seneviratne, "BMI-Based Stability and Performance Design for Fuzzy-Model-Based Control Systems Subject to Parameter Uncertainties," *IEEE Transaction on Systems, Man Cybernetics B*, vol. 37, no. 3, pp. 502–514, June 2007.

[19] L. Zhou, Q. Zhang and C. Yang, "Practical Stability Analysis and Synthesis of a Class of Uncertain T-S Fuzzy Systems," *Lecture Notes in Computer Science*, vol. 4223, pp. 11–20, Sep. 2006.

[20] C. W. Park, H. J. Kang, "Graphical and Numerical Approach to Robust Stability Analysis of Fuzzy Modeled Systems with Parametric Uncertainty and Disturbance," *Fuzzy Sets and Systems*, vol. 151, no. 1, pp. 99-117, 2005.

[21] H. K. Lam, and F. H. F. Leung, "Stability Analysis of Discrete-Time Fuzzy-Model-Based Control Systems with Time Delay: Time Delay-Independent Approach," *Fuzzy Sets and Systems*, vol. 159, no. 8, pp. 990-1000, 2008.

[22] B. Chen, X. Liu, and S. Tong, "Delay-Dependent Stability Analysis and Control Synthesis of Fuzzy Dynamic Systems with Time Delay," *Fuzzy Sets and Systems*, vol. 157, no. 16, pp. 2224-2240, 2006.

[23] H. N. Wu, "Delay-Dependent Stability Analysis and Stabilization for Discrete-Time Fuzzy Systems with State Delay: A fuzzy Lyapunov-Krasovskii Functional Approach," *IEEE Transaction on Systems, Man Cybernetics B*, vol. 36, no. 4, pp. 954–962, Aug. 2006.

[24] Z. Zuo, and Y. Wang, "Robust Stability and Stabilization for Nonlinear Uncertain Time-Delay System via Fuzzy Control Approach," *IET Control Theory & Applications*, vol. 1, no. 1, pp. 422–429, Jan. 2007.

[25] E. Tian, and C. Peng, "Delay-Dependent Stability Analysis and Synthesis of Uncertain T-S Fuzzy Systems with Time Varying Delay," *Fuzzy Sets and Systems*, vol. 157, no. 4, pp. 544-559, 2006.

[26] W. J. M. Kickert and E. H. Mamdani, "Analysis of a Fuzzy Logic Controller," *Fuzzy Sets and Systems*, vol. 1, no.1, pp. 29–44, 1978.

[27] E. Kim, H. Lee and M. Park, "Limit-Cycle Prediction of Fuzzy Control System Based on Describing Function Method," *IEEE Transaction on Fuzzy Systems*, vol. 8, no. 1, pp. 11–22, Apr. 2000.

[28] J. Aracil and F. Gordillo, "Describing Function Method for Stability Analysis of PD and PI Fuzzy Controllers," *Fuzzy Sets and Systems*, vol. 143, no. 2, pp. 233-249, 2004.

[29] G. Abdelnour, J. Y. Cheung, C-. H. Chang and G. Tinetti, "Steady-State Analysis of a Three-Term Fuzzy Controller," *IEEE Transaction on Systems, Man Cybernetics*, vol. 23 , no. 2, pp. 607–610, Mar. 1993.

[30] G. Abdelnour, J. Y. Cheung, C-. H. Chang and G. Tinetti, "Application of Describing Functions in the Transient Response Analysis of a Three-Term Fuzzy Controller," *IEEE Transaction on Systems, Man Cybernetics*, vol. 23 , no. 2, pp. 603–606, Mar. 1993.

[31] M. Braae and D. A. Rutherford, "Selection of Parameters for a Fuzzy Logic Controller," *Fuzzy Sets and Systems*, vol. 2, no.3, pp. 185-199, 1979.

[32] C. J. Harris and C. G. Moore, "Phase Plane Analysis Tools for a Class of Fuzzy Control Systems," *Proceedings of IEEE International Conference on Fuzzy Systems*, San Diego, CA, USA, pp. 511-518, Mar. 8-12, 1992.

[33] H. X. Li and H. B. Gatland, "A New Methodology for Designing a Fuzzy Logic Controller," *IEEE Transaction on Systems, Man Cybernetics*, vol. 25 , no. 3, pp. 505–512, Mar. 1995.

[34] K. S. Ray and D. D. Majumder, "Application of Circle Criteria for Stability Analysis of Linear SISO and MIMO Systems Associated with Fuzzy Logic Controller," *IEEE Transaction on Systems, Man Cybernetics*, vol. 14 , no. 2, pp. 345–349, Mar./Apr. 1984.

[35] R. E. Haber, G. Schmitt-Braess and R. H. Haber, A. Alique and J. R. Alique, "Using Circle Criteria for Verifying Asymptotic Stability in PI-like Fuzzy Control Systems:

Application to the Milling Process," *IEE Proceedings Control Theory and Applications*, vol. 150 , no. 6, pp. 619–627, Nov. 2003.

[36] A. Kandel and Y. Luo and Y.-Q. Zhang, "Stability Analysis of Fuzzy Control Systems," *Fuzzy Sets and Systems*, vol.105, no.1, pp. 33-48, 1999.

[37] E. Furutani, M. Saeki, and M. Araki, "Shifted Popov Criterion and Stability Analysis of Fuzzy Control Systems," *Proceedings of Conference on Decision and Control*, Tucson, AZ, USA, pp. 2790–2795, Dec. 16-18, 1992.

[38] H. Wang, A. Xue, R. Lu, and J. Wang, "Reliable Robust $H_\infty$ Tracking Control for Lur'e Singular Systems with Parameter Uncertainties," *Proceedings of American Control Conference*, Seattle, Washington, USA, pp. 4312–4317, June 11-13, 2008.

[39] G. Arslan, and K. Y. Lee, "Stability Analysis of a Fuzzy Logic Controller," *Proceedings of American Control Conference*, Albuqueraue, New Mexico, USA, pp. 3301–3305, June 4-6, 1997.

[40] T. Mori, T. Nishimura, and Y. Kuroe, "Stability of Lur'e Systems with Interval Plants and General Sector-Type Nonlinearities," *Proceedings of American Control Conference*, Baltimore, Maryland, USA, pp. 1013–1017, June 29-July 1 ,1994.

[41] T. Mori, T. Nishimura, and Y. Kuroe, "Off-axis Circle Criteria for Lur'e Systems with Interval Plants," *Proceedings of Conference on Decision and Control*, Lake Buena Vista, Florida, USA, pp. 585–586, Dec. 14-16, 1994.

[42] Y. Chen, and Y. Zhang, and Q. Li, "Delay-Dependent Absolute Stability of Lur'e Systems with Interval-Varying Delay," *Proceedings of IEEE International Conference on Networking, Sensing and Control*, Sanya, Hainan, China, pp. 1696–1699, April 6-8, 2008.

[43] Q. L. Han, and D. Yue, "Absolute Stability of Lur'e Systems with Time Varying Delay," *IET Control Theory & Applications*, vol. 1, no. 3, pp. 854–859, May 2007.

[44] Q. L. Han, "Absolute Stability of Time-Delay Systems with Sector-Bounded Nonlinearity," *Automatica*, vol. 41, no. 12, pp. 2171-2176, Dec. 2005.

[45] Y. Wang, X. Yan, Z. Zuo, and H. Zhao, "Further Improvements on Delay-Dependent Absolute Stability of Delayed Systems with Sector-Bounded Nonlinearity," *Proceedings of IEEE International Symposium on Intelligent Control*, San Antonio, Texas, USA, pp. 899–904, Sep. 3-5, 2008.

[46] R. Q. Lu, H. Y. Su, and J. Chu, "Robust $H_\infty$ Control for a Class of Uncertain Lur'e Singular Systems with Time-Delay," *Proceedings of Conference on Decision and Control*, Maui, Hawaii, USA, pp. 5585–5590, Dec. 9-12, 2003.

[47] B. Butkiewicz, "Steady-State Error of a System with Fuzzy Controller," *IEEE Transaction on Systems, Man Cybernetics B*, vol. 28, no. 6, pp. 855–860, Dec. 1998.

[48] C. W. Tao and J. S. Taur, "Robust Fuzzy Control for a Plant with Fuzzy Linear Model," *IEEE Transaction on Systems, Man Cybernetics B*, vol. 13, no. 1, pp. 30–41, Feb. 2005.

[49] H. A. Malki, H. Li and G. Chen, "New Design and Stability Analysis of Fuzzy Proportional-Derivative Control Systems," *IEEE Transaction on Fuzzy Systems*, vol. 2, no. 4, pp. 245–254, Nov. 1994.

[50] J. S. Taur and, C. W. Tao "Design and Analysis of Region-Wise Linear Fuzzy Controllers," *IEEE Transaction on Systems, Man Cybernetics B*, vol. 27, no. 3, pp. 526–532, June. 1997.

[51] T. Wada, M. Ikeda, Y. Ohta and D. D. Šiljak, "Parametric Absolute Stability of Lur'e Systems," *IEEE Transaction on Automatic Control*, vol. 43, no. 11, pp. 1649 – 1653, Nov. 1998.

[52] B. J. Choi, S. W. Kwak and B. K. Kim, "Design and Stability Analysis of Single-Input Fuzzy Logic Controller," *IEEE Transaction on Systems, Man Cybernetics B*, vol. 30 , no. 2, pp. 303–309, Apr. 2000.

[53] M. Dahleh, A. Tesi, and A. Vicino, "On the Robust Popov Criterion for Interval Lur'e System," *IEEE Transaction on Automatic Control*, vol. 38, no. 9, pp. 1400–1405, Sep. 1993.

[54] S. P. Bhattacharyya, H. Chapellat and L. H. Keel, *Robust Control: The Parametric Approach*, Prentice-Hall, NJ, 1995.

[55] L. M. Pecora and T. L. Carroll, "Synchronization in Chaotic Systems," *Physical Review Letters*, vol.64, no.8, pp.821–824, 1990.

[56] J. A. K. Suykens, P. F. Curran and L. O. Chua, "Robust Synthesis for Master-Slave Synchronization of Lur'e Systems," *IEEE Transaction Circuits and Systems I*, vol.46, no.7, pp.841–850, 1999.

[57] J. A. K. Suykens, P. F. Curran, J. Vandewalle and .L. O. Chua, "Robust Nonlinear $H^\infty$ Synchronization of Chaotic Lur'e Systems," *IEEE Transaction Circuits and Systems I*, vol.44, no.10, pp.891–904, 1997.

[58] E. N. Sanchez, and J. P. Perez, "Adaptive Recurrent Neural Control for Noisy Chaos Synchronization," *Proceedings of American Control Conference*, Denver, CO; USA, pp.1290–1295, June 4-6, 2003.

[59] E. N. Sanchez, J. P. Perez, J. P.Perez, L. J. Ricalde, and Guanrong Chen, "Chaos Synchronization via Adaptive Recurrent Neural Control," *Proceedings of Conference on Decision and Control*, Orlando, FL, USA, pp.3526–3539, Dec. 4-7, 2001.

[60] M. Boutayeb, "Synchronization and Input Recovery in Digital Nonlinear Systems," *IEEE Transaction Circuits and Systems II*, vol.51, no.8, pp.393–399, 2004.

[61] G. Grassi, and S. Mascolo, "Nonlinear Observer Design to Synchronize Hyperchotic Systems via a Scalar Signal," *IEEE Transaction Circuits and Systems I*, vol.44, no.10, pp.1011–1014, 1999.

[62] O. Morgül, and E. Solak, "Observer Based Synchronization of Chaotic Systems," *Physical Review E*, vol.54, no.5, pp.4803–4811, 1996.

[63] T. L. Liao, and N. S. Huang, "An Observer-Based Approach for Chaotic Synchronization with Application to Secure Communication," *IEEE Transaction Circuits and Systems I*, vol.46, no.9, pp.1144 –1150, 1999.

[64] A. Azemi, and E. E. Yaz, "Sliding-Mode Adaptive Observer Approach to Chaotic Synchronization," *ASME Journal of Dynamic Systems, Measurement and Control*, vol.122, pp.758–765, 2000.

[65] M. Feki, "Synchronization of Chaotic Systems with Parametric Uncertainties Using Sliding Observer," *International Journal of Bifurcation and Chaos*, vol.14, no.7, pp.2467–2475, 2004.

[66] K. Y. Lian, C. S. Chiu, T. S. Chiang, and P. Liu, "Secure Communications of Chaotic Systems with Robust Performance via Fuzzy Observer-Based Design," *IEEE Transaction Circuits and Systems I*, vol.9, no.1, pp.212–220, 2001.

[67] G. Millerioux, and J. Daafouz, "An Observer-based Approach for Input-Independent Global Chaos Synchronization of Discrete-Time Switched Systems," *IEEE Transaction Circuits and Systems I*, vol.50, no.10, pp.1270–1279, 2003.

[68] J. Amirazodi, E. E. Yaz, A. Azemi, and Y. I. Yaz, "Nonlinear Observer Performance in Chaotic Synchronization with Application to Secure Communication," *Proceedings of IEEE Conference on Control Application*, Glasgow, Scotland, UK, pp.76–81, Spet. 18-20, 2002.

[69] H. Nijmerijer, and I. M. Y. Mareels, "An Observer Looks at Synchronization," *IEEE Transaction Circuits and Systems I*, vol.44, no.10, pp.882–890, 1997.

[70] H. Dedieu, and M. J. Ogorzalek, "Identifiability and Identification of Chaotic Systems Based on Adaptive Synchronization," *IEEE Transaction Circuits and Systems I*, vol.44, no.10, pp.948-962, 1997.

[71] O. De Feo, "Self-Emergence of Chaos in the Identification of Irregular Periodic Behavior," *Chaos*, vol.13, no.4, pp.1205-1215, 2003.

[72] C. H. Hyun, J. H. Kim, E. Kim and M. Park, "Adaptive Fuzzy Observer Based Synchronization Design and Secure Communications of Chaotic Systems," *Chaos, Solitons and Fractals*, vol.27, no.4, pp.930-940, 2006.

[73] Y. G. Leu and T. T. Lee, "Adaptive Fuzzy-Neural Observer for a Class of Nonlinear Systems," *Proceedings of IEEE International Conference on Robotics and Automation*, San Francisco, CA, USA, pp.2130–2135, April 24-28, 2000.

[74] T. Schimming and O. D. Feo, "Chaos Synchronization in Noisy Environments using Kalman Filters," in *Chaos in Circuits and Systems*, G. Chen and T. Ueta, Ed. World Scientific, pp.509-527, 2002.

[75] B. Friedland, *Advanced Control System Design*, Prentice-Hall, NJ, 1996.

[76] K. Viswanathan, R. Oruganti and Dipti Srinivasan, "Nonlinear Function Controller: A Simple Alterative to Fuzzy Logic Controller for a Power Electronic Converter," *IEEE Transaction on Industrial Electronics*, vol. 52, no. 5, pp. 1439–1448, Oct. 2005.

[77] P. Horowitz and W. Hill, *The Art of Electronics*, Cambridge University Press, Cambridge, UK, 2000.

[78] S. Franco, *Design with Operational Amplifiers and Analog Integrated Circuits,* 3rd ed., McGraw-Hill, NY, 2002.

[79] B. F. Wu, L. S. Ma, J. W. Perng, H. I. Chin and T. T. Lee, "Stability Analysis of Equilibrium Points in Static Fuzzy Control System with Reference Inputs and Adjustable

Parameters," *Proceedings of IEEE International Conference on Fuzzy Systems*, Vancouver, BC, Canada, pp. 10255-10261, July 16-21, 2006.

[80] Y. G. Leu, "Observer-Based Adaptive Fuzzy-Neural Control for a Class of Nonlinear Systems," Ph.D. thesis, Department of Electrical Engineering, National Taiwan University of Science and Technology, Taipei, Taiwan, 1999.

[81] B. S. Chen, C. H. Lee, and Y. C. Chang, " $H^\infty$ Tacking Design of Uncertain Nonlinear SISO Systems: Adaptive Fuzzy Approach," *IEEE Transaction on Fuzzy Systems*, vol.4, no.1, pp.32-43, 1996.

[82] L. X. Wang, "Design and Analysis of Fuzzy Identifiers of Nonlinear Dynamic Systems," *IEEE Transaction on Automatic Control*, vol.40, no.1, pp.11-23, 1995.

[83] M. Jamshidi, N. Vadiee, and T. J. Ress, *Fuzzy Logic and Control*, Prentice-Hall, NJ, 1993.

[84] L. X. Wang, *Adaptive Fuzzy Systems and Control: Design and Stability Analysis*, Prentice-Hall, NJ, 1994.

[85] C. H. Wang, T. C. Lin, T. T. Lee, and H. L. Liu, "Adaptive Hybrid Intelligent Control for Uncertain Nonlinear Dynamical Systems," *IEEE Transaction on Systems, Man Cybernetics B*, vol.32, pp.583–597, 2002.

# VITA

博 士 生：馬立山(Li-Shan Ma)
指導教授：吳炳飛(Bing-Fei Wu)
論文題目：模糊邏輯控制系統之穩定度分析與應用 (The Stability Analysis and its Application in Fuzzy Control Systems)

## 學歷

1. 80 年 9 月～84 年 6 月　　中原大學電機工程學系
2. 84 年 9 月～86 年 6 月　　中原大學電機工程研究所碩士班
3. 90 年 9 月～迄今　　　　國立交通大學電控工程研究所博士班

## 經歷

1. 86 年 7 月～87 年 6 月　　國立桃園農工電機科 實習教師
2. 87 年 7 月～88 年 8 月　　工業技術研究院電通所 副工程師
3. 88 年 9 月～迄今　　　　建國科技大學電子工程系(所) 講師

# Publication List

## Journal Papers

[1] Jau-Woei Perng, <u>Li-Shan Ma</u>, Bing-Fei Wu and Tsu-Tian Lee, "Describing Function Analysis of Neural Control Vehicle Steering Systems," *International Journal of Information Technology*, Vol. 11, No. 6, pp. 63-73, 2005. (EI)

[2] Bing-Fei Wu, Chao-Jung Chen, Hsin-Han Chiang, Hsin-Yuan Peng, Jau-Woei Perng, <u>Li-Shan Ma</u> and Tsu-Tian Lee, "The Design of An Intelligent Real-Time Autonomous Vehicle, Taiwan *i*TS-1," *Journal of the Chinese Institute of Engineers,* Vol. 30, No. 5, pp. 829-842, 2007. (SCI, EI)

[3] Bing-Fei Wu, <u>Li-Shan Ma</u>, and Jau-Woei Perng ,"Observer-Based Synchronization for Unknown Chaos Systems with Adaptive Fuzzy-Neural Network," *IEICE Transaction on Fundamentals of Electronics, Communications and Computer Sciences*, Vol.E91-A, No. 7, pp. 1797-1805, July 2008. (SCI, EI)

[4] Bing-Fei Wu, <u>Li-Shan Ma</u>, and Jau-Woei Perng ,"The Absolute Stability Analysis in Fuzzy Control Systems with Parametric Uncertainties and Reference Inputs," *IEICE Transaction on Fundamentals of Electronics, Communications and Computer Sciences*, Vol.E92-A, No. 8, pp. 2017-2035, Aug. 2009. (SCI, EI)

[5] Jau-Woei Perng, <u>Li-Shan Ma</u>, and Bing-Fei Wu, "Limit Cycle Prediction of a Neurocontrol Vehicle System Based on Gain-Phase Margin Analysis," accepted for publication in *Neural Computing & Applications*, 2009. (SCI, EI)

# Conference Papers

[1] Bing-Fei Wu, Jau-Woei Perng, Li-Shan Ma, and Ching-Cheng Teng "Analysis and Modeling of Coarse Sun Sensors in Attitude Determination and Control Subsystem for ROCSAT1 Sun Mode," 太空計畫十週年暨華衛一號三週年成果發會論文集, Hsinchu, Taiwan, pp.47-59, May 23, 2002.

[2] Bing-Fei Wu, Li-Shan Ma, Jau-Woei Perng and Tsu-Tian Lee, " $H^\infty$ Tracking-Based Sliding Mode Longitudinal Control of a Platoon of Vehicles," *Proceedings of the 6th IASTED International Conference on Intelligent Systems and Control*, Hawaii, USA, pp.174~179, Aug. 23-25, 2004.

[3] Bing-Fei Wu, Li-Shan Ma, Jau-Woei Perng and Tsu-Tian Lee, " $H^\infty$ Sliding Mode Tracking Control for Chua's Circuit", *Proceedings of IEEE Asia-Pacific Conference on Circuits and Systems*, Tainan, Taiwan, pp. 581~584, Dec. 6-9, 2004.

[4] Jau-Woei Perng, Li-Shan Ma, Bing-Fei Wu and Tsu-Tian Lee, "Robust PI Controller Design for Vehicle Steering Systems," *Proceedings of IASTED International Conference on Intelligent Systems and Control*, Cambridge, MAT, USA, pp. 247~252, Oct. 31-Nov. 2, 2005.

[5] Jau-Woei Perng, Li-Shan Ma, Bing-Fei Wu, and Tsu-Tian Lee, "Describing Function Analysis of Neural Control Vehicle Steering Systems," *Proceedings of International Conference on Intelligent Computing*, HeFei, China, pp. 2587~2596, Aug. 23-26, 2005.

[6] Hsin-Han Chiang, Li-Shan Ma, Jau-Woei Perng, Bing-Fei Wu and Tsu-Tian Lee, "Longitudinal and Lateral Fuzzy Control Systems Design for Intelligent Vehicles," *Proceedings of IEEE International Conference on Networking, Sensing and Control*, Ft. Lauderdale, Florida, USA, pp. 573~578, Apr. 23-25, 2006.

[7] Bing-Fei Wu, Li-Shan Ma, Jau-Woei Perng, Hung-I Chin, and Tsu-Tian Lee, "Adaptive

Synchronization for Unknown Chaotic Systems with Fuzzy-Neural Network Observer", *Proceedings of IEEE International Conference on Engineering of Intelligent Systems*, Islamabad, Pakistan, pp198~203, Apr. 22-23, 2006.

[8] Bing-Fei Wu, <u>Li-Shan Ma</u>, Jau-Woei Perng, Hung-I Chin, and Tsu-Tian Lee, "Stability Analysis of Equilibrium Points in Static Fuzzy Control System with Reference Inputs and Adjustable Parameters," *Proceedings of IEEE International Conference on Fuzzy Systems*, Vancouver, BC, Canada, pp. 10255-10261, Jul. 16-21, 2006.

[9] Bing-Fei Wu, <u>Li-Shan Ma</u>**,** Jau-Woei Perng, Shih-Meng Chang, and Tsu-Tian Lee, "Robust Fuzzy Control Design for an Automatic Vehicle Steering System with State Observer," *Proceedings of International Symposium on Advanced Vehicle Control*, Taipei Taiwan, pp. 369-372, Aug. 20-24, 2006.

[10] Bing-Fei Wu, <u>Li-Shan Ma</u>, Jau-Woei Perng, Hung-I Chin, and Tsu-Tian Lee, "Robust Longitudinal Controller and Observer Design for Vehicles with a Riccati Equation Approach," *Proceedings of SICE-ICASE International Joint Conference*, Busan, Korea, pp. 4955-4960, Oct. 18-21, 2006.

[11] Bing-Fei Wu, <u>Li-Shan Ma</u>, Tien-Yu Liao, and Jau-Woei Perng, "Vehicle Steering Controller Design with Time Domain Specification in Parameter Space," *Proceedings of CACS Automatic Control Conference*, Tamsui, Taiwan, pp. 100-104, Nov. 10-11, 2006.

[12] Bing-Fei Wu, <u>Li-Shan Ma</u>, Jau-Woei Perng, and Tsu-Tian Lee, "Vehicle Steering Systems Design with a PID Type Fuzzy Controller," *Proceedings of National Conference on Fuzzy Theory and Its Applications*, Kaohsiung, Taiwan, pp. B6-2-1-B6-2-5, Dec. 14 -15, 2006.

[13] Bing-Fei Wu, <u>Li-Shan Ma</u>, Jau-Woei Perng, Hung-I Chin, and Tsu-Tian Lee, "Optimal Single-Input PID Type Fuzzy Logic Controller Design with Genetic Algorithm," *Proceedings of International Conference on Machine Learning and Cybernetics*, Hong

Kong, China, pp. 2000-2004, Aug. 19-22, 2007.

[14] Bing-Fei Wu, Li-Shan Ma, Jau-Woei Perng, and Hung-I Chin, "Absolute Stability Analysis in Uncertain Static Fuzzy Control Systems with the Parametric Robust Popov Criterion," *Proceedings of IEEE International Conference on Fuzzy Systems*, Hong Kong, China, pp. 1325-1330, June 1-6, 2008.

[15] Bing-Fei Wu, Li-Shan Ma, Jau-Woei Perng, and Hung-I Chin, "Uncertain Interval PLL Frequency Response Analysis," *Proceedings of 2008 National Symposium on System Science and Engineering Conference*, ILan, Taiwan, June 6-7, 2008.